ΠΑΝΕΠΙΣΤΗΜΙΟ ΚΡΗΤΗΣ

ΙΑΤΡΙΚΗ ΣΧΟΛΗ

Η μηχανική ανεπάρκεια του μεσοσπονδύλιου δίσκου μετά από κάταγμα της τελικής πλάκας ως παράγοντας κινδύνου για παρακείμενα σπονδυλικά κατάγματα.

ΔΙΔΑΚΤΟΡΙΚΗ ΔΙΑΤΡΙΒΗ

Μιχαήλ Ν. Τζερμιαδιανός MD

Ηράκλειο Κρήτης, Φεβρουάριος 2017

Τριμελής Συμβουλευτική Επιτροπή:

Γεώργιος Κοντάκης
Ιωάννης Δαμηλάκης
Καλλιόπη Αλπαντάκη

Επταμελής επιτροπή:

Γεώργιος Κοντάκης
Ιωάννης Δαμηλάκης
Καλλιόπη Αλπαντάκη
Αλεξάνδρα Παπαϊωάννου
Οδυσσέας Ζώρας
Κλειώ Σπανάκη
Δημήτριος Τσέτης

Table of Contents

ABSTRACT

Residual kyphotic deformity of the vertebral body after an osteoporotic fracture has been associated with the increased risk of subsequent, especially adjacent vertebral fractures. However, the role of endplate deformity has not been evaluated. This study tested the hypothesis that the altered pressure profile of the intervertebral disc after an osteoporotic vertebral fracture, even in the absence of kyphotic deformity, will alter load transmission to the adjacent vertebra and increase the risk for adjacent vertebral fracture.

Eight human lower thoracic or thoracolumbar specimens, each consisting of five vertebrae were used. To selectively fracture one of the endplates of the middle VB of each specimen a void was created under the target endplate and the specimen was flexed and compressed until failure. The fractured vertebra was subjected to spinal extension under 150 N preload that restored the anterior wall height and vertebral kyphosis, while the fractured endplate remained significantly depressed. The VB was filled with cement to stabilize the fracture, after complete evacuation of its trabecular content to ensure similar cement distribution under both the endplates. Specimens were tested in flexion extension under 400 N preload while pressure in the discs and strain at the anterior wall of the adjacent vertebrae were recorded. Disc pressure in the intact specimens increased during flexion by 26 ± 14%. After cementation, disc pressure increased during flexion by 15 ± 11% in the discs with un-fractured endplates, while decreased by 19 ± 26.7% in the discs with the fractured endplates. During flexion, the compressive strain at the anterior wall of the vertebra next to the fractured endplate increased by 94 ± 23% compared to intact status ($p<0.05$), while it did not significantly change at the vertebra next to the unfractured endplate (18.2 ± 7.1%, $p> 0.05$). Subsequent flexion with compression to failure resulted in adjacent fracture close to the fractured endplate in six specimens and in a non-adjacent fracture in one specimen, while one specimen had no subsequent fractures.

In healthy discs with intact endplates the nucleus pressure increases during flexion avoiding load concentration on the anterior portion of the vertebral bodies. The increased available space for nucleus after an osteoporotic endplate-

depressed fracture impairs its load bearing abilities and forces the anterior annulus to bear more weight in flexion, resulting in excessive loading on the anterior portion of the adjacent vertebra that predisposes to fracture even after correction of kyphosis. These data suggest that correction of endplate deformity may play a role in reducing the risk of adjacent level fractures.

List of Tables

List of Figures

Abbreviations

BMD: Bone Mineral Density

EMG: Electromyography

FEV1: forced expiratory volume in the first second of the forceful exhalation

FVC: Forced Vital Capacity

MPa: megapascal

N: Newton (One newton is the force needed to accelerate one kilogram of mass at the rate of one metre per second squared in direction of the applied force. At average gravity on earth, (conventionally g = 9.80665 m/s^2), a kilogram mass exerts a force of about 9.8 newtons)

OVCF: Osteoporotic Vertebral Compression Fracture

PBK: Percutaneous Balloon Kyphoplasty

PMMA: polymethylmethacrylate

PVP: Percutaneous Vertebroplasy

ROM: Range of Motion

VB: Vertebral Body

WHO: World Health Organization

Altered disc pressure profile after an osteoporotic vertebral fracture is a risk factor for adjacent vertebral body fracture

I. INTRODUCTION

Osteoporosis is a skeletal disorder characterized by compromised bone strength predisposing a person to an increased risk of fracture. An estimated 75 million people in Europe, the United States, and Japan have osteoporosis [1]. According to the WHO criteria, osteoporosis is defined as a bone mineral density (BMD) that lies 2.5 standard deviations or more below the average value for young healthy women. Osteoporosis is often overlooked and undertreated, however, in large part because it is clinically silent before manifesting as fracture. In the United States, it is estimated that 25% of white postmenopausal women and 35% of women over the age of 65 suffer from osteoporosis, as per it's WHO definition [2].

Osteoporotic vertebral compression fractures (OVCFs) is the most common complication of osteoporosis [3]. They may occur in the absence of trauma or after only minor trauma, such as bending, lifting or turning. One fourth of women reaching menopause can expect to suffer one or more OVCF in their lifetime [4]. Radiographic evidence of OVCF exists in 25% of women over 70 and 50% of women over 80 [3]. In the U.S., of the estimated 1.5 million osteoporotic fractures that occur annually, 700,000 affect the spine [5]. The estimated incidence of OVCF in the EU is 438,700 clinically diagnosed vertebral fractures per year (117 per 100,000 person years) [6]. The incidence of OVCF is likely to increase fourfold in the next 50 years [5].

The majority of OVCF occur in the thoracolumbar junction (T12-L1) and the mid-thoracic spine [3,7,8]. These fractures typically lead to increased kyphosis, which may worsen overtime as OVCF increase in number [9,10]. As posture worsens and kyphosis progresses, patients experience difficulty with balance, back pain, respiratory compromise, and an increased risk of pneumonia. Cooper et al. [11] found that vertebral fractures increased the 5-year risk of mortality by 15%. In a subsequent study, Kado et al. [12] demonstrated that women with one or more fractures had a 1.23-fold increased age-adjusted mortality rate and that women with 5 or more vertebral fractures had a 2.3-fold increased age-adjusted mortality rate.

The presence of an OVCF is an independent predictor of subsequent vertebral fractures regardless of age and BMD [13,14,15,16,17]. After adjustment for age and BMD, a prevalent vertebral fracture is associated with a four- to five-fold increased risk of suffering a subsequent vertebral fracture [7,13,16,18]. The risk of a new vertebral fracture increases with both the number and the severity of prevalent vertebral fractures [7,19,20]. It is estimated that a single fracture increases the risk fivefold for new vertebral fractures, while the presence of two or more fractures increases the risk 12-fold [21]. Similarly, Lindsay et al. [13] reported an incidence of 11.5% of new vertebral fractures within 1 year following one previous OVCF, whereas this incidence was 24% in women with two or more fractures. Others have estimated that a fifth of osteoporotic women with a recent vertebral fracture will sustain a new vertebral fracture within the next 12 months [22]. As the increased incidence of subsequent fractures is independent from parameters as age and BMD, better understanding of their causes might improve therapeutic or preventive measures.

The severity of vertebral collapse and the residual kyphotic deformity have been associated with the risk for subsequent vertebral fractures [7,16,23,24]. Kyphotic deformity shifts the center of gravity forward, resulting in increased forward bending moments, which are in turn compensated by a contraction of the posterior spinal muscles, resulting in an increased load within the kyphotic segment [25,26]. Cadaveric studies have shown that residual kyphosis increased vertebral cortical compressive strain at the adjacent vertebrae, especially in flexion [27,28].

Resurgent interest in the pathomechanics of subsequent OVCF arose after reports of new vertebral fractures after cement augmentation of an OVCF, especially in the vicinity of the cemented fracture [29-35]. These reports have raised concern about a possible correlation of augmentation with the risk of subsequent vertebral fractures. This concern was further increased after reports that subsequent fractures after augmentation tend to occur early, usually within 3 months after the cementation procedure [32,34,36,37,38], and that fractures of vertebrae adjacent to the treated level occur sooner than those of non-adjacent levels [32]. It is often postulated that augmentation, by increasing stiffness to

values greater than that of the adjacent vertebrae, may create a “stress riser” effect that could lead to mechanical failure of non-augmented levels. However, increased adjacent level load transfer following augmentation has not been conclusively shown, and the subsequent OVCFs may result simply from disease progression as indicated by more resent reports [39,40,41]. Adjacent vertebrae may be at a greater risk for fracture after an OVCF even in the absence of cement augmentation as shown by Silverman et al. [42] who reported that 58% of women with one or more fractures had adjacent fractures. Moreover, a temporal clustering of incident fractures within the first few months after the diagnosis of a prevalent fracture has been described even in the absence of cement augmentation [43].

The intervertebral disc plays a significant role in load transmission, and it role in the pathogenesis of adjacent compressive vertebral fractures is not well understood. Heathy intervertebral discs transmit compressive load evenly between adjacent vertebral bodies (VBs), while allowing movements of the vertebral column. This mainly reflects the properties of the nucleus, which is composed of a loose network of fibrous strands that lie in a translucent mucoprotein gel containing various mucopolysaccharides. In a healthy young disc, the water content of the nucleus ranges from 70-90%. The water gives the tissue very low rigidity so that it can deform easily in any direction and equalize the stress applied to it [44]. The nucleus fills 30-50% of the total disc cross sectional area, and is located more posterior than central. The annulus gradually becomes differentiated from the periphery of the nucleus, and forms the outer boundary of the disc. The annulus is made up of a series of 15 to 25 concentric lamellae [45]. well suited to resisting torsion due to the characteristic orientation of the fibers in each layer. Fiber strains rarely exceed 6% under physiologic flexion and extension moments and 8.5% under physiologic axial rotation. The intervertebral disc alone provides most of the compressive stiffness of the motion segment, whereas ligaments and facets contribute significantly to resisting bending moments and axial torsion.

When the disc is compressed, the pressure inside the nucleus increases, generating a tensile hoop stress in the restraining annulus, thus maintaining the

intervertebral disc height. Hoop stress decreases from the inner lamellae of the annulus to the outer lamellae. Cadaveric experiments have shown that a compressive force of 2,000 N stretches the collagen fibers on the outer annulus by less than 2% and causes the annulus to bulge radially by 0.4 to 1.0mm [46]. As the preload increases from 250 N to 4,500 N the height of a motion segment is reduced by 0.9 mm. Approximately half of the height reduction can be attributed to the endplates bulging into the vertebral bodies [47,48]. The annulus also resists compression directly, therefore compressive stresses are distributed almost evenly throughout the entire disc area in a young, non-degenerated disc [49].

Changes in the properties of the disc is expected to alter load transmission between adjacent vertebrae. To theoretically explain how increased stiffness of a cemented vertebral body could endanger the adjacent vertebrae, Baroud et al, [50] utilized a finite element model to simulate the effects of cement. They postulated that in the normal vertebrae, axial cushioning is achieved by a combination of outward bowing of the annulus fibrosis as well as by substantial inward bowing of the vertebral endplates. Using their model, they demonstrated that cement in the treated vertebral body “acts like a pillar” that reduces by 93% the physiologic inward bulge of the endplates of the treated level. Because the endplate of the treated vertebra is resistant to inward bowing, pressure is increased in the disk and enhanced bowing and inward deflection is seen in the endplate on the opposite side of the disk. Augmented inward bowing of the adjacent vertebral endplate would place this vertebra at risk for fracture. They also postulated that the untreated, adjacent vertebra showed a 17% decrease in failure load compared with untreated spinal segments [50]. Polikeit et al [51] confirmed the effect of vertebroplasty on adjacent vertebrae with a finite element model similar to that of Baroud et al [50]. These latter authors demonstrated increased pressure in the adjacent nucleus pulposus both above and below the treated vertebra, which translated into a 20% increased inward deflection of the endplate of the adjacent vertebral body.

However, the increased nucleous polposus pressure theory proposed by the previous studies did not take into account the damage of the endplate caused by the osteoporotic vertebral compression fracture. As the endplate is depressed,

more space becomes available for the nucleus. In vitro experiments have shown that damage to the vertebral body endplate reduces the pressure in the nucleus of the adjacent disc [52,53,54,55]. Furthermore, reduced nuclear pressure generates peaks of compressive stress in the annulus [52,53,55], redistributing in this manner the load transmission to the periphery of the vertebral body. Stress concentrations are affected by posture [53].

The reduction of disc pressure after an OVCF has some biomechanical similarities with the model of disc degeneration. In vitro studies have shown that in a degenerative disc the nucleus becomes depressurized as a result of the reduction of water content and increased fibrosis [McNally Spine 1992]56. This has been confirmed by in vivo studies that showed that the intradiscal pressure was significantly reduced in a degenerated disc [57], and the decrease was in accordance to the degree of disc degeneration as estimated by magnetic resonance imaging [58]. Nucleus depressurization results in an increasingly larger load transmission trough the annulus, especially in the posterior portion [56]. Furthermore, the principal area of load transmission is highly dependent on posture, with a more prominent increase of stress concentrations in the posterior annulus when the segment is extended [57,53]. With disc degeneration, the posterolateral annulus is no longer acting in its role of a nucleus retaining membrane but rather as a region transmitting compressive stress. This is associated with inward bulging of the inner lamellae [59]. In more advanced stages of degeneration with disc space narrowing, it is possible for the neural arch to stress shield the posterior annulus in extension, so that much of the compressive load is transmitted through the neutral arch and the anterior annulus [53]. The facet joints in a healthy spine normally bear approximately 20% of the load, but when there is a loss of disc height due to degenerative changes facet load bearing can be as high as 70% [60].

Research question

The purpose of this biomechanical study was to test the hypothesis that the altered pressure profile of the intervertebral disc after an osteoporotic vertebral fracture, even in the absence of kyphotic deformity, will alter load transmission to

the adjacent vertebra and increase vertical loading of the anterior wall of adjacent vertebrae, predisposing them to wedge fracture.

II. LITERATURE REVIEW

A. Osteoporotic vertebral fractures and their biomechanical effects

1. Biomechanical changes in osteoporotic vertebra before and after a fracture

Osteoporotic vertebral bodies have decreased strength and stiffness, which means that the load needed to cause failure of vertebral bodies and their ability to resist compressive deformation are diminished. Strength and stiffness are diminished in proportion to the severity of osteoporosis, as these entities are strongly correlated to bone density of trabecular bone [61]. Vertebral compression fractures result in further reduction of both strength and stiffness relative to pre-fracture values [62]. The clinical consequences are:

(i) a propensity of progressive collapse of the damaged vertebra after the initial osteoporotic fracture as a result of diminished strength

(ii) pain at the fracture site as a result of increased micromotion resulting from diminished stiffness.

A major complaint of 85% of patients with radiological diagnosis of OVCF is back pain, which may be present as either acute and excruciating, or chronic and persistent [63,64]. Old et al. [65] estimates that chronic back pain affects approximately 75% of patients who suffer OVCFs. Acute back pain is usually caused by a recent OVCF, and in the majority of patients is expected to subside as the fracture heals over a period of approximately 3 months [66]. However, an estimated 33% [67] to 75% [65] of patients may develop chronic back pain. Chronic pain may arise from progressive collapse and deformity or persistent intravertebral motion due to pseudoarthrosis, which can occur with an incidence of 35% per fracture [68].

2. Kyphotic deformity after OVCF

Compression fractures of the spine generally occur from a combination of bending forward and downward pressure on the spine. Bending forward concentrates the pressure on the anterior portion of the spine. The fracture occurs

when the bone actually collapses in the anterior part of the vertebral body and forms a wedge shape. Wedge fractures are the main type of fractures that occur in the thoracic spine, and typically lead to increased kyphosis, which may worsen overtime in persons with prevalent OVCF [9,10]. Painful, crippling kyphotic deformities requiring major surgical intervention may be encountered in elderly patients suffering an OVCF or vertebrae delayed collapse with severe neurological deficits and paraparesis [69].

Spinal deformity itself, independent of pain, is a significant cause of disability resulting directly from the impairment of physical functioning, health, and quality of life [25]. Lung function (FVC, FEV1) are significantly reduced in patients with thoracic fractures and may result in increased morbidity and mortality rate. OVCF is associated with a 23-34% age-adjusted increase in mortality rate compared to patients without OVCF [12,70,71]. It has been reported that each vertebral fracture results in restrictive lung disease causing a 9% loss in predicted forced vital capacity and forced expiratory volume in 1 second [72,73], which may in turn have particularly detrimental effects in patients with pre-existing lung disease.

Sagittal spinal deformity, in patients with OVCF, increases the forward bending moment, and can be counterbalanced by flexing the knees to improve body posture [74]. However, this posture provokes paraspinal muscle fatigue and increases strain in the facets and pars interarticularis, contributing to chronic back pain. Furthermore, the knee flexion manoeuvre requires the contraction and tightening of the thigh muscles, resulting in an impaired gait velocity, reduction of mobility, and a curtailing of most daily activities, irrespective of pain. This impairment of patient functions leads to sleep disorders, increased anxiety and depression, lowered self-esteem, diminished social role, and increased dependency on others [42,75,76,77].

3. Subsequent vertebral fractures after an OVCF

The presence of an OVCF increases the risk for subsequent vertebral fractures [13,15,21]. Lindsay et al. [13] in a prospective clinical study reported an incidence of 19.2% of new vertebral fractures within one year following one or more vertebral fractures in patients with osteoporosis. In women with one

previous fracture the incidence was 11.5%, whereas this incidence was 24% in women with two or more fractures. The study showed that the presence of 1 or more vertebral fractures increases the risk of sustaining a new vertebral fracture by 5-fold during the following year. Similarly, Ross et al. [14] reported that a single fracture increases the risk for new vertebral fractures by 5-fold, while the presence of 2 or more fractures increases the risk by 12-fold. A combination of low bone mass and the presence of 2 or more prevalent fractures increase the risk by 75-fold, relative to women with the highest bone mass and no prevalent fractures [14]. Silverman et al. [75] reported that 58% of women with one or more fractures had fractures at adjacent vertebrae, supporting the high rate of adjacent fractures in the natural history of the disease.

The severity of vertebral collapse [24] and the residual kyphotic deformity have been associated with the risk for subsequent vertebral fractures [16,23,78,79]. Kyphotic deformity shifts the center of gravity forward, resulting in increased forward bending moments, which are in turn compensated by a contraction of the posterior spinal muscles, resulting in an increased load within the kyphotic segment [25,26,80] thus predisposing to further vertebral body fractures adjacent to the original OVCF [13,14,71]. Using anterior wall strain gauges, Kayanja et al. [27,28] showed that after an experimentally induced osteoporotic fracture, the addition of flexion to axial compression increases the axial compressive loads at the adjacent vertebrae, supporting the role of residual kyphosis.

4. Residual kyphotic deformity as a risk for subsequent fractures

Residual kyphotic deformity after a wedge fracture is a risk factor for subsequent vertebral fractures [23,25,71]. Wedge type fractures typically occur in the mid thoracic spine or the thoracolumbar junction [7,81,82,83] The contribution of kyphosis is less likely to be important to the lumbar spine where osteoporotic fractures tend to be biconcave, thus not significantly altering sagittal alignment. Kyphotic deformity after a wedge fracture shifts the physiologic compressive load path anteriorly [84], increasing the strain on the anterior cortex [27]. Thus, residual kyphotic deformity after cement augmentation of a fractured vertebra may produce an eccentric loading on the adjacent levels, inducing additional flexion

moments. Mizrahi et al. [85] showed that eccentric loading of a vertebra can increase peak stresses by up to 2.5 times in vertebrae with reduced vertebral bone mass, possibly due to the development of high tensile and multi-axial stresses in the cortical shell and end plate. Cadaveric studies have shown increased vertebral cortical strain at the adjacent vertebrae, especially in flexion [28].

Kyphotic deformity shifts the center of gravity forward, resulting in increased forward bending moments, which are in turn compensated by a contraction of the posterior spinal muscles [25,26]. As a result, the load within the kyphotic segment is increased. Forward bending moment can be counterbalanced by flexing the knees to improve body posture [74]. This posture decreases the contraction of the posterior spinal muscles; however, the force in the erector spine still remains significantly increased when the wedge deformity of the fractured VB remains uncorrected [26]. A drawback of the knee flexion maneuver is it requires the contraction and tightening of the thigh muscles, resulting in an impaired gait pattern. The risk of hip fractures increases 4.5-fold after a single OVCF and 7.2-fold after two or more OVCFs, [16,86] independently of bone mass density [16], possibly reflecting the impaired gait and increasing the risk of injurious falls [87]. However, the role of residual kyphosis after cement augmentation in increasing the risk for subsequent vertebral fractures is still unclear. In a clinical report the greater the degree of height restoration after vertebroplasty, the higher was the risk for new fractures [88]. Similarly, another study reported that the rate of developing new symptomatic OVCFs after vertebroplasty was inversely correlated with the degree of wedge deformation of treated VBs, therefore with increasing preoperative wedging deformity the risk of developing new symptomatic OVCF decreased [89]. Although one might argue that higher cement volume in the less deformed vertebra may account for the increased rate of developing new fracture, those studies report that risk of new fractures was not related to the volume of cement injected [89].

5. Deformity correction by hyperextension, or by intravertebral balloon inflation

Reduced stiffness in fresh osteoporotic fractures or even in some chronic fracture with progressive collapse or pseudarthrosis can result in increased fracture mobility that can be revealed in dynamic flexion-extension radiographs. In such fractures, spinal extension can at least partially restore vertebral height and kyphosis. Height restoration seen after percutaneous vertebroplasty (PVP) is the result of cementing the fractured vertebra after postural reduction [68,90-93]. The degree of re-expansion has been shown to be inversely related with the time after the onset [90]. However, even in chronic fractures re-expansion is possible especially in cases of progressive vertebral collapse or pseudarthosis. Dynamic fracture mobility has been reported to range between 35% [68] and 68% [91] of fractured VBs. Similarly, the percentage of levels that achieved some degree of correction ranges between 35% [68] to 85% [94,95] or even 92% [93]. Prone position with spinal extension have been reported to improve vertebral kyphosis angle by 3.7 degrees [96] to 8.2 degrees [97], anterior wall height by 19%, and mid vertebral height by 16% [96]. Some authors advocate keeping the patients in the supine position with a soft pillow under the fractured vertebra for 1 to 3 days previous to PVP to enhance postural reduction through adaptation of soft tissues [90].

Inflation of a balloon inside the fractured vertebral body has also been associated with variable results in vertebral height restoration and correction of kyphotic deformity. Significant improvement has been reported to range between 54% [98] and 92% [99] of treated vertebrae. This variation may be influenced by the age of the fracture, the degree of deformity, and other factors. Many authors agree that better chances of correction of both vertebral height and kyphotic deformity can be expected in the more recent fractures [100,101,102]. Phillips et al. [101], in a prospective study of 28 patients with OVCFs, reported that fractures less than 3 months old showed better correction with percutaneous balloon kyphoplasty (PBK). After this initial period, fracture age did not seem to influence the amount of deformity correction achieved with PBK, as long as MRI was consistent with an unhealed fracture [101]. Similarly, Crandall et al. [100] reported

that osteoporotic fractures treated within the initial 10 weeks are more than 5 times as likely to be significantly reducible as compared to fractures older than 4 months. They reported that 20% of chronic fractures and 8% of acute fractures failed to show any vertebral height correction [100]. However, 75% of the chronic fractures were at least partially reducible and kyphosis correction was not statistically different between acute and chronic fractures. Majd et al. [103] reported that in non-healed painful fractures with positive MRI or bone scan treated within 2 days to 2 years from onset, the magnitude of height restoration is not related to fracture age. Other authors [33,96] have also reported no correlation between height restoration and fracture age, or agree that meaningful correction can be achieved even in older fractures when magnetic resonance imaging shows the typical signal changes suggesting incomplete healing [99,102].

There is evidence that inflation of a balloon inside the vertebral body with the technique described for kyphoplasty can achieve additional correction of vertebral deformity compared to postural reduction [96,104]. Voggenreiter et al. [96] reported that in addition to the dynamic, posture-related reduction of deformity, inflation of the balloon achieved a further 50% decrease of vertebral body kyphotic angle and 20% increase of anterior vertebral body height. However, after deflation and removal of the balloon some loss of fracture reduction can be expected [96,105]. Shindle et al. [104] reported that kyphoplasty provided an additional 46.6% restoration of the lost mid vertebral height over the postural correction alone. With operative positioning, 51% of OVCFs had >10% restoration of the central portion of the vertebral body, whereas 91% of fractures improved at least 10% following balloon kyphoplasty. In that study, balloon kyphoplasty enhanced the height reduction >4.5-fold over the positioning maneuver alone and accounted for over 80% of the ultimate reduction. Boszczyk et al. [106] reported that in severe osteoporotic fractures, average correction of the kyphotic angle of was 5% with kyphoplasty, while vertebroplasty failed to achieve correction.

Although correction of the shape of the vertebral body (vertebral kyphosis) appears attractive, some reports failed to reveal any correlation between height restoration of the fractured vertebra and restoration of sagittal alignment of the spine [96,107]. Pradhan et al. [107] reported that the majority of kyphosis

correction by kyphoplasty is limited to the treated vertebra, possibly due to the accommodation of most of the correction by the adjacent discs.

6. Effect of OVCF on the intervertebral disc

In vitro experiments have shown that damage to the vertebral body endplate reduces the pressure in the nucleus of the adjacent disc [52-55]. Maintenance of nucleus hydrostatic pressure has an important role in spinal load transmission, as it allows the annulus to share the physiologic load placed on the spinal segments. Load distribution between the trabecular bone and the cortex is dependent on the properties of the intervertebral discs [108,109]. A significant drop of nucleus pressure after an OVCF forces the annulus to bear axial loads and has been reported to generate peaks of compressive stress in the annulus [52,53,55]. Stress concentrations are affected by posture, and lordosis has been associated with intensified stress in the posterior annulus [53].

This phenomenon is also seen in disc degeneration that reduces the ability of discs to distribute load evenly on the vertebral body, resulting in concentration of load anteriorly in flexion and posteriorly in extension [110]. Using a finite element model, Kurowski and Kubo [108] have demonstrated that a disc with a load bearing nucleus places more load on the trabecular content, whereas a degenerated disc, with no load-bearing nucleus, places most of the load on the cortex. Therefore, disc depressurization after an osteoporotic vertebral fracture has similar effects to disc degeneration on load distribution within the spinal segment. However, the load bearing changes after an osteoporotic vertebral fracture and their effects on the spine have not investigated.

B. Mechanical properties of the intervertebral disc

1. Load transfer properties of the disc

The intervertebral disc is the major load-bearing element in axial compression and flexion. In the young healthy spine, the disc transfers approximately 80% of the compressive load applied to the motion segment [111]. As load is applied to the healthy disc, forces are distributed equally in all directions from within the nucleus, placing the annulus fibers in tension. The collagen fibers of the annulus are well suited to resisting tension. The pressure in the nucleus causes the lamellae of the annulus to bulge outward, stretching the fibers in the annulus. Resistance of the fibers to tensile loading then allows the annulus to contribute to compressive load sharing. Measurements in young, healthy discs using stress profilometry show that most of the disc is under uniform load and, because the stress is equal in the vertical and horizontal directions (isotropic), the nucleus behaves as a fluid [56,112].

Experimental and finite element studies have shown that a compressive load applied to a healthy disc is shared by both the nucleus pulposus and the annulus fibrosus [113]. Adams and McNally [114] showed that when discs are subjected to compressive loading in the neutral posture they generally exhibit a small peak of compressive stress in the posterior annulus and a fairly even compressive stress throughout the nucleus and anterior annulus. In extension, the size of the peak in the posterior annulus increases, while moderately flexed postures usually distribute stresses evenly across the disc. In full flexion, stress peaks appear in the anterior annulus, but are rarely as high as those in the posterior annulus in full extension [114]. Posture also affects the hydrostatic pressure in the nucleus. Under compressive preload of 5,00N, the nucleus pressure is 40% less in 4 degrees of extension than in the neutral posture, reflecting the increased load sharing by the facets in extension [114]. Nucleus pressure rises by 100% in full flexion because flexion stretches the ligaments of the neural arch creating tension that compresses the disc. If the neural arch is removed, the ligamentous tension decreases and the nucleus pressure increases only by 38% in flexion and by 8% in extension [114].

2. Disc degeneration as a model of altered mechanical properties after disc depressurization

Disc degeneration is associated with loss of proteoglycans, and hence loss of hydration, particularly in the nucleus [115]. With disc dehydration and narrowing of the disc space, the nucleus is no longer able to exert a hydrostatic pressure on the annulus, meaning the annular fibers of the disc are no longer subjected to the same tensile stresses, as they would be in a healthy disc with a hydrated nucleus. Instead the annulus in a degenerated disc under compression is more likely to directly bear the axial load from the vertebra above [116].

Disc degeneration can significantly alter the normal load sharing between the components of a functional spinal unit. In vitro studies have shown that in a degenerative disc the nucleus becomes depressurized as a result of the reduction of water content and increased fibrosis [56]. This has been confirmed by in vivo studies that showed that the intradiscal pressure was significantly reduced in a degenerated disc [57], and the decrease was in accordance to the degree of disc degeneration as estimated by magnetic resonance imaging [58]. Nucleus depressurization results in an increasingly larger load transmission trough the annulus, especially in the posterior portion [56]. Furthermore, the principal area of load transmission is highly dependent on posture, with a more prominent increase of stress concentrations in the posterior annulus when the segment is extended [53,57]. With disc degeneration, the posterolateral annulus is no longer acting in its role of a nucleus retaining membrane but rather as a region transmitting compressive stress. This is associated with inward bulging of the inner lamellae [59]. In more advanced stages of degeneration with disc space narrowing, it is possible for the neural arch to stress shield the posterior annulus in extension, so that much of the compressive load is transmitted through the neutral arch and the anterior annulus [53]. The facet joints in a healthy spine normally bear approximately 20% of the load, but when there is a loss of disc height due to degenerative changes facet load bearing can be as high as 70% [60].

C. The preload produced by compressive forces

1. The preload produced by muscles

Loads on the human spine are shared by the osteoligamentous tissues and muscles of the spine. Tensile forces in the paraspinal muscles, which exert a compressive load on the spine, balance the moments created by gravitational and external forces. Since these muscles have a small moment arm from the spinal segment, they amplify the compressive load on the osteoligamentous spine. The preload, produced by muscles, can be considered a compressive load that acts on the spinal segments in vivo during different activities of daily living. The mechanical response of healthy, degenerated or injured spinal segments will be influenced by this preload.

The internal compressive forces on the ligamentous spine have been estimated for different physical tasks using intradiscal pressure and EMG data in conjunction with three-dimensional biomechanical models. The compressive force on the human lumbar spine is estimated to range from 150-300 N during supine and recumbent postures to 1,400 N during relaxed standing with the trunk flexed 30 degrees. The compressive force may be substantially larger when holding a weight in the hands in the static standing posture, and even more so during dynamic lifting. In healthy individuals, the spine sustains these loads without injury or instability [58,111,117].

2. Follower load as a tool to simulate internal compressive forces

The osteoligamentous spine is known to be unstable when subjected to compressive loads. Experiments in which a vertical load was applied at the cephalic end of the thoracolumbar spine specimens caused buckling of the spines at a vertical load of approximately 20 N [118]. Therefore, when a compressive vertical load is applied to a multisegment spine specimen, segmental bending moments and shear forces are induced as a result of the inherent curvatures of the spine. This load application causes large changes in the specimen’s curvatures at relatively small loads.

The concept of follower load has been proposed to apply physiological loads to the spine without inducing additional bending moments or shear forces [119]. Patwardhan et al. [119] showed that the osteoligamentous spine could support a compressive load of physiological magnitude if it were applied along a path that approximated the tangent to the curve of the lumbar spine (**Fig. 1**). Within the follower load path the compressive vector passes through the flexion – extension instantaneous center of rotation of each segment in a given posture of the specimen, thereby minimizing any bending moments and shear forces. This allows a multi-segment thoracic spine specimen to support physiologic compressive preloads without constraining the motion of the vertebrae in the sagittal plane [120].

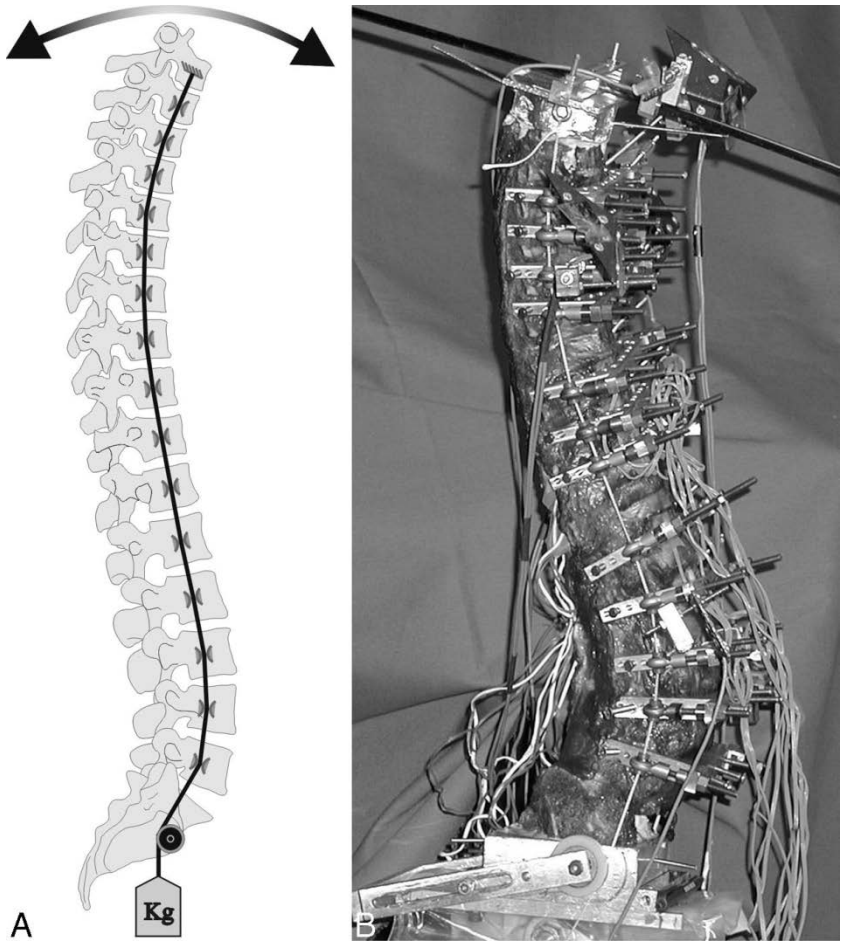

Figure 1. Schematic representation of a thoracolumbar spine specimen subjected to a compressive follower preload and flexion-extension moments. The preload is applied along a path that follows the kypholordotic curve of the thoracolumbar spine. The preload cables are attached bilaterally to the T2 vertebral body, while they pass freely through adjustable guides anchored to each body from T4 to sacrum and are connected to a loading hanger under the specimen. (From Stanley et al Spine 2004 [120])

D. Cement augmentation of osteoporotic vertebral bodies

1. Cement augmentation in the management of OVCFs

Most patients with OVCFs are treated conservatively; however minimally invasive surgical procedures aiming to stabilize a fractured vertebra with the goal of reducing the patient's pain are available. The most commonly used procedures are termed vertebroplasty and kyphoplasty.

Percutaneous Vertebroplasty (PVP) was introduced into the management of osteolytic tumors, and was later successfully applied in the treatment of OVCFs [121-125]. Routine use of the procedure in osteoporosis began in 1995 [126]. PVP involves a percutaneous injection of polymethylmethacrilate (PMMA) cement into the treated vertebral body through a unilateral or bilateral transpedicular or extrapedicular approach [126]. PVP was initially intended to treat pain with no attempt to eliminate spinal deformity. However, mobility in some cases of OVCFs can allow postural reduction of the fractures that can then be stabilized with cement injection by PVP.

Percutaneous balloon kyphoplasty (PBK) was primarily invented for the treatment of osteoporotic vertebral compression fractures (OVCF), when Mark Reiley conceived the idea of using an inflatable balloon to restore height in the OVCF in 1993. The device was approved by the FDA (US Food and Drug Administration) in 1998 [127]. PBK consists of introducing an inflatable bone tamp into the vertebral body to restore vertebral height and kyphotic deformity. The void created after removal of the balloon is filled with cement [127-129].

2. Biomechanical goals of Cement augmentation

The biomechanical goals of cement augmentation are to achieve:

(i) sufficient strength[1] of the VB to prevent progressive collapse,
(ii) sufficient stiffness[2] to prevent instability and painful micromotion

[1] measured by the load needed to cause failure of the vertebral body
[2] the ability to resist compressive deformation

(iii) restoration of physiologic load transfer to prevent subsequent fractures

3. Effects of Augmentation on strength and stiffness of Treated Vertebrae

As osteoporotic vertebrae are at risk of fracture, just restoring pre-fracture strength does not seem a reasonable goal. Attempt to restore the strength to healthy normal values seem more reasonable [130]. Adequate restoration of stiffness limits painful micromotion within the fractured vertebra. Therefore, painful micromotion may persist between fractured trabeculae if cement augmentation results in a significantly decreased stiffness.

Effect of cement volume: The strength and the stiffness of the augmented vertebra increases as a function of the volume of cement injected. As little as 2 mL of cement may restore vertebral strength to its pre-fracture values in all regions of the spine while volumes of 4 mL injected in the thoracic region and 6 mL injected in the lumbar region significantly increase strength [131]. However, as VBs vary considerably in size between regions and spines, restoration of strength may be better correlated to the percentage of the VB filled. Molloy et al. [132] reported that restoration of strength required filling approximately 16% of the VB volume, which corresponds to fill-volumes of 2 mL, 4 mL, and 6 mL for the thoracic, thoracolumbar, and lumbar regions, respectively.

Stiffness is also influenced by the volume of injected cement. Finite element modelling studies have suggested that 14% of vertebral body volume, less than 3 cc of cement in the lumbar spine, is required to restore vertebral compressive stiffness in vertebroplasty, whereas 28% fill (7cc), commonly used in clinical practice, can increase stiffness to almost 50% above the intact value [133]. However, in cadaveric studies [132] it has been reported that restoration of stiffness required approximately 30% of vertebral body volume: 4 mL in the thoracic region and 8 mL in the thoracolumbar region. In the lumbar region, stiffness was not restored even with a cement volume of 8 cc (the maximum volume used in the study). In another study, stiffness restoration was reported to require 4 mL of cement for the thoracic and thoracolumbar spine and 8 cc for the lumbar spine, possibly reflecting the importance of other factors other than

cement volume [131]. In general, existing studies show that larger volumes are needed for stiffness restoration than those required for strength restoration.

Effect of bone mineral density: The increase in strength due to augmentation is inversely related to bone mineral density (BMD) [134-136]. This may be due to the diminished strength of osteoporotic vertebral bodies, but also to the greater degree of filling that can be achieved in osteoporotic vertebrae [134]. In non-osteoporotic, un-fractured vertebrae, cement augmentation does not produce any significant changes in strength [134-136], but as little as 10% fill can result in large increases in compressive strength in osteoporotic lumbar vertebrae [135].

There is debate in the literature concerning whether bone mineral density (BMD) affects the ability of cement augmentation to increase stiffness of vertebral bodies. Heini et al. [134] reported that PMMA injection increased stiffness in osteoporotic vertebrae, but not in normal VBs. The augmentation effect was inversely related to BMD, but as the degree of filling was also inversely related to the BMD, this may reflect differences in the injected volume. Also, in this study vertebral bodies were injected without prior creation of a fracture. Belkoff et al. reported that augmentation of fractured osteoporotic vertebrae did not restore their stiffness to pre-fracture values; [130] although, in a previous study that used both osteoporotic and non-osteoporotic vertebrae, the same authors reported restoration of stiffness [137]. These findings suggest that augmentation of fractured osteoporotic vertebrae can at best restore pre-fracture stiffness; increase in stiffness is unlikely to be achieved.

Similar results have been reported in regards to stiffness of thoracolumbar functional spinal units composed of two adjacent VBs with the intervening disc. Luo et al [138] reported that a vertebral fracture reduced motion segment stiffness in both bending and compression. Specimens with low BMD had more severe fractures, greater changes in stiffness following the fracture, and showed the greatest changes in stiffness following vertebroplasty. However, motion segment stiffness did not exceed pre-fracture values [138].

Effect of cement composition: Cements used for vertebral body augmentation are commonly altered by the addition of various opacifiers to increase visibility, and by increasing the monomer-to-polymer ratio to decrease viscosity, increase working time, and facilitate injection through a cannula [70,139,140]. Such alterations change the cement's mechanical properties.

In an ex vivo biomechanical study Belkoff et al. [141] compared Simplex P (Stryker-Howmedica-Osteonics, Rutherford, NJ, USA) mixed as directed by the manufacturer (10% BaSo4, and monomer-to-polymer powder ratio of 0.56 mL/g) with Simplex P modified as used in vertebroplasty (30% BaSo4, monomer-to-powder ratio of 0.71 mL/g). They reported that fractured vertebrae that were augmented with vertebroplasty using the original Simplex P resulted in significantly greater strength relative to their pre-fracture values, while those repaired with modified Simplex P resulted in significantly greater strength in the thoracic region, and restoration of strength in the lumbar region. Post-augmentation stiffness also depends on cement composition. Fractured vertebral bodies injected with Simplex P bone cement were restored to pre-fracture stiffness levels, while those injected with Cranioplastic bone cement had significantly less stiffness [137]. Furthermore, the material properties of Cranioplastic are diminished when the cement is mixed as typically used in vertebroplasty [142]. Cranioplastic used in vertebroplasty studies resulted in lower vertebral body stiffness values than those in the intact state [62,130,141]. This does not appear to cause concern, as both cements are used clinically and there are no reported complications related to insufficient stiffness restoration.

Effect of the technique of augmentation: In vertebroplasty, bone cement interdigitates into the cancellous bone, infiltrating the space between trabeculae; hence, at the periphery of cement mass, there are spikes of cement anchoring within the trabecular bone. In the balloon kyphoplasty model, a void is created within the VB; a layer of packed trabeculae displaced by balloon inflation surrounds this void. Three different and distinctive zones can theoretically be differentiated within the treated VB: an outer zone of intact bone, an intermediate zone of packed trabeculae and a central zone of cement.

Both vertebroplasty and kyphoplasty can significantly increase the strength of fractured vertebrae to above pre-fracture values. However, in one comparative study the increase was greater after vertebroplasty [143]. In another cadaveric study, it was shown that although fractured VBs treated with kyphoplasty were initially taller that those treated with vertebroplasty they finally became shorter after repetitive cycling loading due to progressive loss of their height. Therefore, the cancellous bone around cement zone is susceptible to further collapse, being the weakest link in the chain of load transmission [Kim 2006]144. In vertebroplasty, cement interdigitation throughout the VB may allow for better load transfer between the upper and lower endplates of the augmented vertebra. It is possible that, even if subsequent collapse is not significant, microfractures at the non-augmented bone might account for relapse of pain after an initially successful augmentation procedure. Furthermore, there is evidence that loss of correction after vertebroplasty is greater for OVCF with clefts [145]. Pseudarthrotic cavity, being possibly less permeable to injected cement, prevents the cement from interdigitating the cancellous bone, leaving an area of non-augmented trabeculae around the cement mass. A re-fracture of an augmented VB has been reported in a clinical series [38]. Therefore, to prevent further collapse of the treated vertebra, an attempt for the widest possible cement distribution within the treated vertebral body seems justified.

Uni-lateral versus bi-lateral cement injection: Most studies show that both bi-pedicular and uni-pedicular cement injections result in significant increase in strength; although the increase is reported to be greater with bi-pedicular injection [62,135]. In a finite element model, a posterolateral approach resulted in a higher stiffness than the bi-pedicular approach for all tested fill volumes [133]. Simulation of uni-pedicular injections resulted in equal or higher stiffness predictions compared with bi-pedicular or posterolateral cases. However, asymmetrical distribution of cement from a uni-pedicular approach resulted in a medial-lateral bending deformation toward the untreated side when uniform compressive load was applied, increasing the risk of collapse on the non-augmented side [133]. However, in a cadaveric study lateral injection of 3.5 mL of cement restored stiffness of fractured vertebra to pre-fracture values, while central injections of the same volume resulted in significantly less stiffness [146]. When a larger amount of

cement was used (7 mL), both central and lateral injections restored initial stiffness [146].

4. Effects of Augmentation on load transfer to the adjacent vertebrae

The ideal cement augmentation of an osteoporotic vertebral fracture should also restore physiologic load transfer. However, the reported rate of new vertebral fractures, especially in the vicinity of the cemented fracture, [29-35] has raised concern about a possible correlation of cement augmentation and increased risk of subsequent vertebral fractures. This concern is further increased from the increasing evidence that subsequent fractures after cement augmentation tend to occur early, within 1 to 3 months in the follow-up period [31,32,34,36-38], and that fractures of vertebrae adjacent to the treated level occur sooner than those of nonadjacent levels [31].

The increased stiffness of the augmented vertebrae has been proposed as a risk factor for adjacent fractures after cement augmentation. Berlemann et al. [147], using an osteoporotic functional spinal unit composed of two VBs and the intervening disc, showed a decrease in the failure strength after cement augmentation in one vertebra. The ultimate failure strength of the functional units treated with injection of cement was 19% lower than in the matched untreated controls, and there was a trend towards lower failure loads with increased filling with cement. However, these specimens were tested without first creating a compression fracture. As mentioned previously, the stiffness of a fractured vertebra after cement injection is generally smaller or at best restored to the intact (pre-fracture) value. Thus, the increased strains in the adjacent vertebrae cannot be attributed to the higher stiffness of the augmented vertebra.

Rigid cement augmentation underneath the endplates has been proposed to act as an upright pillar that reduces the inward bulge of the endplates of the augmented vertebra, resulting in increased nucleus pressure and an increased inward bulge of the adjacent endplate [50,51]. However, as shown in cadaveric studies, even though cement augmentation can increase nucleus pressure, the resultant pressure is still below the level of the pre-fracture condition [54], a finding that contradicts the hypothesis of increased end plate bulge of the

adjacent vertebra. Although stiffness of the augmented vertebra is influenced by cement volume, cement volume has not been shown to correlate with the rate of subsequent fractures in clinical studies [148]. For example, injection of 3-6 ml of PMMA cement per vertebral body in one study resulted in subsequent fracture in 52% of patients [29], while in another study using an average amount of 9 ml resulted in subsequent fractures in 12.4% of patients [36]. Since the majority of subsequent fractures that can be attributed to cement augmentation tend to occur in the first one to three months after the procedure, the difference reported between the two studies is unlikely to be greatly influenced by differences in the follow-up period.

Concerns about the role of intradiscal cement leakage in increasing the risk of adjacent fractures have been raised after a report that in 71.4% of patients, the new fractures were associated with cement leakage into the disc [149]. In that study, VBs adjacent to a disc with cement leakage had a 58% chance of developing a new fracture, compared with 12% of vertebral bodies adjacent to a disc without cement leakage. Similarly, in another study cement leakage into the disc was a significant predictor of new vertebral body fracture after vertebroplasty [148]. However, others failed to reveal any significant relation between cement extravasation into the disc and the occurrence of a new fracture [37,150]. Voormolen et al. [37] reported that although cement leakage to adjacent disc occurred in 30% of treated vertebra, only 7% of the new fractures that occurred adjacent to the treated VB occurred in relation to cement leakage to the adjacent disc space.

5. Effect of kyphosis reduction in the incidence of subsequent fractures.

Some investigators postulate that decreased kyphotic deformity that can be achieved during cement augmentation techniques may actually decrease subsequent fracture risk [151,152,153]. Kasperk et al. [151] reported that at the 6 months follow up, 12.5% of patients who underwent augmentation developed new fractures, as compared to 30% of patients who were treated conservatively. At 12 months follow up, the incidence of new fractures was 17.5% for PBK and 50% for the conservatively treated patients [152]. Regarding the incidence of the adjacent level fractures in that series, at 6 months it was 6% in the kyphoplasty treated

group versus 12% in the conservatively treated patients, and at 12 months was 7.1% for kyphoplasty versus 9.7% for the conservatively treated patients [152]. Furthermore, these two reports [151,152] suggest that most of the new fractures tent to occur within the first six months. Similarly, Komp et al. [153] reported new vertebral fractures in 37% of patients treated with kyphoplasty and 65% of patients treated conservatively, at 6 months. Only 40% of the new fractures after kyphoplasty were at adjacent VBs, while 100% of fractures in the conservatively treated group were adjacent to the old fracture.

III. MATERIALS AND METHODS

Laboratory

The present study was conducted at the Musculoskeletal Biomechanics Laboratory of the department of Orthopaedic Surgery and Rehabilitation of Loyola University, Stritch School of Medicine, IL, USA. The Laboratory is located at the Edward Hines, Jr. VA Hospital Rehabilitation Research and development Center at Maywood Illinois, USA, and is directed by Avinash G. Patwardhan.

Specimens and Experimental Set-Up

Eight fresh frozen human lower thoracic (T7-T11) or thoracolumbar (T10-L2) specimens (age 56-82) were used; each consisting of 5 vertebrae. The specimens were from five females and three males whose ages ranged from 56 to 82 years (average 69 ± 8.5 years). Specimens were radiographically screened to exclude existing osteoporotic fractures, severe intervertebral space narrowing, bridging osteophytes and vertebral metastasis. The specimens were thawed at room temperature (20°C) 24 hours before testing. The paravertebral muscles were dissected, while keeping the discs, ligaments and posterior bony structures intact. The cephalad and caudal vertebrae of each specimen were anchored in cups using bone cement and pins.

The specimen was fixed to the testing apparatus at the caudal end and was free to move at the cephalad end. A moment was applied by controlling the flow of water into bags attached to 50 cm loading arms fixed to the cephalad vertebra (**Fig. 2**). The long moment arm used to apply the moment loading resulted in nearly equal bending moments at each level. A six-axis load cell (Model MC3A-6-250, AMTI Inc., Newton, Massachusetts) was placed under the specimen to measure the applied loads and moments. The apparatus allowed for continuous cycling of the specimen between specified maximum moment endpoints in flexion and extension.

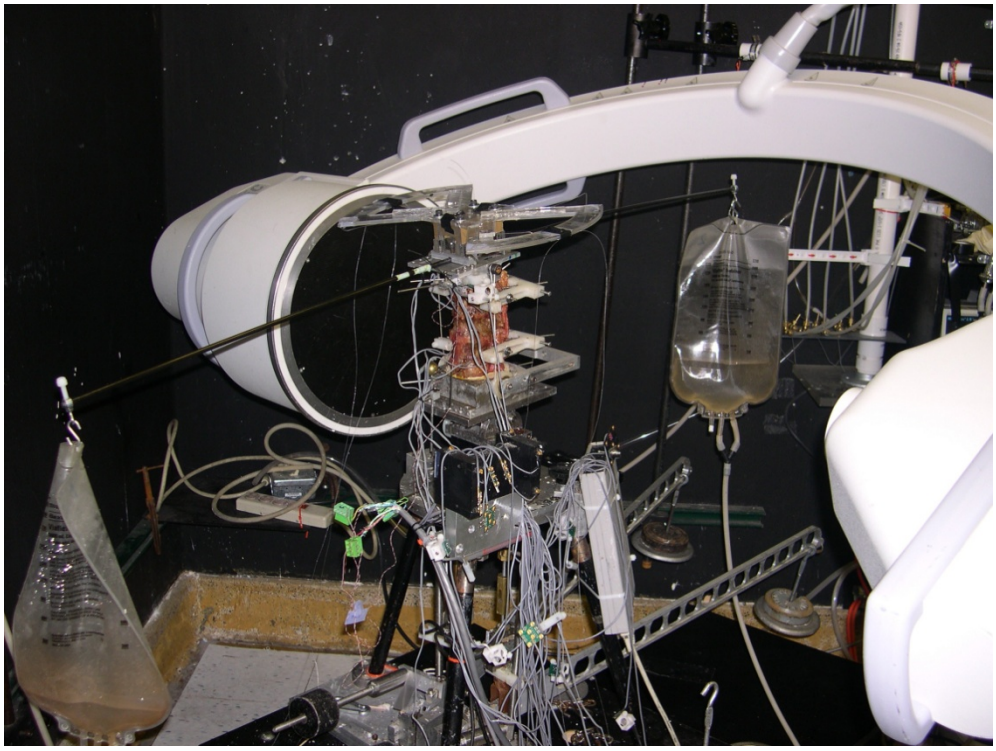

Figure 2. Specimen mounted at the testing apparatus.

Range of motion measurements: The motion of the cephalad vertebra of the specimen relative to the caudal one was measured using an optoelectronic motion measurement system (model 3020, Optotrak; Northen Digital, Waterloo, Ontario, Canada). In addition, biaxial angle sensors (model 902-45; Applied Geomechanics, Santa Cruz, California) were mounted on the cephalad and caudal vertebrae to allow real time feedback for the optimization of the preload path..

Disc pressure measurements: The spines were instrumented with miniature pressure transducers (model 060S-1000, Precision Measurement Co., Ann Arbor, Michigan) in the nucleus of the discs above and below the middle vertebra. These pressure transducers are specifically designed for biological and medical applications where an absolute minimum intrusion volume is required. Their function is based on strain gauge technology (**Fig. 3**). They were calibrated prior to the testing of each specimen using a pressure chamber.

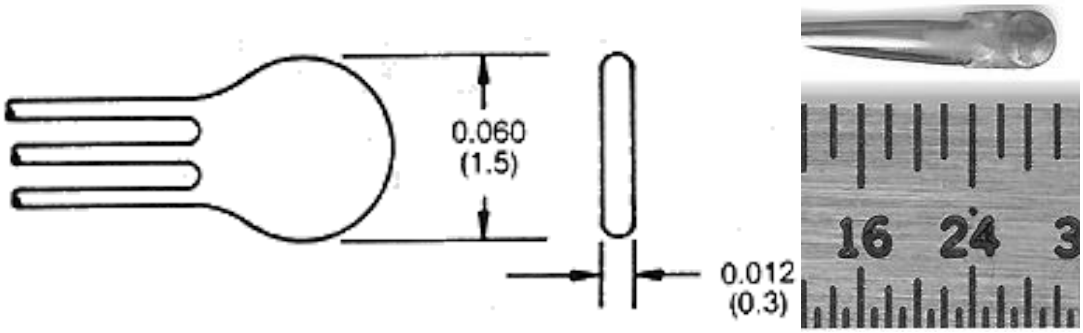

Figure 3. Miniature pressure sensor (1.5 X 0.3 mm). The transducer utilizes a 350-ohm foil strain gauge attached to a stable substrate. It is furnished with a 3-conductor stranded copper lead wire.

Strain measurement: The anterior wall of the vertebral bodies adjacent to the middle vertebra were instrumented with single element strain gauges (FLA-2-11-3L, Sokki Kenkyujo, Tokio) to measure vertical (compressive) strain (**Fig. 4, 5**).

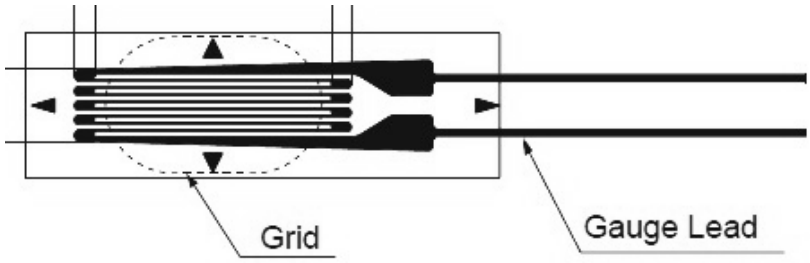

Figure 4. Single element strain gauge. Tension causes the electrical resistance of the grid to increase, while compression causes resistance decrease. Resistance is measured between gauge leads.

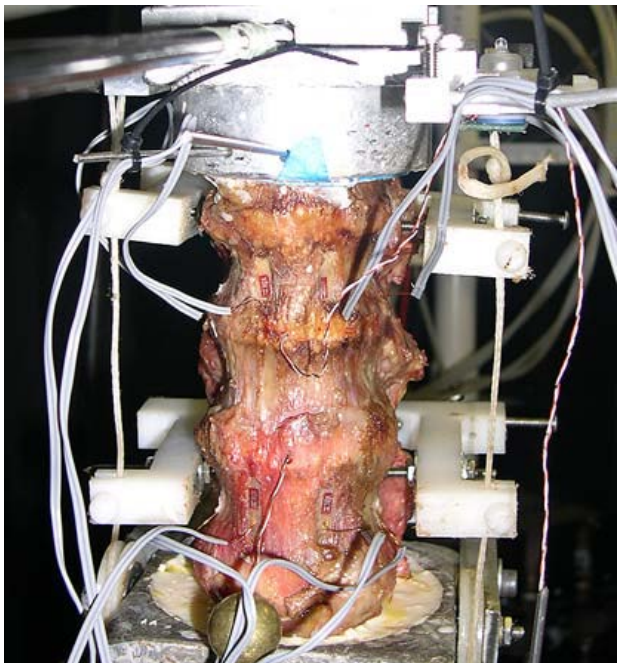

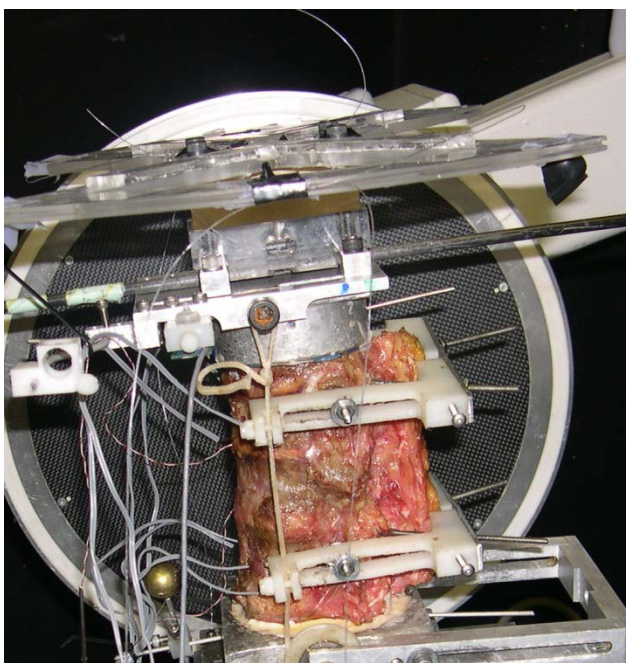

Figure 5. Photograph of a specimen positioned on the testing apparatus. Strain gauges are mounted at the anterior walls and pressure sensors in the discs. Bilateral loading cables pass through guides mounted at the posterior elements

Strain measures the deformation of an elastic material caused by the application of an external force. Compressive strain is the strain that appears due to the application of compressive force. In compressive force, there is a decrease in the dimension of the body. The ratio of the decrease in the length of the body to the original length is called compressive strain.

A strain gauge (**Fig. 4**) is a device used to measure strain. Its function is based on the principle that the electric resistance of a metal changes proportionally to the mechanical deformation caused by an external force applied to it. If a strip of conductive metal is stretched, it will become skinnier and longer, both changes resulting in an increase of electrical resistance. Conversely, if placed under compressive force (without buckling), it will broaden and shorten and its resistance will decrease. If these stresses are kept within the elastic limit of the metal strip, the strip can be used as a measuring element for physical force, the amount of applied force inferred from measuring its resistance. Normally, this resistance change is very small and requires a Wheatstone bridge circuit to convert the small resistance change to a more easily measured voltage change (**Fig. 6**).

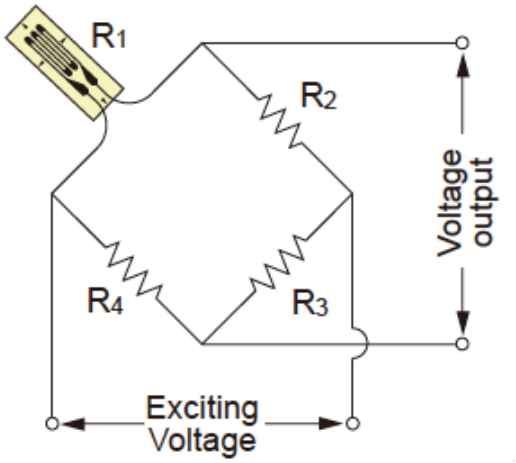

Figure 6. The single element strain gauges used to measure anterior cortical strain is connected in a quarter bridge (Wheatstone bridge) configuration. An instrument called a strainmeter configures the Wheatstone bridge and supplies exciting voltage. Voltage output varies according to compressive strain changes to the gauge.

Application of preload: The concept of the follower load was used to apply compressive preload to the specimens [119]. The compressive preload was applied along a path that followed the curve of the spine. By applying a compressive load along the follower load path the segmental bending moments and shear forces due to the preload application are minimized [154]. This allows a multi-segment thoracic spine specimen to support physiologic compressive preloads without constraining the motion of the vertebrae in the sagittal plane [120]. The preload was applied using bilateral loading cables that were attached to the cup holding the cephalad vertebra. The cables passed freely through guides anchored to the vertebrae adjacent to the target vertebra (**Fig. 5**). To avoid the creation of stress risers, the cable guide mounting technique did not violate the cortices of the vertebral bodies adjacent to the target vertebra. The loading cables were connected to loading actuators under the specimen. The cable guide mounts allowed anterior-posterior adjustments of the follower load path. The alignment of the preload path was optimized by adjusting the cable guide locations to minimize changes in the sagittal alignment of the specimen when compressive load up to 400 N was applied. The cables were coated with

radiopaque barium solution to be visible on x-ray images. A calibration marker (a radiopaque ball, 25.4 mm in diameter) was visible on each x-ray image.

Experimental Protocol

Each specimen was first tested intact under flexion-extension moments (±6Nm) with a 400N compressive preload. Pressure was recorded at the discs above and below the middle vertebra and compressive strain was recorded at the anterior wall of the adjacent vertebrae. Total range of motion (ROM) was measured using the optoelectronic motion measurement system.

Experimental Creation of OVCF:

A novel technique was utilized to selectively fracture only one of the endplates of the middle VB of each specimen. Through a small opening on the

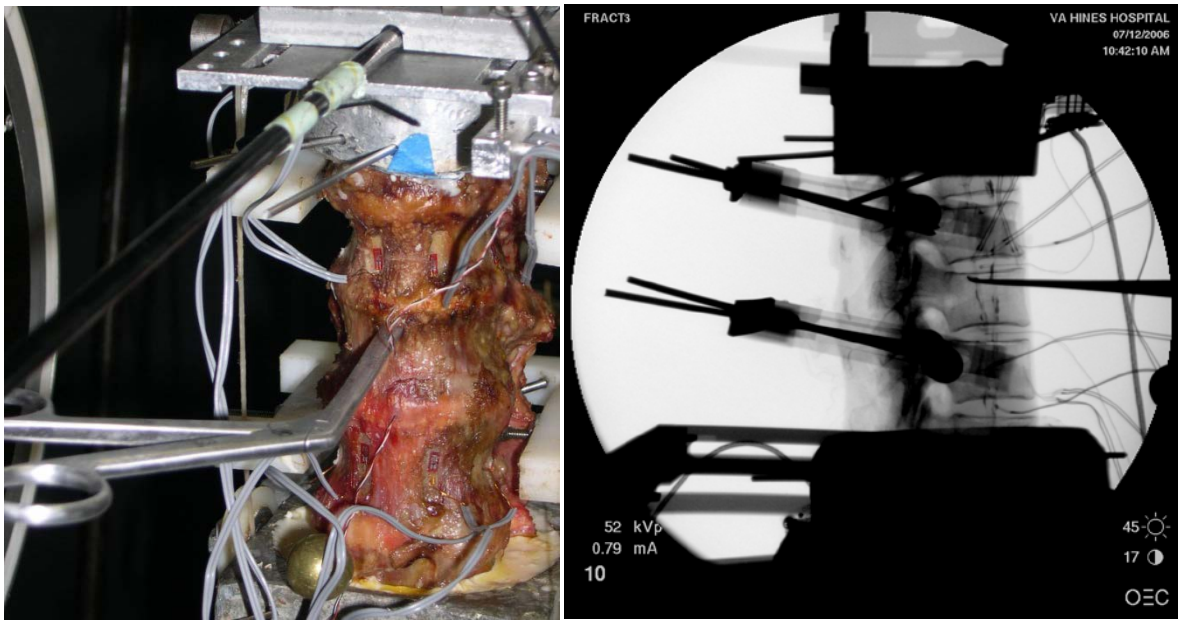

anterior wall close to the target endplate, a void was created selectively under the endplate and was extended to one-third of the VB trabecular content; thereby creating a “stress-riser”. The endplate was carefully scraped free of trabecular connections using curettes and pituitaries (**Fig. 7**). The void was randomly assigned under the upper endplate in four specimens and under the lower endplate in four. The specimen was flexed to 5 Nm and compressed using the loading cables until a fracture under the target endplate was observed on fluoroscopy or until a load limit of 700 N was reached (**Fig. 8**). The maximum load limit of 700 N was used to avoid the likelihood of failure of the other endplate or other that the target vertebra; as this load magnitude is significantly less than the failure load reported in the literature [131,136,155]. If no fracture was observed on fluoroscopy, the instruments were reintroduced, the void was extended, and the specimen was again loaded in flexion and compression. After the fracture was established, the specimen remained under a physiologic compressive preload of 150 N. This value of compressive preload was selected taking into account the reported range of compressive preload on the lumbar spine in the prone position [58].

Figure 7. A) A pituitary is used to create a void in the upper half of the 3rd VB through a small anterior opening. B) A curette used under fluoroscopy for the same reason.

Figure 8. Digital fluoroscopy images of a specimen. A) Intact specimen. The

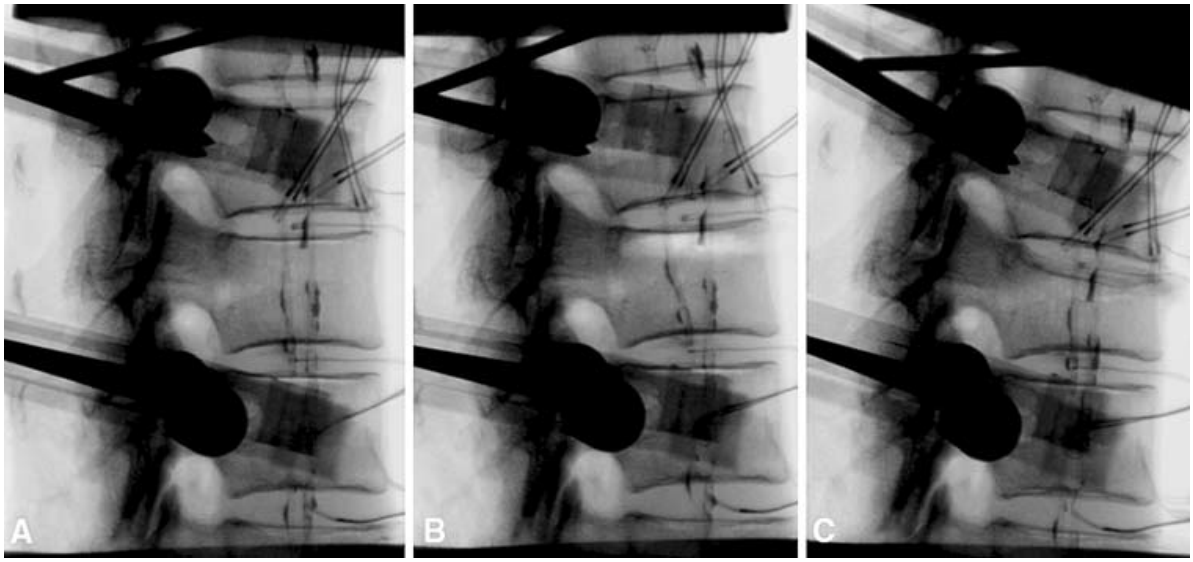

bilateral loading cables, coated with radiopaque barium solution, are visible on the X-ray images. B) Radiographic appearance of the void created under the upper endplate of the middle vertebra. C) Image of the wedge fracture affecting only the upper part of the index vertebra.

Reduction of the Vertebral Kyphotic Deformity Using Spinal Extension:

The fracture was reduced by applying extension moment to the specimen under 150 N preload, aiming to completely restore the pre-fracture anterior wall height and therefore correct the vertebral kyphosis angle (**Fig. 9A**). The extension was applied using upward force on the anterior loading arm fixed to the uppermost vertebra. After stabilization of the reduced fracture by cement injection into the void through the anterior opening, (**Fig. 9b**), the rest of the trabecular content in the middle VB was evacuated through a separate small anterior opening. The undamaged endplate was carefully scraped free of trabecular connections, and the rest of the VB was completely filled with cement under fluoroscopy to ensure proper cement distribution (**Fig. 9c**). Careful abrasion of both endplates ensured similar cement distribution near them. The specimen was then retested in flexion-extension (± 6 Nm) under 400 N preload, and

measurements of pressures at the discs adjacent to the middle vertebra and anterior wall compressive strains at the adjacent vertebrae were recorded.

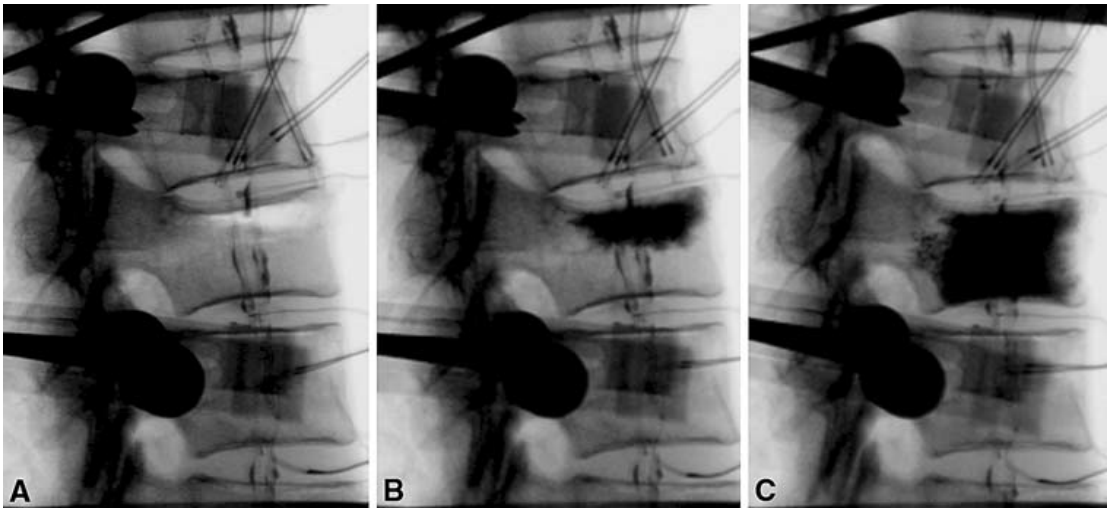

Figure 9. Digital fluoroscopy images of a specimen A) Reduction of anterior wall height and vertebral kyphosis angle with extension of the specimen while under 150 N preload. B) Cement augmentation of the fracture. C) Image showing the uniform distribution of cement under both endplates after careful abrasion of the un-fractured endplate.

Experimental Creation of Subsequent Fractures:

As a final step, the specimen was placed in flexion to 5 Nm and loaded in compression using the bilateral loading cables connected to actuators. The compressive load was gradually increased from 0 to 3,000 N or until a subsequent fracture was observed on fluoroscopy with a simultaneous sudden drop in the force versus time curve of the actuators.

Data Analysis

The heights at the anterior wall and mid vertebral portion, as well as the vertebral kyphosis angle of the index vertebra were measured in the intact status, after the index fracture and after the reduction and augmentation. Mid vertebral height was measured using the depressed central endplate. Vertebral kyphosis angle was measured between the two end plates of the index vertebra. Measurements were performed on digital fluoroscopy images using computer software (Image Pro Plus, Media Cybernetics Inc). Flexion range of motion of the

specimen was calculated as the angular change of the apical vertebra relative to the caudal one from the neutral posture to 6 Nm flexion. The force to failure for the index and the subsequent fractures was defined as the peak point of the force versus time curve. The strain gauges used to measure anterior cortical strain were single element gauges and were connected in a quarter bridge (referring to Wheatstone bridge) configuration (**Fig. 6**). In addition, the pressure sensors used to measure intervertebral disc pressure (model 060S) were quarter bridge diaphragm transducers. Strain gauges and transducers connected in a quarter bridge configuration are not capable of temperature compensation. These devices cannot be trusted to give absolute measurements since the output of the quarter bridge is a combination of thermal drift and measured value. Therefore, the disc pressure and adjacent vertebral wall compressive strain were normalized so that values in neutral position under 400 N preload were taken to zero, to compensate for thermal-drifting of sensors. As a result, the change in pressure and strain from neutral to full flexion before and after the creation and augmentation of the index fracture were used for analysis. Two specimens were excluded from pressure and strain analyses because of anterior slippage of pressure sensors during the experiment that resulted in inaccurate pressure recordings. The data were analysed using repeated measures analysis of variance (ANOVA) with a significance level of a = 0.05 using the commercial statistics package SPSS (SPSS Inc., Chicago, IL).

IV. RESULTS

Morphometric values

In the intact specimens, vertebral kyphosis at the middle vertebra was 8.5 ±2.2 degrees, anterior wall height was 21.2 ± 2.7 mm, and mid vertebral height was 20.1 ± 2.9 mm (Table 1). An average of 540 ± 150N compressive load was required to fracture the target endplate of the index vertebra. No radiographic evidence of fractures at the non-target endplate or adjacent vertebral bodies was observed in any of the specimens. After the index fracture, vertebral kyphosis was 12.6 ± 2.4, anterior wall height was 17.2 ± 3.1 mm and mid vertebral height was 14.3 ± 3.3 mm. A mean 4.6 ± 0.8 Nm extension moment, under 150 N preload, was sufficient to restore the kyphosis angle of the index vertebra to its intact value (8.8 ± 1.6 degrees, $p=0.38$). The anterior wall height was restored to 20.8 ± 2.6 degrees, and the difference from the intact value, although statistically significant ($p=0.04$), was small. Mid vertebral height remained significantly lower compared to intact (16.4 ± 3.0 mm, $p<0.01$). Total flexion ROM of the specimens increased from 4.7 ± 1.4 in the intact to 6.1 ± 2.4 degrees after augmentation of the middle VB fracture. This increase was statistically significant ($p<0.05$).

Table 1. Morphometric values of the middle vertebra of the specimens measured in the intact state, after the experimentally created fracture and after reduction of the fracture and augmentation of the vertebra with bone cement. Flexion range of motion (ROM) refers to the angular displacement of the specimen after application of 5 Nm flexion moment under 400 N preload

	Intact	Fractured VB	Reduced and cemented Fx
Vertebral Kyphosis (deg)	8.5±2.2	12.6 ± 2.4	8.8±1.6
Anterior Height (mm)	21.2±2.7	17.2 ± 3.1	20.8±2.6
Mid VB Height (mm)	20.1±2.9	14.3 ± 3.3	16.4±3.0
Flexion ROM (deg)	4.7 ±1.4	-	6.1 ±2.4

Pressure values

In the intact specimen, the pressure in the disc adjacent to the endplate assigned to remain un-fractured was 1.21 ± 1.82 MPa in the neutral posture under 400 N preload. Application of 6 Nm flexion moment increased disc pressure by 0.14 ± 0.11 MPa, representing an increase of 27.19 ± 17.4% from the pressure value in the neutral posture. After augmentation of the index fracture, the disc pressure in the neutral posture under 400 N preload was 1.34 ± 1.55 MPa. Application of 6 Nm flexion moment increased disc pressure by 0.13 ± 0.10 MPa, representing an increase of 15.8 ± 10.1% from the value in the neutral posture. The pressure change due to a flexion moment in the disc with undamaged endplates was not affected by the augmentation of the index fracture ($p = 0.55$). The disc pressure in the intact specimen adjacent to the endplate to be fractured was 0.51 ± 0.25 MPa in the neutral posture under preload. Application of 6 Nm flexion moment increased the pressure by 0.14 ± 0.10 MPa, representing an increase of 26.3 ± 9.5% from the pressure value in the neutral posture. After augmentation of the index fracture, the disc pressure at that level was 0.43 ± 0.13 MPa in the neutral posture under 400 N preload. Application of 6 Nm flexion decreased disc pressure by 0.07 ± 0.14 MPa, representing a decrease of 19.0 ±

26.8% from the value in the neutral posture (**Fig. 10**). The pressure change due to the application of the flexion moment in the disc with fractured endplate was significantly different from the intact (p = 0.02).

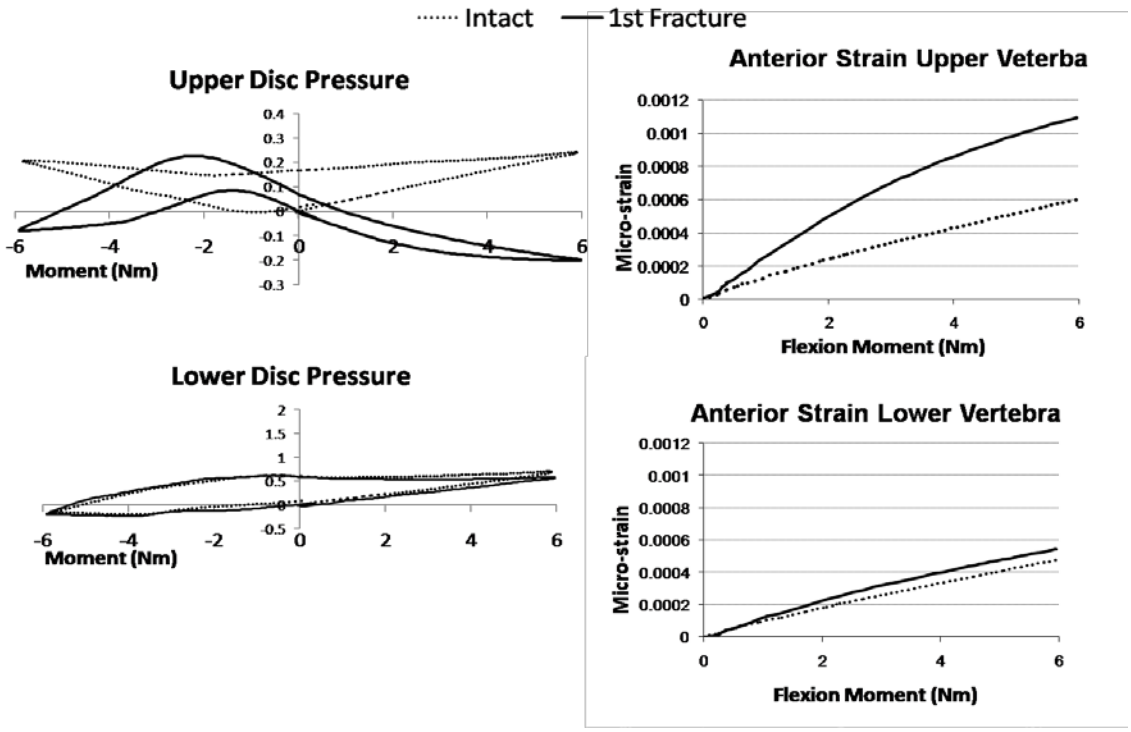

Figure 10. Graphs showing the changes in the disc pressure (MPa) and anterior wall strain of the adjacent VBs (microstrain) after the selective damage to the upper endplate of the specimen shown in Figs. 4 and 5. Data were collected during flexion-extension runs, under 400 N preload. Pressure and strain values were normalized so that values in neutral position under 400 N preload were taken to zero.

Strain values

In the intact specimen, the compressive strain at the anterior wall of the VB adjacent to the endplate assigned to remain unfractured increased by 447.8 ± 100.4 microstrain due to the application of 6 Nm flexion moment as compared to the strain value in the neutral posture. After augmentation of the index fracture, the strain increased by 522.6 ± 131.5 microstrain from the neutral posture to 6 Nm

flexion. (Fig. 6). This difference represents a nonsignificant change of 18.2 ± 7.1% in the anterior wall compressive strain of the adjacent vertebra next to the unfractured endplate, before and after the index fracture ($p > 0.05$). The strain at the anterior wall of the VB of the intact specimen adjacent to the endplate assigned for the index fracture increased by 413.2 ± 232.4 microstrain from the neutral posture to 6 Nm flexion. After augmentation of the index fracture, the strain increased by 836.2 ± 499.2 microstrain from the neutral posture to 6 Nm flexion. This difference represents a 94.2 ± 22.8% increase in the compressive strain of the anterior wall of the adjacent vertebra next to the damaged endplate, before and after the index fracture ($p < 0.05$). The maximum strain values seen in this study at 6 Nm of flexion were below 0.08% in all cases.

Subsequent Fractures

Subsequent compressive loading of the specimens in 5 Nm flexion resulted in a fracture of the adjacent VB close to the fractured endplate in six specimens and in a distal fracture at the uppermost VB in one specimen (Table 2). Maximum load applied with the actuators failed to create a fracture in one of the specimens. The fractures of the adjacent vertebrae began as a depression in the anterior portion of the endplate (**Fig. 10**) that became gradually deeper as loading continued until the anterior wall finally failed. The failure load for the adjacent fractures was 1450 ± 402 N.

Table 2. Location of Subsequent Fractures in Correlation to the Damaged Endplate of the Index Vertebra.

Specimen	Endplate Fx	Subsequent Fx
1	lower	no fracture
2	upper	upper adjacent
3	lower	non adjacent
4	lower	lower adjacent
5	upper	upper adjacent
6	upper	upper adjacent
7	lower	lower adjacent

8	upper	upper adjacent

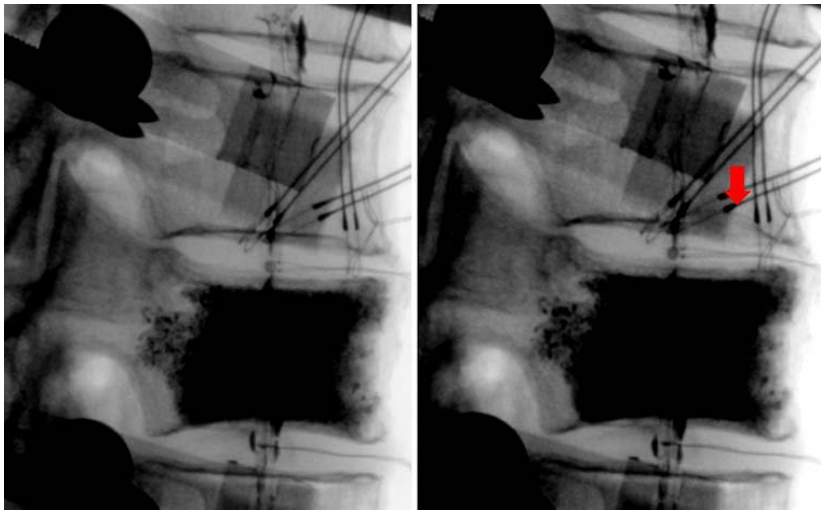

Figure 11. Digital fluoroscopy images of the specimen shown in Figs. 4 and 5 showing the initiation of a subsequent fracture at the anterior portion of the lower endplate of the upper adjacent vertebra (arrow), next to the damaged endplate of the index vertebra.

V. DISCUSSION

This biomechanical study focused on the role of the endplate deformity after a fracture as a risk factor for subsequent adjacent vertebral fractures. Cement was used only to stabilize the fracture and allow subsequent testing. The cementation technique used in this experiment is not relevant to any technique used in clinical practice. Because of the concerns existing in the literature about the presence of cement in the augmented vertebrae and how it may change their load bearing properties [50,51,147], both the endplates were carefully scraped free of any trabecular connections to ensure similar cement distribution underneath them. Therefore, any possible effect of cement presence under the endplates was a common denominator. Furthermore, restoration of the vertebral kyphosis angle by restoring the pre-fracture anterior wall height eliminated residual kyphosis as a risk factor for adjacent fractures leaving the endplate disruption as the only causal variable for the observed effects.

Experimental creation of a vertebral compression fracture is associated with uncertainty in both fracture pattern and location. Centrum defects have been previously used to assist in reproducing osteoporotic fractures in a target vertebra [28,84,156]. The fracture model used in the current study allowed creating a predictable fracture not only at a target vertebra but more specifically under the target endplate. The morphology of the fracture could also be controlled. The fracture began as depression of the weakened endplate. As the compressive load was increased, the anterior wall failed and the fracture progressed to a wedge shaped while sparing the non-weakened endplate. In the current study, compressive loading was continued until the anterior wall height was reduced by approximately 25%.

Both in vivo [58,117] and in vitro [54] studies have shown that in the intervertebral disc, the greatest pressures are exhibited in the forward flexed position under compression in activities such as lifting. The present study agrees with these findings. Furthermore, previous in vitro studies have documented that nuclear pressure is substantially reduced after an osteoporotic vertebral fracture [52,54,138,157] as more space becomes available for the nucleus. Findings from the current study indicate a more specific impairment in the mechanical properties

of the disc after endplate depression. The nucleus pressure is further decreased during flexion as compared to the already decreased value in the neutral posture reported in the literature. This abnormal mechanical behavior was accompanied with a simultaneous increase of the anterior wall compressive strain of the juxtaposed adjacent vertebra, which nearly doubled in flexion compared to the compressive stain in the intact status. On the contrary, the mechanical behavior of the undamaged disc of the fractured vertebra was not significantly affected and the compressive strain of the juxtaposed vertebral body was also not significantly altered. Previous investigators showed that anterior wall strain of adjacent vertebrae is increased with compressive load, but is more dramatically affected by flexion than by axial compression [27,28,158-161]. Therefore, we can speculate that the small strain increase in the VB adjacent to the intact endplate found in this study could be explained by the increased flexion ROM that was observed after the fracture.

Cement augmentation using different surgical techniques, has been reported to only partially restore nucleus pressure, and the resultant pressure does not reach the pre-fracture condition [54,157]. Our findings that after endplate fracture disc pressure is decreased during flexion as compared to the neutral posture are in contrast to previous experimental findings. Ananthakrishnan et al. [54] reported slightly higher disc pressure in flexion compared to the neutral position under axial compression after vertebroplasty for a VCF. In that study, pressure after vertebroplasty for an experimentally created vertebral fracture increased from 674 ± 111 kPa in the neutral posture under preload to 769 ± 165 kPa in the flexed position. This may suggest that the extension maneuver used in the present study to correct the vertebral kyphosis angle may have a detrimental effect on load transfer. Spinal extension exerts a ligamentotaxis effect through the anterior longitudinal ligament and annulus on the periphery of the fractured VB. Lacking tensile properties, the nucleus cannot exert a ligamentotaxis effect on the central part of the endplate, therefore central depression remains even after complete anterior wall reduction. In our study, disarticulation of the index vertebra at the end of the experiment revealed severe central depression of the endplate despite anterior height restoration in all of our specimens (**Fig. 11**). In this context, elevation of the periphery of the endplate by spinal extension may enhance the

relative central depression, leading to further compromise of nucleus mechanics. Clinical reports indicated that a greater degree of height restoration after vertebroplasty was associated with higher risk for new fractures [88,162]. Similarly, another study reported that the rate of developing new symptomatic OVCFs after vertebroplasty was inversely correlated with the degree of wedge deformity of cemented vertebrae [89]. Although one might argue that higher cement volume in the less deformed vertebra may account for the increased rate of developing new fracture, those studies report that the risk of new fractures was not related to the volume of cement injected [89,162]. Further clinical and biomechanical investigations are needed before reaching a definite conclusion.

Figure 12. Photograph of a disarticulated middle vertebra at the end of the experiment showing severe central depression of the endplate despite anterior wall height restoration and kyphosis correction.

It has been proposed that adjacent level load transfer through the vertebral centrum can be measured through adjacent disc pressure, while transfer through the vertebral shell can be measured through vertebral wall strain [28,54]. Strain gauges bonded to the bone have been widely used to detect cortical bone

deformation from load application. Surface strain distribution in the lumbar vertebrae measured by strain gauges has been shown to be directly proportional to compressive load [161]. Strain distribution, measured by surface strain gauges, has also been used as an indicator of the region where vertebral burst fracture initiates [158]. Similarly, stress concentration on the anterior cortex has been used to predict adjacent fracture risk after an osteoporotic compression fracture [27,28]. Therefore, the findings from the current study support the hypothesis that endplate depression after fracture leads to significant reduction of load transfer through the centrum and increases adjacent level cortical strain, compensating for a lack of centrum support. The anterior shift of the load transfer path in flexion results in excessive load concentration in the anterior portion of the vertebra. After loading the cemented specimens to failure, nearly all subsequent fractures were located at the vertebra next to the damaged endplate. The fractures started as a depression of the anterior portion of the endplate close to the anterior wall, which subsequently led to anterior wall collapse as loading continued.

Among spontaneous osteoporotic fractures, isolated superior endplate fractures are substantially more common than isolated inferior endplate fractures. A clinical study has reported that isolated inferior endplate fractures were more commonly seen at subsequent fractures next to cemented vertebral bodies. It has been suggested that this localization implicates the cement as causative factor of the adjacent fractures, as the fractures occur immediately above the cemented vertebral body [32]. However, we observed this location of adjacent fractures only in cases with a damaged upper endplate of the cemented vertebra. Our findings suggest that endplate deformity, and not cement augmentation per se, is the reason for this atypical fracture localization.

The temporal clustering of subsequent fractures after cement augmentation in the first 2 to 3 months after the procedure has been proposed as an indication of increased risk after cement injection. However, a similar temporal clustering of incident fractures within 8 months of diagnosis of a prevalent fracture has been described in the natural history of un-cemented OVCFs [43]. Although there is a discrepancy between the high risk periods for subsequent fractures, the non augmented OVCFs have the additional risk of progressive collapse in the early

follow-up period. The results from the current study support the hypothesis that alterations in load transfer after the prevalent fracture may predispose the fractured VB to progressive collapse. When the fracture is augmented or adequately healed, the strength of the vertebral body is significantly increased, and alterations in load transfer constitute a threat to the adjacent vertebrae.

In vivo studies have reported that patients with degenerative discs have reduced nuclear pressure in all positions [58]. According to the hypothesis of the current study, those patients should also be at risk for osteoporotic vertebral fractures. This has been supported by a report that disc space narrowing is associated with an increased risk of vertebral fractures despite the higher BMD associated with spine osteoarthritis [163].

VI. CONCLUSIONS SUGGESTIONS

This study suggests that endplate depression after an osteoporotic vertebral fracture impairs the ability of the disc to distribute load evenly to the adjacent segments. Load shifts to the anterior portion of the adjacent vertebrae as flexion increases while simultaneously the disc nucleons pressure declines. This concentration of load may contribute to increased subsequent fracture risk after an osteoporotic vertebral fracture. The altered mechanical behavior of the nucleus can be ascribed to the increased available space after the endplate depression. Biomechanical studies have shown that extension moments can increase the anterior wall height and reduce vertebral kyphosis; however, the middle height of the fractured vertebra cannot be significantly corrected [84].

Current vertebral augmentation procedures for the treatment of osteoporotic VCFs have focused on the reduction of kyphosis angle and restoration of anterior vertebral body height with postural reduction or with the use of inflatable bone tamps [104,164,165]. The current study suggests that in addition to restoring spinal sagittal alignment, the ability to reduce the entire fractured endplate is important to restore load transmission across the fractured level. Based on these data, cement augmentation techniques should aim to end-plate reduction as an important maneuver during the procedure. In cases of anterior height restoration by spinal extension maneuver, one may consider prophylactic augmentation of the adjacent fracture in cases where severe endplate depression still remains.

Εκτενής Ελληνική αναφορά

Η μηχανική ανεπάρκεια του μεσοσπονδυλίου δίσκου μετά από κάταγμα της τελικής πλάκας ως παράγοντας κινδύνου για παρακείμενα σπονδυλικά κατάγματα.

Εισαγωγή

Η παρουσία ενός οστεοπορωτικού σπονδυλικού κατάγματος αυξάνει τον κίνδυνο εμφάνισης νέων σπονδυλικών καταγμάτων [13-17]. Η κυφωτική παραμόρφωση που προκύπτει από την κατάρρευση του σπονδυλικού σώματος έχει συσχετιστεί με τον κίνδυνο δημιουργίας νέων καταγμάτων [7,16,23,24]. Η κύφωση μετατοπίζει το κέντρο βάρους του σώματος προς τα εμπρός με αποτέλεσμα την αύξηση της ροπής των καμπτικών δυνάμεων, που με τη σειρά τους αντιρροπούνται από τη σύσπαση των οπίσθιων σπονδυλικών μυών με αποτέλεσμα την αύξηση του συμπιεστικού φορτίου στο κυφωτικό τμήμα [25,26]. Μελέτες σε πτωματικά παρασκευάσματα έχουν δείξει ότι η κύφωση μετά από σφηνοειδή κατάγματα αυξάνει το συμπιεστική καταπόνηση στον πρόσθιο φλοιό των παρακείμενων του κατάγματος σπονδύλων κατά την κάμψη [27,28].

Ο μεσοσπονδύλιος δίσκος κατέχει ένα σημαντικό ρόλο στη μεταφορά του φορτίου στη σπονδυλική στήλη και ο ρόλος του στη παθογένεση των παρακείμενων σπονδυλικών καταγμάτων δεν είναι επαρκώς κατανοητός. Ο υγιής δίσκος μεταφέρει με ομαλό τρόπο τα φορτία στα παρακείμενα σπονδυλικά σώματα, κυρίως λόγω των ιδιοτήτων του πηκτοειδούς πυρήνα [44].

Αλλαγές στις μηχανικές ιδιότητες του δίσκου αναμένεται να διαταράξουν της φυσιολογική μεταφορά φορτίου σε παρακείμενους σπονδύλους. Εργαστηριακά δεδομένα δείχνουν ότι η βλάβη στην τελική πλάκα του σπονδυλικού σώματος μειώνει την υδροστατική πίεση στον παρακείμενο μεσοσπονδύλιο δίσκο [52-55] και αυξάνει τα συμπιεστικά φορτία στο δακτύλιο [52,53,55], ανακατανέμοντας με τον τρόπο αυτό τα φορτία προς την περιφέρεια του σπονδυλικού σώματος. Η καταπόνηση επηρεάζεται επιπλέον από την κάμψη [53].

Ερευνητικό ερώτημα:

Ο σκοπός της εμβιομηχανικής αυτής εργασίας ήταν να ελέγξει την υπόθεση ότι η αλλαγή στις μηχανικές ιδιότητες του μεσοσπονδύλιου δίσκου μετά από κάταγμα της παρακείμενης τελικής, ακόμη και επί απουσίας κυφωτικής παραμόρφωσης, θα αλλάξει την μεταφορά των φορτίων στους παρακείμενους

σπονδύλους και θα αυξήσει την κάθετη συμπίεση του πρόσθιου τοιχώματος, προδιαθέτοντας σε σφηνοειδές κάταγμα.

Υλικό και Μέθοδος

Εργαστήριο: Η μελέτη πραγματοποιήθηκε στο εργαστήριο εμβιομηχανικής μυοσκελετικού συστήματος που στεγάζεται στο Edward Hines, Jr. VA Hospital Maywood Illinois, USA και συνεργάζεται με το Loyola University, Stritch School of Medicine, IL, USA.

Παρασκευάσματα και προετοιμασία: Χρησιμοποιήθηκαν οκτώ ανθρώπινα φρέσκα κατεψυγμένα κατώτερα θωρακικά (Θ7-Θ11) ή θωρακοοσφυϊκά (Θ10-Ο2) παρασκευάσματα. Το κάθε ένα αποτελούνταν από πέντε σπονδύλους. Τα παρασκευάσματα προερχόταν από πέντε γυναίκες και τρεις άνδρες ηλικίας από 56 έως 82 ετών (μέση 69 ± 8,5 έτη). Όλα ελέγχθηκαν ακτινολογικά για να αποκλειστεί η παρουσία καταγμάτων ή άλλης οστικής παθολογικής διεργασίας όπως μεταστατικών εστιών, ή σοβαρής εκφύλισης των μεσοσπονδύλιων δίσκων με οστεόφυτα που γεφυρώνουν τα σπονδυλικά σώματα. Τα παρασκευάσματα αφέθηκαν να ξεπαγώσουν σε θερμοκρασία δωματίου (20 C) για 24 ώρες πριν τη χρήση τους. Καθαρίστηκαν από τους μαλακούς ιστούς, δίνοντας προσοχή στην διατήρηση δίσκων και συνδέσμων και τυλίχτηκαν με βρεγμένο απορροφητικό χαρτί για την πρόληψη αφυδάτωσης των ιστών.

Ο ανώτερος και ο κατώτερος σπόνδυλος κάθε παρασκευάσματος τοποθετήθηκαν μέσα σε μεταλλικά κυπέλλια και στερεώθηκαν με βελόνες Kirschner και ακρυλικό οστικό τσιμέντο. Το παρασκεύασμα, μέσω του κατώτερου κυπέλλιου, στερεώθηκε σταθερά στο μηχανισμό εφαρμογής των φορτίων, ενώ το άνω άκρο του μπορούσε να κινείται ελεύθερα. Στο άνω κυπέλλιο προσαρμόστηκε μία μεταλλική ράβδος 50 εκατοστών, στα άκρα της οποίας κρεμόταν δύο πλαστικοί σάκοι που μπορούσαν να γεμίζουν με νερό από αντλίες υπό τον έλεγχο υπολογιστή. Μέσω της ράβδου μπορούσε να ασκηθεί ροπή κάμψης ή έκτασης στο παρασκεύασμα ελεγχόμενη από τη ροή του νερού στο πρόσθιο ή τον οπίσθιο σάκο. Η μακριά μεταλλική ράβδος που χρησιμοποιήθηκε για την εφαρμογή της ροπής είχε σαν αποτέλεσμα την ομοιόμορφη κατανομή των καμπτικών ροπών σε κάθε σπονδυλικό επίπεδο. Ένας μετρητής [six-axis load cell (Model MC3A-6-250,

AMTI Inc., Newton, MA)] τοποθετήθηκε κάτω από το παρασκεύασμα για να καταγράφονται οι εφαρμοζόμενες ροπές και τα αξονικά φορτία και να παρέχει ανατροφοδότηση στον υπολογιστή που έλεγχε την εφαρμογή ροπής. Με τον τρόπο αυτό το παρασκεύασμα μπορούσε να κινηθεί ομαλά μεταξύ της μέγιστης κάμψης (ροπή +6Nm) και της μέγιστης έκτασης (ροπή -6Nm).

Η κίνηση του ανώτερου σπονδύλου του παρασκευάσματος σε σχέση με τον κατώτερο -ακίνητο σπόνδυλο μετριόταν με ένα οπτικο-ηλεκτρονικό σύστημα (opto-electronic motion measurement system (model 3020, Optotrak; Northen Digital, Waterloo, ON, Canada). Επιπρόσθετα διαξονικά ηλεκτρονικά γωνιόμετρα (Model 902-45, Applied Geomechanics, Santa Cruz, CA) τοποθετημένα στον ανώτερο και τον κατώτερο σπόνδυλο χρησιμοποιήθηκαν για βελτιστοποίηση της πορείας των καλωδίων προφόρτισης.

Για την εφαρμογή συμπιεστικού προ-φορτίου στα παρασκευάσματα χρησιμοποιήθηκε η τεχνική της φόρτισης που ακολουθεί την κυρτότητα της σπονδυλικής στήλης (follower load). Το πλεονέκτημα της είναι ότι επιτρέπει την εφαρμογή συμπιεστικού φορτίου καθ’ όλη τη διάρκεια της κίνησης, χωρίς την δημιουργία επιπρόσθετων ροπών στο παρασκεύασμα [119]. Με το τρόπο αυτό ένα πολυτμηματικό σπονδυλικό παρασκεύασμα μπορεί να υποβληθεί σε φυσιολογικά συμπιεστικά φορτία (μιμούμενα την επίδραση του βάρους του σώματος και της μυϊκής τάσης) χωρίς να παρεμποδίζεται η κίνηση των σπονδύλων στο οβελιαίο επίπεδο. Το φορτίο εφαρμόστηκε μέσω δύο καλωδίων συμπίεσης που ήταν προσδεμένα στο μεταλλικό κυπέλλιο του ανώτερου σπονδύλου. Τα καλώδια διερχόταν ελεύθερα από ρυθμιζόμενους οδηγούς που βρίσκονταν καθηλωμένοι στους σπονδύλους πάνω και κάτω από τον μεσαίο σπόνδυλο. Οι οδηγοί των καλωδίων ήταν προσδεμένοι στους σπονδύλους χωρίς να παραβιάζεται η συνέχεια του τοιχώματος του σπονδυλικού σώματος, ώστε να μην δημιουργούνται σημεία επικέντρωσης φορτίου (stress risers) που θα μπορούσαν να προκαλέσουν κατάγματα ή artifacts στην καταγραφή της τάσης. Αυτό έγινε δυνατό με τη χρήση ενός πλαστικού πέταλου (ανοικτό προς τα εμπρός) το οποίο βιδώθηκε στα οπίσθια στοιχεία του σπονδύλου και δεν είχε καμία επαφή με τις οπίσθιες αρθρώσεις τα σπονδυλικά σώματα ή τους δίσκους. Οι οδηγοί επέτρεπαν την πρόσθια - οπίσθια ρύθμιση της πορείας του κάθε

καλωδίου στο οβελιαίο επίπεδο. Η τελική πορεία του καλωδίου βελτιστοποιήθηκε ρυθμίζοντας την θέση των οδηγών στο οβελιαίο επίπεδο, ώστε να ελαχιστοποιηθεί η κίνηση του παρασκευάσματος κατά την εφαρμογή συμπιεστικού φορτίου από 0 ως 400 N [119]. Τα καλώδια προσαρμόστηκαν σε μηχανισμό εφαρμογής φορτίου (loading actuators) και καλύφθηκαν με ακτινοσκιερό βαριούχο διάλυμα για να είναι ορατά στην ακτινοσκόπηση.

Κατά την διάρκεια της κίνησης των παρασκευασμάτων λαμβάνονταν ακτινοσκοπικές εικόνες από φορητό C arm. Μια μεταλλική σφαίρα με διαστάσεις 25,4 χιλιοστά τοποθετήθηκε μπροστά από κάθε παρασκεύασμα για να υπολογιστεί η μεγέθυνση των ακτινολογικών εικόνων (calibration marker).

Στους σπονδύλους πάνω και κάτω από το μεσαίο σπόνδυλο κάθε παρασκευάσματος τοποθετήθηκαν μετρητές τάσης (single element strain gauges, FLA-2-11- 3L, Sokki Kenkyujo, Tokyo), δύο στο πρόσθιο και από ένα σε κάθε πλάγιο τοίχωμα του σώματος του. Στη θέση εφαρμογής των μετρητών αφαιρέθηκε τοπικά το περιόστεο για να διασφαλιστεί η επαφή τους με τον οστικό φλοιό. Στους μεσοσπονδύλιους δίσκους εκατέρωθεν του μεσαίου σπονδύλου τοποθετήθηκαν μετρητές πίεσης (pressure transducers model 060S-1000, Precision Measurement Co., Ann Arbor, MI) στον πηκτοειδή πυρήνα. Τα δεδομένα από τους μετρητές φιλτραρίστηκαν και καταγράφηκαν με συχνότητα 4 Hz.

Πειραματικό πρωτόκολλο

Έλεγχος στο άθικτο παρασκεύασμα: Αρχικά κάθε παρασκεύασμα ελέγχθηκε άθικτο κατά την ομαλή κίνησή του υπό την επίδραση ροπών (±6 Nm) με ταυτόχρονη συμπιεστική φόρτιση 400 N ώστε να προσομοιώνεται η δράση των μυών και του βάρους του σώματος. Κατά τη δοκιμασία γινόταν καταγραφή της πίεση στους δίσκους άνω και κάτω του μεσαίου σπονδύλου και της τάσης (strain) στο πρόσθιο τοίχωμα των παρακείμενων σπονδύλων. Το εύρος κίνησης του παρασκευάσματος καταγραφόταν από το οπτο-ηλεκτρονικό σύστημα.

Δημιουργία κατάγματος της τελικής πλάκας: Για την δημιουργία του επιλεκτικού κατάγματος στη μία μόνο τελική πλάκα του μεσαίου σπονδύλου χρησιμοποιήθηκε μια νέα πειραματική τεχνική. Από μια μικρή οπή 3 χιλιοστών στο

πρόσθιο τοίχωμα του σπονδυλικού σώματος αφαιρέθηκε το σπογγώδες οστό κάτω από την επιλεγμένη τελική πλάκα. Το κενό που δημιουργήθηκε εκτεινόταν ως το ένα τρίτο του σπονδυλικού σώματος. Με τυχαία επιλογή το κενό δημιουργήθηκε πλησίον της άνω τελικής πλάκας σε τέσσερα παρασκευάσματα και της κάτω πλάκας στα υπόλοιπα τέσσερα. Ακολούθως, τα παρασκευάσματα τοποθετήθηκαν σε θέση κάμψης, εφαρμόζοντας ροπή κάμψης 5 Nm και υποβλήθηκαν σε αξονική συμπίεση έως τη διαπίστωση κατάγματος στην τελική πλάκα κατά τον ακτινοσκοπικό έλεγχο ή μέχρι ένα ανώτερο όριο φόρτισης 700 N. Το ανώτατο όριο των 700 N χρησιμοποιήθηκε για να αποφευχθεί η πιθανότητα κάκωσης σε άλλες τελικές πλάκες, καθώς το όριο αυτό είναι σημαντικά μικρότερο από τα φορτία που απαιτούνται για τη θραύση των σπονδύλων κατά τη βιβλιογραφία [131,136,155] Αν μέχρι το όριο αυτό δεν παρατηρείτο κάταγμα, το κενό επεκτεινόταν και το παρασκεύασμα υποβαλλόταν ξανά σε κάμψη και συμπίεση. Μετά τη δημιουργία του κατάγματος το παρασκεύασμα παρέμενε υπό συμπιεστική φόρτιση 150N. Η τιμή αυτή επελέγη λαμβάνοντας υπόψιν το εύρος των τιμών συμπιεστικού προφορτίου στην οσφυϊκή μοίρα κατά την πρηνή θέση [58].

***Ανάταξη της κυφωτικής παραμόρφωσης με την έκταση*:** Το κάταγμα ανατάχθηκε εφαρμόζοντας ροπή έκτασης υπό την επίδραση συμπιεστικού φορτίου 150 N με στόχο την αποκατάσταση του ύψους του πρόσθιου τοιχώματος και κατ΄ επέκταση την ανάταξη της κυφωτικής παραμόρφωσης του σπονδυλικού σώματος. Η ροπή έκτασης εφαρμόστηκε με χρήση προς τα πάνω δύναμης στο πρόσθιο τμήμα της μεταλλικής ράβδου που βρισκόταν στο κυπέλλιο του άνω σπονδύλου. Το αναταγμένο κάταγμα σταθεροποιήθηκε με την πλήρωση της κοιλότητας με πολυμεθακρυλικό τσιμέντο. Ακολούθως, το υπόλοιπο σπονδυλικό σώμα εκκενώθηκε πλήρως από το σπογγώδες του περιεχόμενο μέσω μιας δεύτερης μικρής οπής στο πρόσθιο τοίχωμα και ακολούθησε η πλήρωση του με ακρυλικό τσιμέντο. Με τον προσεκτικό καθαρισμό και των δύο τελικών πλακών από τις οστικές δοκίδες διασφαλίστηκε η ομοιόμορφη κατανομή του τσιμέντου στην εγγύτητά τους, ώστε η παρουσία του να αποτελεί κοινό παράγοντα για την παραμορφωμένη και την άθικτη πλάκα.

Τα παρασκευάσματα υποβλήθηκαν σε δοκιμασία κάμψης έκτασης (ροπή ±6 Nm) υπό συμπιεστικό φορτίο 400N, πρώτα άθικτα και κατόπιν μετά την δημιουργία και ανάταξη του πειραματικού κατάγματος στον μεσαίο σπόνδυλο. Κατά τη δοκιμασία αυτή καταγράφηκε η πίεση στους δίσκους πάνω και κάτω από το μεσαίο σπόνδυλο, καθώς και η τάση στο πρόσθιο τοίχωμα των παρακείμενων σπονδύλων.

Δημιουργία νέων καταγμάτων: Κάθε παρασκεύασμα τοποθετήθηκε σε κάμψη με ροπή 5 Nm και υποβλήθηκε σε σταδιακά αυξανόμενο συμπιεστικό φορτίο από 0 έως 3000 N ή ώσπου ένα επακόλουθο κάταγμα να παρατηρηθεί στο ακτινοσκοπικό έλεγχο ταυτόχρονα με μια απότομη πτώση στην γραφική παράσταση δύναμης προς το χρόνο.

Ανάλυση των δεδομένων: Μετρήθηκε το ύψος του σπονδυλικού σώματος στο πρόσθιο τοίχωμα και στη μεσότητα, καθώς και η κυφωτική γωνία του σπονδύλου στο άθικτο παρασκεύασμα, μετά τη δημιουργία του κατάγματος καθώς και μετά την ανάταξη και σταθεροποίηση με το τσιμέντο. Το ύψος στη μεσότητα μετρήθηκε λαμβάνοντας υπ΄ όψη την κατάσπαση της κεντρική του περιοχή. Η κυφωτική γωνία μετρήθηκε ως η γωνία ανάμεσα στην άνω και την κάτω τελική πλάκα. Οι μετρήσεις έγιναν στις ψηφιακές ακτινοσκοπικές εικόνες χρησιμοποιώντας το πρόγραμμα Image Pro Plus (Media Cybernetics Inc). Το εύρος κίνησης κατά την κάμψη υπολογίστηκε ως η αλλαγή στη γωνία του ανώτερου σπονδύλου σε σχέση με τον κατώτερο από την ουδέτερη θέση ως την κάμψη με 6Nm. Η δύναμη που χρειάστηκε για τη θραύση των σπονδύλων καθορίστηκε από το ανώτερο σημείο στην καμπύλη δύναμης προς χρόνο.

Οι μετρητές strain και πίεσης δεν μπορούν να δώσουν αξιόπιστες απόλυτες τιμές καθώς η συνδεσμολογία που χρησιμοποιήθηκε δεν επιτρέπει τη αντιστάθμιση της αλλαγής της θερμοκρασίας. Τα δεδομένα που δίνουν εξαρτώνται από ένα συνδυασμό της μετρούμενης τιμής και της αλλαγής στη θερμοκρασία. Για το λόγο αυτό η πίεση στους δίσκους και το strain στα τοιχώματα των σπονδύλων προσαρμόστηκαν ώστε οι τιμές στην ουδέτερη θέση υπό προφορτίο 400 N ελήφθησαν ως μηδενική τιμή για να αντισταθμίσουν τη θερμική αλλαγή. Αυτό είχε σαν αποτέλεσμα να χρησιμοποιηθούν για την ανάλυση όχι οι απόλυτες τιμές αλλά

οι αλλαγές στην πίεση και το strain από την ουδέτερη θέση στη πλήρη κάμψη, στο άθικτο παρασκεύασμα και μετά την τσιμέντωση του αναταγμένου κατάγματος.

Δύο παρασκευάσματα αποκλειστήκαν από τη ανάλυση δεδομένων για την πίεση του δίσκου καθώς οι μετρητές πίεσης μετακινήθηκαν προς τα εμπρός, στην περιοχή του δακτυλίου, με αποτέλεσμα μη ακριβείς μετρήσεις. Τα δεδομένα αναλύθηκαν με repeated measures analysis of variance (ANOVA) με επίπεδο σημαντικότητας a = 0,05 χρησιμοποιώντας το εμπορικό στατιστικό πακέτο SPSS (SPSS Inc., Chicago, IL).

Αποτελέσματα

Μορφομετρικά στοιχεία: Στα άθικτα παρασκευάσματα η κυφωτική γωνία του μεσαίου σπονδύλου ήταν 8,5 ± 2,2°, το ύψος του πρόσθιου τοιχώματος ήταν 21,2 ± 2,7 mm και το ύψος στη μεσότητα του σπονδυλικού σώματος ήταν 20.1 ± 2,9 mm (**Πίνακας 1**). Το συμπιεστικό φορτίο που χρειάστηκε για την επίτευξη του επιλεκτικού κατάγματος στον μεσαίο σπόνδυλο ήταν 540 ± 150 N. Δεν υπήρξε καμία ένδειξη κατάγματος σε άλλη τελική πλάκα πέρα από την αναμενόμενη κατά τον ακτινοσκοπικό έλεγχο σε κανένα από τα παρασκευάσματα. Μετά το αρχικό κάταγμα η κυφωτική γωνία του σπονδύλου αυξήθηκε σε 12,6 ± 2,4°, το ύψος του προσθίου τοιχώματος μειώθηκε σε 17,2 ± 3,1 mm και της μεσότητας του σώματος σε 14,3 ± 3,3 mm. Κατά μέσο όρο χρειάστηκαν 4,6 ± 0,8 Nm ροπή έκτασης, υπό προφορτίο 150 N, για να αποκατασταθεί η κυφωτική γωνία του μεσαίου σπονδύλου στην αρχική τιμή του άθικτου σπονδύλου (8,8 ± 1,6°, p = 0,38). Το ύψος του πρόσθιου τοιχώματος αποκαταστάθηκε σε 20,8 ± 2,6 mm και η διαφορά από τον άθικτο σπόνδυλο αν και στατιστικά σημαντική (p = 0,04), ήταν μικρή. Το ύψος στη μεσότητα του σπονδυλικού σώματος παρέμεινε σημαντικά μειωμένο σε σχέση με τα άθικτα παρασκευάσματα (16,4 ± 3,0 mm, p < 0,01). Το εύρος κίνησης κατά την κάμψη αυξήθηκε από 4,7 ± 1,4° στα άθικτα παρασκευάσματα σε 6,1 ± 2,4° μετά την ενίσχυση με τσιμέντο του κατάγματος στο μεσαίο σπόνδυλο. Η αύξηση ήταν στατιστικά σημαντική (p<0,05).

Ενδοδισκική πίεση: Στα άθικτα παρασκευάσματα, η πίεση στους δίσκους που γειτνίαζαν με την τελική πλάκα που είχε προγραμματιστεί να παραμείνει άθικτη ήταν 1,21 ± 1,82 MPa στην ουδέτερη θέση υπό προφορτίο 400 N. Η

εφαρμογή καμπτικής ροπής 6 Nm αύξησε την πίεση στους δίσκους κατά 0,14 ± 0,11 MPa, που αντιπροσωπεύει μια αύξηση 27,19 ± 17,4% σχετικά με την πίεση στη ουδέτερη θέση. Μετά την ενίσχυση με οστικό τσιμέντο του αρχικού κατάγματος η πίεση στους δίσκους στην ουδέτερη θέση υπό προφορτίο 400 N ήταν 1,34 ± 1,55 MPa. Η εφαρμογή καμπτικής ροπής 6 Nm αύξησε την πίεση στους δίσκους κατά 0,13 ± 0,10 MPa, που αντιπροσωπεύει μια αύξηση κατά 15,8 ± 10,1% από την τιμή στην ουδέτερη θέση. Η αλλαγή στη πίεση από την εφαρμογή της καμπτικής ροπής στο δίσκο με τη μη σπασμένη τελικά πλάκα δεν επηρεάστηκε σημαντικά από την έγχυση του τσιμέντου (p = 0,55).

Στα άθικτα παρασκευάσματα, η πίεση στους δίσκους που γειτνίαζαν με την τελική πλάκα που είχε προγραμματιστεί να σπάσει ήταν 0,51 ± 0,25 MPa στην ουδέτερη θέση υπό προφορτίο 400 N. Η εφαρμογή ροπής κάμψης 6 Nm αύξησε την πίεση κατά 0,14 ± 0,11 MPa, που αντιπροσωπεύει μια αύξηση 26,3 ± 9,5% σχετικά με την πίεση στη ουδέτερη θέση. Μετά την τσιμέντωση του αρχικού κατάγματος η πίεση στους δίσκους στην ουδέτερη θέση υπό προφορτίο 400 N ήταν 0,43 ± 0,13 MPa. Η εφαρμογή καμπτικής ροπής 6 Nm μείωσε την πίεση στους δίσκους κατά 0,07 ± 0,14 MPa, που αντιπροσωπεύει μια μείωση κατά 19.0 ± 26.8% από την τιμή στην ουδέτερη θέση (**εικ. 10**). Η αλλαγή στη πίεση από την εφαρμογή της καμπτικής ροπής στο δίσκο με τη σπασμένη τελικά πλάκα ήταν σημαντικά διαφορετική από το άθικτο παρασκεύασμα (p = 0.02).

Συμπιεστική τάση: Στα άθικτα παρασκευάσματα, η συμπιεστική τάση στο πρόσθιο τοίχωμα των σπονδύλων που γειτνίαζαν με την τελική πλάκα που είχε προγραμματιστεί να παραμείνει άθικτη αυξήθηκε κατά 447.8 ± 100.4 micro- strain κατά την κάμψη 6 Nm υπό προφορτίο 400 N σε σύγκριση με την ουδέτερη θέση. Μετά την τσιμέντωση του αρχικού κατάγματος η τάση αυξήθηκε κατά 522.6 ± 131.5 microstrain με την κάμψη 6 Nm. Η διαφορά αυτή αντιπροσωπεύει μια μη σημαντική αλλαγή της τάξης του 18,2 ± 7.1% στη συμπιεστική τάση του πρόσθιου τοιχώματος των παρακείμενων σπονδύλων δίπλα από τη μη σπασμένη τελική πλάκα, πριν και μετά το επιλεκτικό κάταγμα. (p>0,05). Στα άθικτα παρασκευάσματα, η συμπιεστική τάση στο πρόσθιο τοίχωμα των σπονδύλων που γειτνίαζαν με την τελική πλάκα που είχε προγραμματιστεί να σπάσει αυξήθηκε κατά 413.2 ± 232.4 microstrain από την ουδέτερη θέση στη κάμψη 6

Nm, υπό προφορτίο 400 N. Μετά την τσιμέντωση του αρχικού κατάγματος η τάση αυξήθηκε κατά 836.2 ± 499.2 microstrain κατά την κάμψη 6 Nm. Η διαφορά αντιπροσωπεύει μια αύξηση 94,2 ± 22,8% στη συμπιεστική τάση στο πρόσθιο τοίχωμα των παρακείμενων σπονδύλων δίπλα στη σπασμένη τελική πλάκα ($p<0,05$).

Επακόλουθα κατάγματα: Επακόλουθη συμπίεση των παρασκευασμάτων σε θέση 5Nm κάμψης είχε σαν αποτέλεσμα τη δημιουργία νέου κατάγματος σε σπονδυλικό σώμα παρακείμενο στη αρχικά σπασμένη τελική πλάκα σε έξι παρασκευάσματα και σε ένα απομακρυσμένο κάταγμα στο άνω σπονδυλικό σώμα σε ένα. Η εφαρμογή του μέγιστου συμπιεστικού φορτίου των 3000 N δεν κατάφερε να δημιουργήσει νέο κάταγμα σε ένα από τα παρασκευάσματα. Η δημιουργία των παρακείμενων καταγμάτων ξεκινούσε σαν μια κατάσπαση στην πρόσθια περιοχή της τελικής πλάκας που γινόταν προοδευτικά βαθύτερη καθώς η φόρτιση αυξανόταν έως ότου το πρόσθιο τοίχωμα τελικά ενέδιδε. Το φορτίο που χρειάστηκε ήταν κατά μέσο όρο 1450 ± 402 N**.**

Συζήτηση

Η παρούσα εμβιομηχανική μελέτη επικεντρώθηκε στο ρόλο της παραμόρφωσης της τελικής πλάκας ενός σπονδύλου μετά από ένα οστεοπορωτικό κάταγμα ως παράγοντα κινδύνου για την δημιουργία παρακείμενων σπονδυλικών καταγμάτων. Το ακρυλικό τσιμέντο χρησιμοποιήθηκε μόνο για τη σταθεροποίηση του κατάγματος ώστε να επιτραπεί η συνέχιση του πειράματος. Η τεχνική έγχυσης του τσιμέντου στην παρούσα πειραματική εργασία δεν έχει σχέση με τις τεχνικές που χρησιμοποιούνται κλινικά. Παρόλα αυτά, επειδή στην βιβλιογραφία υπάρχει η ανησυχία ότι η παρουσία του τσιμέντου στο σπονδυλικό σώμα μπορεί να αλλάζει τις ιδιότητες μεταφοράς φορτίου [50,51,147], και οι δύο τελικές πλάκες καθαρίστηκαν καλά από όλες τις υποκείμενες οστικές δοκίδες ώστε να εξασφαλιστεί ομοιόμορφη κατανομή του τσιμέντου κάτω από αυτές. Με τον τρόπο αυτό, οποιαδήποτε επίδραση θα μπορούσε να έχει η παρουσία του τσιμέντου μέσα στο σπονδυλικό σώμα ήταν ένα κοινός παράγοντας και για τις δύο τελικές πλάκες. Επιπρόσθετα, η αποκατάσταση της κυφωτικής γωνίας του σπονδυλικού σώματος μετά την αποκατάσταση του ύψους του πρόσθιου τοιχώματος στην προ του κατάγματος τιμή, εξάλειψε την υπολειπόμενη κύφωση ως παράγοντα κινδύνου για παρακείμενα κατάγματα. Με τον τρόπο αυτό η παραμόρφωση της τελικής πλάκας παρέμεινε η μοναδική μεταβλητή για τα φαινόμενα που παρατηρήθηκαν.

Η πειραματική δημιουργία ενός συμπιεστικού σπονδυλικού κατάγματος σχετίζεται με αβεβαιότητα ως προς τον τύπο και την εντόπιση του κατάγματος. Προηγούμενες μελέτες έχουν περιγράψει τη δημιουργία κενού χώρου στο κέντρο του σπονδυλικού σώματος για την επίτευξη κατάγματος σε ένα επιλεγμένο σπόνδυλο ενός παρασκευάσματος [28,82,156]. Το μοντέλο που περιγράφεται στην παρούσα εργασία επιτρέπει την δημιουργία ενός απολύτως προβλέψιμου κατάγματος όχι μόνο σε ένα συγκεκριμένο σπόνδυλο, αλλά κάτω από κάποια συγκεκριμένη τελική πλάκα. Η μορφολογία του κατάγματος μπορεί επίσης να ελεγχθεί. Το κάταγμα ξεκινούσε σα μια εμβύθιση της εξασθενημένης τελικής πλάκας και καθώς το συμπιεστικό φορτίο αυξανόταν οδηγούσε σε κατάρρευση του πρόσθιου τοιχώματος με προοδευτική δημιουργία τυπικού κατάγματος με σφηνοειδές σχήμα, ενώ η μη εξασθενημένη τελική πλάκα παρέμενε ανέπαφη.

Στην παρούσα μελέτη η συμπιεστική φόρτιση συνεχιζόταν ως τη απώλεια ύψους του πρόσθιου τοιχώματος της τάξης του 25%.

Μελέτες in vivo [58,117], και in vitro [54] έχουν δείξει ότι οι μεγαλύτερες πιέσεις στο μεσοσπονδύλιο δίσκο ασκούνται κατά την πρόσθια κάμψη υπό συμπιεστική φόρτιση, όπως για παράδειγμα στην άρση βάρους. Η παρούσα μελέτη βρίσκεται σε συμφωνία με αυτά τα ευρήματα. Επιπροσθέτως, προηγούμενες in vitro μελέτες έχουν δείξει ότι η πίεση στον πηκτοειδή πυρήνα ελαττώνεται σημαντικά μετά από ένα οστεοπορωτικό κάταγμα [52,54,138,157], καθώς με την κατάσπαση της τελικής πλάκας αυξάνεται ο χώρος που είναι διαθέσιμος για τον πυρήνα. Τα ευρήματα της παρούσης μελέτης υποδεικνύουν μια πιο συγκεκριμένη διαταραχή στις μηχανικές ιδιότητες του δίσκου μετά την κατάσπαση της τελικής πλάκας. Η πίεση του πυρήνα ελαττώνεται ακόμη περισσότερο κατά την κάμψη, πέρα από την αρχική αναμενόμενη ελάττωση στην ουδέτερη θέση που αναφέρεται στη βιβλιογραφία. Αυτή η μη φυσιολογική εμβιομηχανική συμπεριφορά συνοδεύεται από μια ταυτόχρονη αύξηση της συμπίεσης του πρόσθιου τοιχώματος του παρακείμενου σπονδύλου, η οποία σχεδόν διπλασιάστηκε σε σχέση με αυτή του άθικτου παρασκευάσματος. Αντιθέτως, οι μηχανικές ιδιότητες του μη κατεστραμμένου δίσκου του σπασμένου σπονδύλου δεν επηρεάστηκαν σημαντικά με συνέπεια και τα συμπιεστικά φορτία στον παρακείμενο σπόνδυλο να μην αλλάξουν. Προηγούμενες μελέτες έχουν δείξει ότι η συμπιεστική καταπόνηση στους παρακείμενους σπονδύλους αυξάνεται με την εφαρμογή συμπιεστικού φορτίου, αλλά η αύξηση είναι περισσότερο δραματική από την κάμψη παρά από την αξονική φόρτιση [27,28,158,159,160,161]. Μπορούμε άρα να υποθέσουμε ότι η μικρή αύξηση στη συμπιεστική καταπόνηση στα σπονδυλικά σώματα δίπλα σε μη σπασμένες τελικές πλάκες που βρέθηκε στην παρούσα μελέτη θα μπορούσε να εξηγηθεί από την αύξηση στο εύρος κίνησης που παρατηρήθηκε μετά το κάταγμα.

Έχει αναφερθεί ότι η ενίσχυση με τσιμέντο των σπονδυλικών καταγμάτων με τις διάφορες τεχνικές που χρησιμοποιούνται κλινικά μπορεί μόνο μερικώς να αποκαταστήσει την πίεση του πυρήνα, καθώς η προκύπτουσα πίεση δεν μπορεί να φτάσει τις τιμές προ του κατάγματος [54,157]. Τα ευρήματά της παρούσας μελέτης ότι μετά το κάταγμα η πίεση στο δίσκο μειώνεται κατά την κάμψη αν

συγκριθεί με την πίεση στην ουδέτερη θέση έρχονται σε αντίθεση με προηγούμενα εργαστηριακά ευρήματα. Οι Ananthakrishnan et al. [54] ανέφεραν ελαφρά αυξημένες πιέσεις στο δίσκο κατά την κάμψη σε σχέση με την ουδέτερη θέση μετά από σπονδυλοπλαστική για οστεοπορωτικά κατάγματα. Αυτό μπορεί να υποδεικνύει ότι ο χειρισμός έκτασης που χρησιμοποιήθηκε στην παρούσα μελέτη για τη ανάταξη της σπονδυλικής κύφωσης μπορεί να έχει αρνητικές συνέπειες στη μεταφορά του φορτίου. Η έκταση ασκεί συνδεσμόταξη (ligamentotaxis) μέσω της τάσης που αναπτύσσεται στον πρόσθιο επιμήκη σύνδεσμο και τον ινώδη δακτύλιο. Η τάση αυτή μπορεί να ανατάξει την περιφέρεια του σπονδυλικού σώματος. Ο πυρήνα μη διαθέτοντας ικανότητα να αναπτύξει τάση (tensile properties) αδυνατεί να ανατάξει την κεντρική κατάσπαση της τελικής πλάκας με συνδεσμόταξη. Αυτό έχει σαν αποτέλεσμα την παραμονή της κεντρικής παραμόρφωσης της τελικής πλάκας ακόμη και όταν το ύψος του πρόσθιου τοιχώματος έχει αποκατασταθεί πλήρως. Σε αυτό το πλαίσιο, η ανόρθωση της περιφέρειας της τελικής πλάκας από τον χειρισμό έκτασης μπορεί να κάνει πιο έντονη την κεντρική εμβύθιση, έχοντας σαν αποτέλεσμα την μεγαλύτερη επιδείνωση των μηχανικών χαρακτηριστικών του πυρήνα. Κλινικές αναφορές έχουν δείξει ότι η μεγαλύτερη αποκατάσταση του ύψους του κατάγματος από την σπονδυλοπλαστική μπορεί να σχετίζεται με μεγαλύτερη πιθανότητα νέων καταγμάτων [88,162]. Παρόμοια ευρήματα έδειξε και άλλη μελέτη με την αναφορά της ότι η συχνότητα εμφάνισης νέων καταγμάτων μετά από σπονδυλοπλαστική ήταν αντιστρόφως ανάλογη με την βαρύτητα της σπονδυλικής κύφωσης μετά την επέμβαση [89]. Παρά το ότι θα μπορούσε κάποιος να υποθέσει ότι οι μεγαλύτεροι όγκοι τσιμέντου που χρειάζονται οι λιγότερο παραμορφωμένοι σπόνδυλοι μπορεί να σχετίζονται με την εμφάνιση νέων καταγμάτων, οι μελέτες αυτές δεν έδειξαν ότι ο κίνδυνος νέων καταγμάτων σχετίζεται με τον όγκο του τσιμέντου [89,162].

Συμπεράσματα Προτάσεις

Σαν συμπέρασμα, η παρούσα εργασία δείχνει ότι η κατάσπαση της τελικής πλάκας μετά από ένα οστεοπορωτικό κάταγμα επηρεάζει την ικανότητα του δίσκου να κατανέμει ομαλά τα φορτία στα παρακείμενα σπονδυλικά σώματα. Το φορτίο αυξάνεται υπέρμετρα στην πρόσθια περιοχή του σπονδυλικού σώματος καθώς προχωράει η κάμψη της σπονδυλικής στήλης, ενώ ταυτόχρονα η πίεση στον πυρήνα του δίσκου μειώνεται. Η συγκέντρωση του φορτίου στην πρόσθια πλευρά του παρακείμενου σπονδυλικού σώματος αυξάνει τον κίνδυνο κατάγματος. Οι τρέχουσες τεχνικές ενίσχυσης σπονδυλικών σωμάτων μετά από κατάγματα έχουν επικεντρωθεί στην ανάταξη της κυφωτική γωνίας και στην αποκατάσταση του πρόσθιου τοιχώματος με ανάταξη κατά την τοποθέτηση του ασθενή σε πρηνή θέση ή με τη χρήση μπαλονιών για την έκπτυξη του σπονδυλικού σώματος [104,164,165]. Η παρούσα μελέτη υποδεικνύει ότι εκτός από την ανάταξη της παραμόρφωσης στο οβελιαίο επίπεδο, η αποκατάσταση της παραμόρφωσης της τελικής πλάκας είναι σημαντική για την εξομάλυνση της μεταφοράς του φορτίου από το επίπεδο που έχει υποστεί το κάταγμα.

References

1. Kanis JA on behalf of the WHO Scientific Group (2007). Assessment of osteoporosis at the primary health care level. Technical Report. WHO Collaborating Centre for Metabolic Bone Diseases, University of Sheffield, UK.
2. Word Health Organization. Assessment of fracture risk and its application to screening for postmenopausal osteoporosis. WHO 1994, pp1-129.
3. Kanis JA, McClosky EV. The Epidemiology of vertebral osteoporosis. Bone 1992;13:S1-S10.
4. Melton LJ. Epidemiology of spinal osteoporosis. Spine 1997;22(24S):2S–11S.
5. Riggs BL, Melton LJ 3rd. The worldwide problem of osteoporosis: insights afforded by epidemiology. Bone 1995;17(5 Suppl):505S-511S
6. Cooper C, Atkinson EJ, O'Fallon WM, Melton LJ 3rd. Incidence of clinically diagnosed vertebral fractures: a population-based study on Rochester, Minnesota, 1985-1989. J Bone Miner Res 1992;7(2):221-227.
7. Nevitt MC, Ross PD, Palermo L, Musliner T, Genant HK, Thompson DE. Association of prevalent vertebral fractures, bone density, and alendronate treatment with incident vertebral fractures: effect of number and spinal location of fractures. The Fracture Intervention Trial Research Group. Bone 1999;25:613-619.
8. Lee YL, Yip KM. The osteoporotic spine. Clin Orthop 1996;323:91-97.
9. Cortet B, Roches E, Logier R, Houvenagel E, Gaydier-Souquières G, Puisieux F, Delcambre B. Evaluation of spinal curvatures after a recent osteoporotic vertebral fracture. Joint Bone Spine. 2002;69(2):201-8.
10. Milne JS, Williamson J. A longitudinal study of kyphosis in older people. Age Ageing. 1983;12(3):225-33.
11. Cooper C, Atkinson EJ, Jacobsen SJ, O'Fallon WM, Melton LJ 3rd. Population-based study of survival after osteoporotic fractures. Am J Epidemiol. 1993;137(9):1001-5.

12. Kado DM, Browner WS, Palermo L, Nevitt MC, Genant HK, Cummings SR. Vertebral body fractures and mortality in older women: A prospective study. Study of Osteoporotic Fracture Research Group. Arch Intern Med 1999;159(11):1215-1220.
13. Lindsay R, Silverman SL, Cooper C, Hanley DA, Barton I, Broy SB, Licata A, Benhamou L, Geusens P, Flowers K, Stracke H, Seeman E. Risk of new vertebral fracture in the year following a fracture. JAMA 2001;285(3):320-323.
14. Ross PD, Davis JW, Epstein RS, Wasnich RD. Pre-existing fractures and bone mass predict vertebral fracture incidence in women. Arch Intern Med 1991;114:919-923.
15. Melton LJ 3rd, Atkinson EJ, Cooper C, O'Fallon WM, Riggs BL. Vertebral fractures predict subsequent fractures. Osteoporos Int. 1999;10(3):214-21.
16. Black DM, Arden NK, Palermo L, Pearson J, Cummings SR. Prevalent vertebral deformities predict hip fractures and new vertebral fractures but not wrist fracture. Study of Osteoporotic Fractures Research Group. J Bone Miner Res 1999;14(5):821-828.
17. McCloskey EV, Vasireddy S, Threlkeld J, Eastaugh J, Parry A, Bonnet N, Beneton M, Kanis JA, Charlesworth D. Vertebral fracture assessment (VFA) with a densitometer predicts future fractures in elderly women unselected for osteoporosis. J Bone Miner Res 2008;23:1561-1568.
18. Cauley JA, Hochberg MC, Lui LY, Palermo L, Ensrud KE, Hillier TA, Nevitt MC, Cummings SR. Long-term risk of incident vertebral fractures. JAMA 2007;298:2761-2767.
19. Bouxsein ML, Chen P, Glass EV, Kallmes DF, Delmas PD, Mitlak BH. Teriparatide and raloxifene reduce the risk of new adjacent vertebral fractures in postmenopausal women with osteoporosis. Results from two randomized controlled trials. J Bone Joint Surg Am 2009;91:1329-1338.
20. Siris ES, Genant HK, Laster AJ, Chen P, Misurski DA, Krege JH. Enhanced prediction of fracture risk combining vertebral fracture status and BMD. Osteoporos Int 2007;18:761-770.

21. Ross PD, Genant HK, Davis JW, Miller PD, Wasnich RD. Predicting vertebral fracture incidence from prevalent fractures and bone density among non-black, osteoporotic women. Osteoporos Int 1993;3(3):120–126.
22. Johnell O, Oden A, Caulin F, Kanis JA. Acute and long-term increase in fracture risk after hospitalization for vertebral fracture. Osteoporos Int 2001;12:207-214.
23. Pongchaiyakul C, Nguyen ND, Jones G et al. Asymptomatic vertebral deformity as a major risk factor for subsequent fractures and mortality: a long-term prospective study. J Bone Miner Res 2005;20(8):1349–1355.
24. The European Prospective Osteoporosis Study (EPOS) Group. Determinants of the size of incident vertebral deformities in European men and women in the sixth to ninth decades of age: the European Prospective Osteoporosis Study (EPOS). J Bone Miner Res 2003;18:1664–1673.
25. Yuan H, Brown C, Phillips FM. Osteoporotic spinal deformity: a biomechanical rationale for the clinical consequences and treatment of vertebral body compression fractures. J Spinal Disord 2004;17:236–242.
26. Rohlmann A, Zander T, Bergmann G. Spinal loads after osteoporotic vertebral fractures treated by vertebroplasty or kyphoplasty. Eur Spine J 2006;15(8):1255–1264.
27. Kayanja MM, Ferrara LA, Lieberman IH. Distribution of anterior cortical shear strain after a thoracic wedge compression fracture. Spine J 2004;4(1):76–87.
28. Kayanja MM, Togawa D, Lieberman IH. Biomechanical changes after the augmentation of experimental osteoporotic vertebral compression fractures in the cadaveric thoracic spine. Spine J 2005;5(1):55–63.
29. Grados F, Depriester C, Cayrolle G, Hardy N, Deramond H, Fardellone P. Long-term observations of vertebral osteoporotic fractures treated by percutaneous vertebroplasty. Rheumatology 2000; 39:1410-1414.

30. Legroux-Gerot I, Lormeau C, Boutry N, Cotten A, Duquesnoy B, Cortet B. Long-term follow-up of vertebral osteoporotic fractures treated by percutaneous vertebroplasty. Clin Rheumatol 2004;23(4):310-317.
31. Trout AT, Kallmes DF, Kaufmann TJ. New fractures after vertebroplasty: adjacent fractures occur significantly sooner. Am J Neuroradiol 2006;27(1):217-223.
32. Trout AT, Kallmes DF, Layton KF, Thielen KR, Hentz JG. Vertebral endplate fractures: an indicator of the abnormal forces generated in the spine after vertebroplasty. J Bone Miner Res 2006;21(11):1797–1802.
33. Ledlie JT, Renfro MB. Kyphoplasty treatment of vertebral fractures: 2-year outcomes show sustained benefits. Spine 2006;31(1):57-64.
34. Fribourg D, Tang C, Sra P, Delamarter R, Bae H. Incidence of subsequent vertebral fracture after kyphoplasty. Spine 2004;29(20):2270-2277.
35. Lavelle WF, Cheney R. Recurrent fracture after vertebral kyphoplasty. Spine J 2006;6(5):488-493.
36. Uppin A, Hirsch J, Centenera L, Pfiefer B, Pazianos A, Choi I. Occurrence of new vertebral fracture after percutaneous Vertebroplasty in patients with osteoporosis. Radiology 2003;226(1):119-124.
37. Voormolen MH, Lohle PN, Juttmann JR, et al. The risk of new osteoporotic vertebral compression fractures in the year after percutaneous vertebroplasty. J Vasc Interv Radiol 2006;17(1):71-76.
38. Tanigawa N, Komemushi A, Kariya S, Kojima H, Shomura Y, Sawada S. Radiological follow-up of new compression fractures following percutaneous vertebroplasty. Cardiovasc Intervent Radiol 2006;29(1):92–96.
39. Klazen CA, Venmans A, de Vries J, van Rooij WJ, Jansen FH, Blonk MC, Lohle PN, Juttmann JR, Buskens E, van Everdingen KJ, Muller A, Fransen H, Elgersma OE, Mali WP, Verhaar HJ.Percutaneous vertebroplasty is not a risk factor for new osteoporotic compression

fractures: results from VERTOS II. AJNR Am J Neuroradiol. 2010;31(8):1447-50

40. Han SL, Wan SL, Li QT, Xu DT, Zang HM, Chen NJ, Chen LY, Zhang WP, Luan C, Yang F, Xu ZW.Is vertebroplasty a risk factor for subsequent vertebral fracture, meta-analysis of published evidence? Osteoporos Int. 2015;26(1):113-22.
41. Zhang YZ, Kong LD, Cao JM, Ding WY, Shen Y. Incidence of subsequent vertebral body fractures after vertebroplasty. J Clin Neurosci. 2014;21(8):1292-7
42. Silverman SL. The clinical consequences of vertebral compression fractures. Bone 1992;13(supp 1):261–267.
43. Kaplan FS, Scherl JD, Wisneski R, et al. The cluster phenomenon in patients who have multiple vertebral compression fractures. Clin Orthop Relat Res 1993;(297):161–167.
44. Adams MA, McNally DS, Dolan P. ‘Stress’ distributions inside intervertebral discs. The effects of age and degeneration. J Bone Joint Surg Br 1996;78(6):965–972.
45. Marchand F, Ahmed AM Investigation of the laminate structure of lumbar disc annulus fibrosus. Spine 1990;15:402-410.
46. Stokes IA. Surface strain on human intervertebral discs. J Orthop Res 1987;5:348-355.
47. Brinckmann P, Frobin W, Hierholzer E et al. Deformation of the vertebral endplate under axial loading of the spine. Spine 1983;8:851-856.
48. Holmes AD, Hukins DW, Freemont AJ. Endplate displacement during compression of lumbar vertebra-disc vertebra segments and the mechanisms of failure. Spine 1993;18:128-135.
49. Adams MA, Dolan P, Hutton WC. The stages of disc degeneration as revealed by discograms. J bone Joint Surg [Br] 1986;68:36-41.
50. Baroud G, Nemes J, Heini P, Steffen T. Load shift of the intervertebral disc after a vertebroplasty: a finite-element study. Eur Spine J 2003;12(4):421–426.

51. Polikeit A, Nolte LP, Ferguson SJ. The effect of cement augmentation on the load transfer in an osteoporotic functional spinal unit, finite element analysis. Spine 2003;28:991–996.
52. Adams MA, McNally DS, Wagstaff J, Goodship AE. Abnormal stress concentrations in lumbar intervertebral discs following damage to the vertebral body: a cause of disc failure. Eur Spine J 1993;1:214–221.
53. Adams MA, Freeman BJ, Morrison HP, Nelson IW, Dolan P. Mechanical initiation of intervertebral disc degeneration. Spine 2000;25(13):1625–1636.
54. Ananthakrishnan D, Berven S, Deviren V et al. The effect on anterior column loading due to different vertebral augmentation techniques. Clin Biomech (Bristol, Avon) 2005;20:25–31.
55. Dolan P, Luo J, Pollintine P, Landham PR, Stefanakis M, Adams MA. Intervertebral disc decompression following endplate damage: implications for disc degeneration depend on spinal level and age. Spine (Phila Pa 1976) 2013;38(17):1473-81.
56. McNally DS, Adams MA. Internal intervertebral disc mechanics as revealed by stress profilometry. Spine 1992;17(1):66-73
57. McNally DS, Shackleford IM, Goodship AE, Mulholland RC. In vivo stress measurements can predict pain on discography. Spine 1996;21(22):2580-2587.
58. Sato K, Kikuchi S, Yonezawa T. In vivo intradiscal pressure measurement in healthy individuals and in patients with ongoing back problems. Spine 1999;24(23):2468-74.
59. McNally DS. The objectives of the biomechanical evaluation of spinal instrumentation have changed. Eur Spine J 2002;11Suppl2]:S171-S185.
60. Adams MA, Hutton WC. The mechanical function of the lumbar apophyseal joints. Spine 1983;8(3):327-30.
61. Mow VC, Hayes WC. Basic orthopaedic biomechanics. New York: Raven Press, 1999.
62. Tohmeh AG, Mathis JM, Fenton DC, Levine AM, Belkoff SM. Biomechanical efficacy of unipedicular versus bipendicular

vertebroplasty for the management of osteoporotic compression fractures. Spine 1999;24(17):1772-1776.

63. Lyritis GP, Mayasis B, Tsakalakos N, Lambropoulos A, Gazi S, Karachalios T, Tsekoura M, Yiatzides A. The natural history of osteoporotic vertebral fracture. Clin Reumatol 1989;8(Suppl.2):66-69.
64. Sinaki M. Exercise and Physical Therapy. In Lawrence Riggs and Joseph Melton (Ed) Osteoporosis: Etiology, Diagnosis and Management, edited by B, Raven Press, NY, 1988 p401.
65. Old JL, Calvert M. Vertebral compression fractures in the elderly. Am Fam Physician 2004;69(1):111-1116.
66. Eck JC, Hodges SD, Humphreys SC. Vertebroplasty: A new treatment strategy for osteoporotic compression fractures. Am J Ortop 2002;31(3)123-128.
67. Cyteval C, Sarrabere MP, Roux JO, Thomas E, Jorgensen C, Blotman F, Sany J, Taourel P. Acute osteoporotic vertebral collapse: open study on percutaneous injection of acrylic surgical cement in 20 patients. AJR Am J Roentgenol 1999;173(6):1685–1690.
68. McKiernan F, Faciszewski T. Intravertebral clefts in osteoporotic vertebral compression fractures. Arthritis Rheum 2003;48(5):1414-1419.
69. Hadjipavlou AG, Katonis PG, Tzermiadianos MN, Tsoukas GM, Sapkas G. Principles of management of osteometabolic disorders affecting the aging spine. Eur Spine J 2003;12(Suppl. 2):S113–S131.
70. Cotten A, Boutry N, Cortet B, Assaker R, Demondion X, Leblond D, Chastanet P, Duquesnoy B, Deramond H. Percutaneous vertebroplasty: State of the Art; Radiographics 1998;18(2):311-320.
71. Linville DA 2nd. Vertebroplasty and kyphoplasty. Southern Medical J 2002;95:583-587.
72. Leech JA, Dulberg C, Kellie S, Pattee L, Gay J. Relationship of lung function to severity of osteoporosis in women. Am Rev Respir Dis 1990;141(1):68-71.
73. Schlaich C, Minne HW, Bruckner T, Wagner G, Gebest HJ, Grunze M, Ziegler R, Leidig-Bruckner G. Reduced pulmonary function in patients with spinal osteoporotic fractures. Osteoporos Int 1998;8(3):261–267.

74. Raisadeh K. Surgical management of adult kyphosis: idiopathic, posttraumatic and osteoporotic. Semin Spine Surg 1999;10:367-381.
75. Silverman SL, Minshall ME, Shen W, Harper KD, Xie S. The relationship of health-related quality of life to prevalent an incident vertebral fractures in postmenopausal women with osteoporosis. Arthritis Reum 2001;44(11):2611-2619.
76. Lyles KW, Gold DT, Shipp KM, Pieper CF, Martinez S, Mulhausen PL. Association of osteoporotic compression fractures with impaired functional status. Am J Med 1993;94:595-601.
77. Hall SE, Criddle RA, Comito TL, Prince RL. A case-control study of quality of life and functional impairment in women with long-standing vertebral osteoporotic fracture. Osteoporos Int 1999;9(6):508-15.
78. Huang MH, Barrett-Connor E, Greendale GA, Kado DM. Hyperkyphotic posture and risk of future osteoporotic fractures: the Rancho Bernardo study. J Bone Miner Res. 2006;21(3):419-23.
79. Roux C, Fechtenbaum J, Kolta S, Said-Nahal R, Briot K, Benhamou CL. Prospective assessment of thoracic kyphosis in postmenopausal women with osteoporosis. J Bone Miner Res. 2010;25(2):362-8
80. Briggs AM, van Dieën JH, Wrigley TV, Greig AM, Phillips B, Lo SK, Bennell KL. Thoracic kyphosis affects spinal loads and trunk muscle force. Phys Ther. 2007;87(5):595-607.
81. De Smet AA, Robinson RG, Johnson BE, Lukert BP. Spinal compression fractures in osteoporotic women: patterns and relationship to hyperkyphosis. Radiology 1988;166:497-500.
82. Hedlund LR, Gallagher JC, Meeger C, Stoner S. Change in vertebral shape in spinal osteoporosis. Calcif Tissue Int. 1989;44(3):168-72.
83. Lee YL, Yip KM. The osteoporotic spine. Clin Orthop 1996;323:91-97.
84. Gaitanis IN, Carandang G, Phillips FM, Magovern B, Ghanayem AJ, Voronov LI et al. Restoring geometric and loading alignment of the thoracic spine with a vertebral compression fracture: effects of balloon (bone tamp) inflation and spinal extension. Spine J 2005;5(1):45–54.
85. Mizrahi J, Silva MJ, Keaveny TM, Edwards WT, Hayes WC. Finite-element stress analysis of the normal and osteoporotic lumbar vertebral body. Spine 1993;18(14):2088-2096.

86. Ismail AA, Cockerill W, Cooper C, et al. Prevalent vertebral deformity predicts incident hip though not distal forearm fracture: results from the European Prospective Osteoporosis Study. Osteoporosis Int 2001;12(2):85-90.
87. Kado DM, Huang MH, Nguyen CB, Barrett-Connor E, Greendale GA. Hyperkyphotic posture and risk of injurious falls in older persons: the Rancho Bernardo Study. J Gerontol A Biol Sci Med Sci. 2007;62(6):652-7.
88. Kim SH, Kang HS, Choi JA, Ahn JM. Risk factors of new compression fractures in adjacent vertebrae after percutaneous vertebroplasty. Acta Radiol 2004;45(4):440–445.
89. Lee WS, Sung KH, Jeong HT, et al. Risk factors of developing new symptomatic vertebral compression fractures after percutaneous vertebroplasty in osteoporotic patients. Eur Spine J 2006;15(12):1777–1783.
90. Chin DK, Kim YS, Cho YE, Shin JJ. Efficacy of postural reduction in osteoporotic vertebral compression fractures followed by percutaneous vertebroplasty. Neurosurgery 2006;58(4):695-700.
91. Carlier RY, Gordji H, Mompoint D, et al. Osteoporotic vertebral collapse: percutaneous vertebroplasty and local kyphosis correction. Radiology 2004;233:891-898.
92. Jang JS, Kim DY, Lee SH. Efficacy of percutaneous vertebroplasty in the treatment of intravertebral pseudarthrosis associated with noninfected avascular necrosis of the vertebral body. Spine 2003;28(14):1588-1592.
93. Teng MM, Wei CJ, Wei LC, et al. Kyphosis correction and height restoration effects of percutaneous vertebroplasty. Am J Neuroradiol 2003;24(9):1893-1900.
94. Hiwatashi A, Moritani T, Numaguchi Y, Westesson PL. Increase in vertebral body height after vertebroplasty. Am J Neuroradiol 2003;24(2):185-189
95. Dublin AB, Hartman J, Latchaw RE, et al. The vertebral body fracture in osteoporosis: restoration of height using percutaneous vertebroplasty. Am J Neuroradiol 2005;26(3):489-492.

96. Voggenreiter G. Balloon kyphoplasty is effective in deformity correction of osteoporotic vertebral compression fractures. Spine 2005;30(24):2806-12.
97. Orler R, Frauchiger LH, Lange U, Heini PF. Lordoplasty: report on early results with a new technique for the treatment of vertebral compression fractures to restore the lordosis. Eur Spine J 2006;15(12):1769-1775.
98. Grohs JG, Matzner M, Trieb K, Krepler P. Minimal invasive stabilization of osteoporotic vertebral fractures: a prospective nonrandomized comparison of vertebroplasty and balloon kyphoplasty. J Spinal Disord Tech 2005;18(3):238-242.
99. Gaitanis I, Hadjipavlou AG, Katonis PG, et al. Balloon kyphoplasty for the treatment of pathological vertebral compressive fractures. Eur Spine J 2005;14(3):250-260.
100. Crandall D, Slaughter D, Hankins PJ, et al. Acute versus chronic vertebral compression fractures treated with Kyphoplasty: early results. Spine J 2004;4(4):418-424.
101. Phillips FM, Ho E, Campbell-Hupp M, et al. Early radiographic and clinical results of balloon kyphoplasty for the treatment of osteoporotic vertebral compression fractures. Spine 2003;28(19):2260-2267.
102. Berlemann U, Franz T, Orler R, Heini PF. Kyphoplasty for treatment of osteoporotic vertebral fractures: a prospective non-randomized study. Eur Spine J 2004;13(6):496-501.
103. Majd ME, Farley S, Holt RT. Preliminary outcomes and efficacy of the first 360 consecutive kyphoplasties for the treatment of painful osteoporotic vertebral compression fractures. Spine J 2005;5:244-255.
104. Shindle MK, Gardner MJ, Koob J, Bukata S, Cabin JA, Lane JM. Vertebral height restoration in osteoporotic compression fractures: kyphoplasty balloon tamp is superior to postural correction alone. Osteoporos Int 2006;17(12):1815–1819.
105. Heini PF, Orler R. Kyphoplasty for treatment of osteoporotic vertebral fractures. Eur Spine J 2004;13(3):184-192.

106. Boszczyk BM, Bierschneider M, Schmid K, et al. Microsurgical interlaminary vertebro- and kyphoplasty for severe osteoporotic fractures. J Neurosurg 2004;100:Suppl Spine:32–37.
107. Pradhan BB, Bae HW, Kropf MA, et al. Kyphoplasty reduction of osteoporotic vertebral compression fractures: correction of local kyphosis versus overall sagittal alignment. Spine 2006;31(4):435-441.
108. Kurowski P, Kubo A. The relationship of degeneration of the intervertebral disc to mechanical loading conditions on lumbar vertebrae. Spine 1986;11:726–731.
109. Liu L, Pei F, Song Y et al. The influence of the intervertebral disc on stress distribution of the thoracolumbar vertebrae under destructive load. Chin J Traumatol 2002;5:279–283
110. Pollintine P, Dolan P, Tobias JH, Adams MA. Intervertebral disc degeneration can lead to "stress-shielding" of the anterior vertebral body: a cause of osteoporotic vertebral fracture. Spine 2004;29(7):774-782.
111. Schultz A. Loads in the lumbar spine. In Jayson MVI, ed. The Lumbar Spine and Back Pain. Edinburg: Churchill Livingstone, 1987:204-214.
112. McNally DS, Adams MA, Goodship AE. Development and validation of a new transducer for intradiscal pressure measurement. J Biomed Eng 1992;14:495-8.
113. Goel VK, Weinstein JN, Patwardhan A. Biomechanics of the intact ligamentous spine. Chapter 6, In: Biomechanics of the spine-Clinical and surgical perspective, Edited by V. K. Goel and J. N. Weinstein, CRC Press, 1990; pp. 97-156.
114. Adams, McNally DS,ChinnH, et al. Posture and the compressive strength of the lumbar spine. Clin Biomech 1994;95-14.
115. McDevitt CA. Proteoglycans of the intervertebral disc. Chapter 6, In: The Biology of the intervertebral disc, Vol. 1, Edited by Peter Ghosh, CRC Press, 1988; pp. 151-170.
116. Gunzburg R, Parkinson R, Moore R, Cantraine F, Hutton W, Vernon-Roberts B, Fraser R. A cadaveric study comparing discography, magnetic resonance imaging, histology, and mechanical behavior of the human lumbar disc. Spine 1992;17(4):417-426.

117. Nachemson AL. Disc pressure measurements. Spine 1981;6(1):93-7.
118. Lucas DB, Bresler B. Stability of the Ligamentous Spine. San Francisco: University of California, Biomechanics Laboratory; Technical Report No. 40; 1961.
119. Patwardhan AG, Havey RM, Meade KP, et al. A follower load increases the load-carrying capacity of the lumbar spine in compression. Spine 1999;24:1003–9.
120. Stanley SK, Ghanayem AJ, Voronov LI, Havey RM, Paxinos O, Carandang G, Zindrick MR, Patwardhan AG. Flexion-extension response of the thoracolumbar spine under compressive follower preload. Spine 2004;29(22):E510-4
121. Galibert P, Deramond H, Rosat P, Le Gars D. Preliminary note on the treatment of vertebral angioma by percutaneous acrylic vertebroplasty. Neurochirurgie 1987;33: 166-8.
122. Kaemmerlen P, Thiesse P, Bouvard H, et al. Percutaneous vertebroplasty in the treatment of metastases: technic and results. J Radiol 1989;70:557-62.
123. Kaemmerlen P, Thiesse P, Jonas P, et al. Percutaneous injection of orthopaedic cement in metastatic vertebral lesions. N Engl J Med 1989;321:121.
124. Cotten A, Dewatre F, Cortet B, et al. Percutaneous vertebroplasty for osteolytic metastases and myeloma: effects of the percentage of lesion filling and the leakage of methylmethacrylate at clinical follow-up. Radiology 1996;200:525-30.
125. Lapras C, Mottolese C, Deruty R, et al. Percutaneous injection of methyl-methacrylate in the treatment of severe vertebral osteolysis (Galibert's technic). Ann Chir 1989;43:371-6.
126. Jensen ME, Evans AJ, Mathis JM, et al. Percutaneous polymethylmethacrylate vertebroplasty in the treatment of osteoporotic vertebral body compression fractures: technical aspects. AJNR Am J Neuroradiol 1997;18:1897-904.
127. Garfin SR, Yuan HA, Reiley MA. New technologies in spine: kyphoplasty and vertebroplasty for treatment of painful osteoporotic fractures. Spine 2001;26:1511-15.

128. Lieberman IH, Dudeney S, Reinhardt MK, Bell G. Initial outcome and efficacy of “kyphoplasty” in the treatment of painful osteoporotic vertebral compression fractures. Spine 2001;26:1631-738.
129. Dudeney S, Lieberman IH, Reinhardt MK, Hussein M. Kyphoplasty in the treatment of osteolytic vertebral compression fractures as a result of multiple myeloma. J Clin Oncol 2002;20:2382-7.
130. Belkoff SM, Mathis JM, Erbe EM, Fenton DC. Biomechanical evaluation of a new bone cement for use in vertebroplasty. Spine 2000;25(9):1061-1064.
131. Belkoff SM, Mathis JM, Jasper LE, Deramond H. The biomechanics of vertebroplasty: the effect of cement volume on mechanical behavior. Spine 2001; 26:1537-1541.
132. Molloy S, Mathis JM, Belkoff SM. The effect of vertebral body percentage fill on mechanical behavior during percutaneous vertebroplasty. Spine. 2003;28(14):1549-1554.
133. Liebschner MA, Rosenberg WS, Keaveny TM. Effects of bone cement volume and distribution on vertebral stiffness after vertebroplasty. Spine 2001;26(14):1547-1554.
134. Heini PF, Berlemann U, Kaufmann M, Lippuner K, Fankhauser C, van Landuyt P. Augmentation of mechanical properties in osteoporotic vertebral bones-a biomechanical investigation of vertebroplasty efficacy with different bone cements. Eur Spine J 2001;10(2):164-171.
135. Higgins KB, Harten RD, Langrana NA, Reiter MF. Biomechanical effects of unipedicular vertebroplasty on intact vertebrae. Spine 2003;28(14):1540-1548.
136. Tomita S, Kin A, Yazu M, Abe M. Biomechanical evaluation of kyphoplasty and vertebroplasty with calcium phosphate cement in a simulated osteoporotic compression fracture. J Orthop Sci 2003;8:192-197.
137. Belkoff SM, Maroney M, Fenton DC, Mathis JM. An in vitro biomechanical evaluation of bone cements used in percutaneous vertebroplasty. Bone 1999;25(2 Suppl):23S-26S.
138. Luo J, Skrzypiec DM, Pollintine P, Adams MA, Annesley-Williams DJ, Dolan P. Mechanical efficacy of vertebroplasty: influence of cement

type, BMD, fracture severity, and disc degeneration. Bone 2007;40(4):1110-1119.

139. Deramond H, Depriester C, Toussaint P, et al Percutaneous vertebroplasty. Semin Musculoskelet Radiol 1997;1:285-295.
140. Mathis JM, Barr JD, Belkoff SM, Barr MS, Jensen ME, Deramond H. Percutaneous vertebroplasty: a developing standard of care for vertebral compression fractures. AJNR Am J Neuroradiol 2001;22(2):373-381.
141. Belkoff SM, Mathis JM, Jasper LE, Deramond H. An ex vivo biomechanical evaluation of hydroxyapatite cement for use with vertebroplasty. Spine 2001;26(14):1542-1546.
142. Jansen LE, Deramont H, Matis JM, et al. The effect of monomer-to-powder ratio on the material properties of cranioplastic. Bone 1999;25(Suppl):27-29.
143. Belkoff SM, Mathis JM, Fenton DC, Scribner RM, Reiley ME, Talmadge K. An ex vivo biomechanical evaluation of an inflatable bone tamp used in the treatment of compression fracture. Spine 2001;26(2):151-156.
144. Kim MJ, Lindsey DP, Hannibal M, Alamin TF. Vertebroplasty versus kyphoplasty: biomechanical behavior under repetitive loading conditions. Spine 2006;31(18):2079-2084
145. Ha KY, Lee JS, Kim KW, Chon JS. Percutaneous vertebroplasty for vertebral compression fractures with and without intravertebral clefts. JBJS Br 2006;88B:629-633.
146. Molloy S, Riley LH 3rd, Belkoff SM. Effect of cement volume and placement on mechanical-property restoration resulting from vertebroplasty. AJNR Am J Neuroradiol 2005;26(2):401-404.
147. Berlemann U, Ferguson SJ, Nolte LP, Heini PF. Adjacent vertebral failure after vertebroplasty: a biomechanical investigation. J Bone Joint Surg Br 2002;84:748-752.
148. Komemushi A, Tanigawa N, Kariya S, Kojima H, Shomura Y, Komemushi S, Sawada S. Percutaneous vertebroplasty for osteoporotic compression fracture: Multivariate study of predictors of

new vertebral body fracture. Cardoivasc Intervent Radiol 2006;29:580-585.

149. Lin EP, Ekholm S, Hiwatashi A, Westesson PL. Vertebroplasty: cement leakage into the disc increases the risk of new fracture of adjacent vertebral body. Am J Neuroradiol 2004;25(2):175-180.
150. Syed MI, Patel NA, Jan S, et al. Intradiskal extravasation with low-volume cement filling in percutaneous vertebroplasty. Am J Neuroradiol 2005;26(9):2397-401.
151. Kasperk C, Hillmeier J, Noldge G, et al. Treatment of painful vertebral fractures by kyphoplasty in patients with primary osteoporosis: a prospective nonrandomized controlled study. J Bone Miner Res 2005;20(4):604-612.
152. Grafe IA, Da Fonseca K, Hillmeier J, et al. Reduction of pain and fracture incidence after kyphoplasty: 1-year outcomes of a prospective controlled trial of patients with primary osteoporosis. Osteoporos Int 2005;16(12):2005-2012.
153. Komp M, Ruetten S, Godolias G. Minimally invasive therapy for functionally unstable osteoporotic vertebral fracture by means of kyphoplasty: a prospective comparative study of 19 surgically and 17 conservatively treated patients. J Miner Stoffwechs 2004;1(suppl 1):13-15.
154. Patwardhan AG, Havey RM, Carandang G, Simonds J, Voronov LI, Ghanayem AJ et al. Effect of compressive follower preload on the flexion-extension response of the human lumbar spine. J Orthop Res 2003;21:540–546.
155. Belkoff SM, Mathis JM, Deramond H et al. An ex vivo biomechanical evaluation of hydroxyapatite cement for use with kyphoplasty. AJNR Am J Neuroradiol 2001;22:1212–1216
156. Windhagen HJ, Hipp JA, Silva MJ, Lipson SJ, Hayes WC. Predicting failure of thoracic vertebrae with simulated and actual metastatic defects. Clin Orthop Relat Res 1997;(344):313-9.
157. Farooq N, Park JC, Pollintine P, Annesley-Williams DJ, Dolan P. Can vertebroplasty restore normal load-bearing to fractured vertebrae? Spine 2005;30(15):1723–1730.

158. Hongo M, Abe E, Shimada Y, Murai H, Ishikawa N, Sato K. Surface strain distribution on thoracic and lumbar vertebrae under axial compression. Spine 1999;24:1197–1202.
159. Lin HS, Liu YK, Adams KH. Mechanical response of the lumbar intervertebral joint under physiological (complex) loading. J Bone Joint Surg 1978;60(1):41–55.
160. Ranu HS. Measurement of pressures in the nucleus and within the annulus of the human spinal disc due to extreme loading. Proc Inst Mech Eng [H] 1990;204:141–145.
161. Shah JS, Hampson WG, Jayson MI. The distribution of surface strain in the cadaveric lumbar spine. J Bone Joint Surg 1978;60-B(2):246–251.
162. Lin CC, Chen IH, Yu TC, Chen A, Yen PS. New symptomatic compression fracture after percutaneous vertebroplasty at the thoracolumbar junction. AJNR Am J Neuroradiol 2007;28(6):1042–1045.
163. Sornay-Rendu E, Munoz F, Duboeuf F, Delmas PD (2004) Disc space narrowing is associated with an increased vertebral fracture risk in postmenopausal women: the OFELY Study. J Bone Miner Res 19(12):1994–1999
164. Hadjipavlou AG, Tzermiadianos MN, Katonis PG, Szpalski M. Percutaneous vertebroplasty and balloon kyphoplasty for the treatment of osteoporotic vertebral compression fractures and osteolytic tumours. J Bone Joint Surg Br 2005;87(12):1595–1604
165. Hulme PA, Krebs J, Ferguson SJ, Berlemann U. Vertebroplasty and kyphoplasty: a systematic review of 69 clinical studies. Spine 2006;31(17):1983–2001.

Citations

Article: Tzermiadianos MN, Renner SM, Phillips FM, Hadjipavlou AG, Zindrick MR, Havey RM, Voronov M, Patwardhan AG. Altered disc pressure profile after an osteoporotic vertebral fracture is a risk factor for adjacent vertebral body fracture. Eur Spine J. 2008 Nov;17(11):1522-30

Cited in 20 publications

1. Chen C, Li D, Wang Z, Li T, Liu X, Zhong J. Safety and Efficacy Studies of Vertebroplasty, Kyphoplasty, and Mesh-Container-Plasty for the Treatment of Vertebral Compression Fractures: Preliminary Report. PLoS One 2006 Mar 10;11(3):e0151492
2. Padányi C, Misik F, Papp Z, Vitanovics D, Balogh A, Veres R, Lipóth L, Banczerowski P. [Treatment of osteoporotic vertebral compression fracture with PMMA augmented pedicle screw fixation] Osteoporoticus kompressziós csigolyatörések kezelése pmma-augmentált csavaros transpedicularis rögzitéssel] Ideggyogyaszati Szemle 2015 Jan 30;68(1-2):52-8
3. Landham PR, Gilbert SJ, Baker-Rand HL, Polintine P, Robson Brown KA, Adams MA, Dolan P. Pathogenesis of vertebral anterior wedge deformity: a 2-stage process? Spine 2015 Jun 15;40(12):902-8.
4. Baeesa SS, Krueger A, Aragón FA, Noriega DC. The efficacy of a percutaneous expandable titanium device in anatomical reduction of vertebral compression fractures of the thoracolumbar spine. Saudi Medical Journal 2015 Jan;36(1):52-60
5. Doulgeris JJ, Gonzalez-Blohm SA, Aghayev K, Shea TM, Lee WE, Hess DP, Vrionis FD. Axial rotation mechanics in a cadaveric lumbar spine model: A biomechanical analysis. The Spine Journal 2014 Jul 1;14(7):1272-9
6. Tontz B Jr. Perspective: Vertebral Compression Fractures Caused by Osteoporosis and Available Treatments. Topics in Pain Management 2014 Jan;29(6):7-9
7. Liu XW, Kong XY, Zhong J, (...), Du YX, Sun G. Bone filling mesh container repairs vertebral compression fractures: Biomechanical changes. Journal of Clinical Rehabilitative Tissue Engineering Research 2014 Apr;18(16):2487-

92
8. Xie ZY, Liu XW, Zhong J, (...), Du YX, Sun G. Calcium phosphate bone cement and biodegradable mesh-like microporous balloon for vertebroplasty. Journal of Clinical Rehabilitative Tissue Engineering Research 2014 18(47): 7566-72
9. Yi X, Lu H, Tian F, Wang Y, Li C, Liu X, Li H. Recompression in new levels after percutaneous vertebroplasty and kyphoplasty compared with conservative treatment. Archives of Orthopaedic and Trauma Surgery 2014 Jan;134(1):21-30
10. Li JC, Liu PJ, He YL, Zhao WD, Liang DZ, Mao BY. Primary development and biomechanics of single vertebrae internal fixation system for thoracolumbar compression fracture. Journal of Clinical Rehabilitative Tissue Engineering Research 2014 Feb 18(9):1350-55
11. Yamada K, Suzuki A, Takahashi S, (...), Koike T, Nakamura H. MRI evaluation of lumbar endplate and facet erosion in rheumatoid arthritis. J Spinal Disord Tech 2014 Jun;27(4):E128-35
12. Dolan P, Luo J, Pollintine P, Landham PR, Stefanakis M, Adams MA. Intervertebral disc decompression following endplate damage: Implications for disc degeneration depend on spinal level and age. Spine 2013 Aug 1;38(17):1473-81
13. Peng XT, Liu XW, Li M, Zhong J, Wei DX, He DN, Sun G. Vertebral bodies implanted with biodegradable reticulated balloon and calcium phosphate cement: Changes in the vertebral biomechanics. Chinese Journal of Tissue Engineering Research 2013;17(51):8795-00
14. Doulgeris JJ, Aghayev K, Gonzalez-Blohm SA, Del Valle M, Waddell J, Lee WE 3rd, Vrionis FD. Comparative analysis of posterior fusion constructs as treatments for middle and posterior column injuries: An in vitro biomechanical investigation. Clinical Biomechanics 2013 Jun;28(5):483-9
15. Choi WH, Oh SH, Lee CJ, Rhim JK, Chung BS, Hong HJ. Usefulness of SPAIR Image, Fracture Line and the Adjacent Discs Change on Magnetic Resonance Image in the Acute Osteoporotic Compression Fracture Korean Journal of Spine, 2012 Sep;9(3):227-31
16. Renner SM, Tsitsopoulos PP, Dimitriadis AT, (...), Ringelstein JG, Patwardhan AG. Restoration of spinal alignment and disk mechanics

following polyetheretherketone wafer kyphoplasty with StaXx FX. American Journal of Neuroradiology 2011 Aug;32(7):1295-300
17. Verdoia C, Macchi V, Bernieri J, Corradini C. Criticality of kyphoplasty and vertebroplasty. Aging Clin Exp Res. 2011 Apr;23(2 Suppl):47-8.
18. Hadley C, Awan OA, Zoarski GH. Biomechanics of vertebral bone augmentation. Neuroimaging Clin N Am 2010 May;20(2):159-67.
19. Pratelli E, Cinotti I, Pasquetti P. Rehabilitation in osteoporotic vertebral fractures. Clin Cases Miner Bone Metab 2010 Jan;7(1):45-7
20. Heyde CE, Rohlmann A, Weber U, Kayser R. [Stabilization of the osteoporotic spine from a biomechanical viewpoint] Stabilisierung der osteoporotischen Wirbelsäule unter biomechanischen Gesichtspunkten. Orthopäde 2010 Apr;39(4):407-16

Eur Spine J (2008) 17:1522–1530
DOI 10.1007/s00586-008-0775-x

ORIGINAL ARTICLE

Altered disc pressure profile after an osteoporotic vertebral fracture is a risk factor for adjacent vertebral body fracture

Michael N. Tzermiadianos · Susan M. Renner · Frank M. Phillips · Alexander G. Hadjipavlou · Michael R. Zindrick · Robert M. Havey · Michael Voronov · Avinash G. Patwardhan

Received: 29 October 2007 / Revised: 2 August 2008 / Accepted: 31 August 2008 / Published online: 16 September 2008

Abstract This study investigated the effect of endplate deformity after an osteoporotic vertebral fracture in increasing the risk for adjacent vertebral fractures. Eight human lower thoracic or thoracolumbar specimens, each consisting of five vertebrae were used. To selectively fracture one of the endplates of the middle VB of each specimen a void was created under the target endplate and the specimen was flexed and compressed until failure. The fractured vertebra was subjected to spinal extension under 150 N preload that restored the anterior wall height and vertebral kyphosis, while the fractured endplate remained significantly depressed. The VB was filled with cement to stabilize the fracture, after complete evacuation of its trabecular content to ensure similar cement distribution under both the endplates. Specimens were tested in flexion-extension under 400 N preload while pressure in the discs and strain at the anterior wall of the adjacent vertebrae were recorded. Disc pressure in the intact specimens increased during flexion by 26 ± 14%. After cementation, disc pressure increased during flexion by 15 ± 11% in the discs with un-fractured endplates, while decreased by 19 ± 26.7% in the discs with the fractured endplates. During flexion, the compressive strain at the anterior wall of the vertebra next to the fractured endplate increased by 94 ± 23% compared to intact status ($p < 0.05$), while it did not significantly change at the vertebra next to the un-fractured endplate (18.2 ± 7.1%, $p > 0.05$). Subsequent flexion with compression to failure resulted in adjacent fracture close to the fractured endplate in six specimens and in a non-adjacent fracture in one specimen, while one specimen had no adjacent fractures. Depression of the fractured endplate alters the pressure profile of the damaged disc resulting in increased compressive loading of the anterior wall of adjacent vertebra that predisposes it to wedge fracture. This data suggests that correction of endplate deformity may play a role in reducing the risk of adjacent fractures.

Keywords Osteoporosis · Compression fractures · Adjacent fractures · Cement augmentation · Biomechanics · Intervertebral disc

M. N. Tzermiadianos · R. M. Havey · A. G. Patwardhan (✉)
Department of Orthopaedic Surgery and Rehabilitation,
Loyola University Medical Center, 2160 S. First Avenue,
Maywood, IL 60153, USA
e-mail: apatwar@lumc.edu

M. N. Tzermiadianos · A. G. Hadjipavlou
University Hospital of Crete, Heraklion, Crete, Greece

S. M. Renner · R. M. Havey · M. Voronov · A. G. Patwardhan
Department of Veterans Affairs,
Edward Hines Jr. VA Hospital, Hines, IL, USA

F. M. Phillips
Rush University, Chicago, IL, USA

M. R. Zindrick
Hinsdale Orthopaedic Associates, Hinsdale, IL, USA

Introduction

The presence of an osteoporotic vertebral compression fracture (OVCF) increases the risk for subsequent vertebral fractures [27, 30, 38]. Lindsay et al. [27] reported an incidence of 11.5% of new vertebral fractures within 1 year following one previous OVCF, whereas this incidence was 24% in women with two or more fractures. Similarly, Ross et al. [38] reported that a single fracture increases the risk fivefold for new vertebral fractures, while the presence of two or more fractures increases the risk 12-fold. Silverman

et al. [42] reported that 58% of women with one or more fractures had adjacent fractures, supporting the high rate of adjacent fractures in the natural history of the disease. In a similar fashion, new vertebral fractures, especially at the adjacent vertebral bodies, have been reported after cement augmentation of an osteoporotic vertebral fracture [11, 13, 21, 22, 24, 45, 48–51].

The severity of vertebral collapse and the residual kyphotic deformity have been associated with the risk for subsequent vertebral fractures [9, 35, 46]. Kyphotic deformity shifts the center of gravity forward, resulting in increased forward bending moments, which are in turn compensated by a contraction of the posterior spinal muscles, resulting in an increased load within the kyphotic segment [37, 52]. Using anterior wall strain gauges, Kayanja et al. [17, 18] showed that after an experimentally induced osteoporotic fracture, the addition of flexion to axial compression increases the axial compressive loads at the adjacent vertebrae, supporting the role of residual kyphosis.

In vitro experiments have shown that damage to the vertebral body endplate reduces the pressure in the nucleus of the adjacent disc [1, 3, 4] and generates peaks of compressive stress in the annulus, usually posteriorly to the nucleus [1, 3]. Stress concentrations are affected by posture, and lordosis has been associated with intensified stress in the posterior anulus [3]. Furthermore, load distribution between the trabecular centrum of the vertebral body and the cortex is dependent on the properties of the intervertebral disc [20, 28]. Therefore, the altered mechanical properties of the intervertebral disc after an osteoporotic compression fracture with endplate depression are expected to change load distribution to the adjacent areas of the spine.

The purpose of this biomechanical study was to test the hypothesis that the altered pressure profile of the intervertebral disc after an osteoporotic vertebral fracture, even in the absence of kyphotic deformity, will alter load transmission to the adjacent vertebra and increase vertical loading of the anterior wall of adjacent vertebrae, predisposing them to wedge fracture.

Materials and methods

Specimens and experimental set-up

Eight fresh frozen human lower thoracic (T7–T11) or thoracolumbar (T10–L2) specimens each consisting of five vertebrae were used. The specimens were from five females and three males whose ages ranged from 56 to 82 years (average: 69 ± 8.5 years). Specimens were radiographically screened to exclude existing osteoporotic fractures, severe intervertebral space narrowing, bridging osteophytes and signs of vertebral metastasis. The specimens were thawed at room temperature (20°C) 24 h before testing. The paravertebral muscles were dissected, while keeping the discs, ligaments and posterior bony structures intact. The cephalad and caudal vertebrae of each specimen were anchored in cups using bone cement and pins.

The specimen was fixed to the testing apparatus at the caudal end and was free to move at the cephalad end. A moment was applied by controlling the flow of water into bags attached to 50-cm loading arms fixed to the cephalad vertebra. The long moment arm used to apply the moment loading resulted in nearly equal bending moments at each level. A six-axis load cell (Model MC3A-6-250, AMTI Inc., Newton, MA) was placed under the specimen to measure the applied loads and moments. The apparatus allowed for continuous cycling of the specimen between specified maximum moment endpoints in flexion and extension.

The motion of the cephalad vertebra of the specimen relative to the caudal one was measured using an optoelectronic motion measurement system (model 3020, Optotrak; Northen Digital, Waterloo, ON, Canada). In addition, biaxial angle sensors (model 902–45; Applied Geomechanics, Santa Cruz, CA) were mounted on the cephalad and caudal vertebrae to allow real time feedback for the optimization of the preload path. The spines were instrumented with pressure transducers (model 060S-1000, Precision Measurement Co., Ann Arbor, MI) in the nucleus of the discs above and below the middle vertebra. The pressure transducers were calibrated prior to the testing of each specimen using a pressure chamber. The anterior wall of the vertebral bodies adjacent to the middle vertebra were instrumented with single element strain gauges (FLA-2-11-3L, Sokki Kenkyujo, Tokio) to measure vertical (compressive) strain (Fig. 1).

The concept of the follower load was used to apply compressive preload; therefore, the preload was applied along a path that followed the curve of the spine [32]. An advantage of follower load application is that segmental bending moments and shear forces due to the preload application are minimized [33]. This allows a multi-segment thoracic spine specimen to support physiologic compressive preloads without constraining the motion of the vertebrae in the sagittal plane [44]. The preload was applied using bilateral loading cables attached to the cup holding the cephalad vertebra. The cables passed freely through guides anchored to the vertebrae adjacent to the target vertebra (Fig. 1). To avoid the creation of stress risers, the cable guide mounting technique did not violate the cortices of the vertebral bodies adjacent to the target vertebra. The cable guide mounts allowed anterior–posterior adjustments of the follower load path. The alignment of the preload path was optimized by adjusting the cable

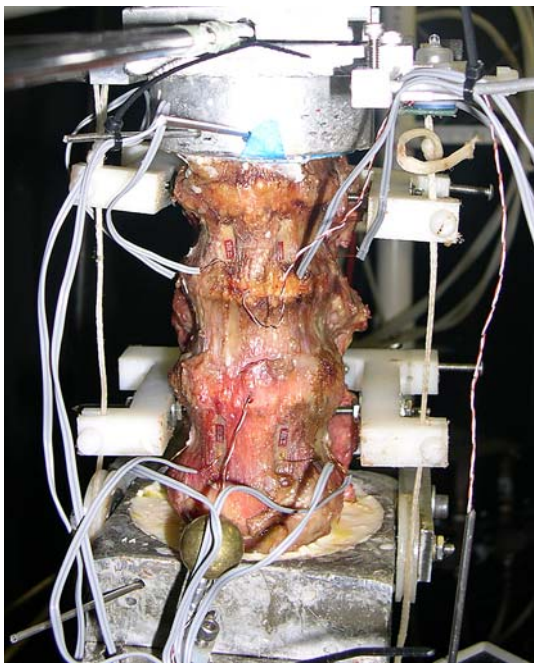

Fig. 1 Photograph of a specimen positioned on the testing apparatus. Strain gauges are mounted at the anterior walls and pressure sensors in the discs. Bilateral loading cables pass through guides mounted at the posterior elements

guide locations to minimize changes in the sagittal alignment of the specimen when compressive load up to 400 N was applied. The loading cables were connected to loading actuators under the specimen and were coated with radiopaque barium solution to be visible on X-ray images. A calibration marker (a radiopaque ball, 25.4 mm in diameter) was visible on each X-ray image.

Experimental protocol

Each specimen was first tested intact under flexion-extension moments (±6 Nm) with a 400 N compressive preload. Pressure was recorded at the discs above and below the middle vertebra and compressive strain was recorded at the anterior wall of the adjacent vertebrae. Total range of motion (ROM) of the specimen was measured using the optoelectronic motion measurement system.

Experimental creation of VCF

A novel technique was utilized to selectively fracture only one of the endplates of the middle VB of each specimen. Through a small opening on the anterior wall close to the target endplate, a void was created selectively under the endplate and was extended to one-third of the VB trabecular content; thereby creating a "stress-riser". (Fig. 2a, b). The endplate was carefully scraped free of trabecular connections using curettes and pituitaries. The void was randomly assigned under the upper endplate in four specimens and under the lower endplate in four. The specimen was flexed to 5 Nm and compressed using the loading cables until a fracture under the target endplate was observed on fluoroscopy or until a load limit of 700 N was reached (Fig. 2c). The maximum load limit of 700 N was used to avoid the likelihood of failure of the other endplate or other than the target vertebra; as this load magnitude is significantly less than the failure load reported in the literature [6, 7, 47]. If no fracture was observed on fluoroscopy, the instruments were reintroduced, the void was extended, and the specimen was again loaded in flexion and compression. After the fracture was established, the specimen remained under a physiologic compressive preload of 150 N. This value of compressive preload was selected taking into account the reported range of compressive preload on the lumbar spine in the prone position [39].

Reduction of the vertebral kyphotic deformity using spinal extension

The fracture was reduced by applying extension moment to the specimen under 150 N preload, aiming to completely

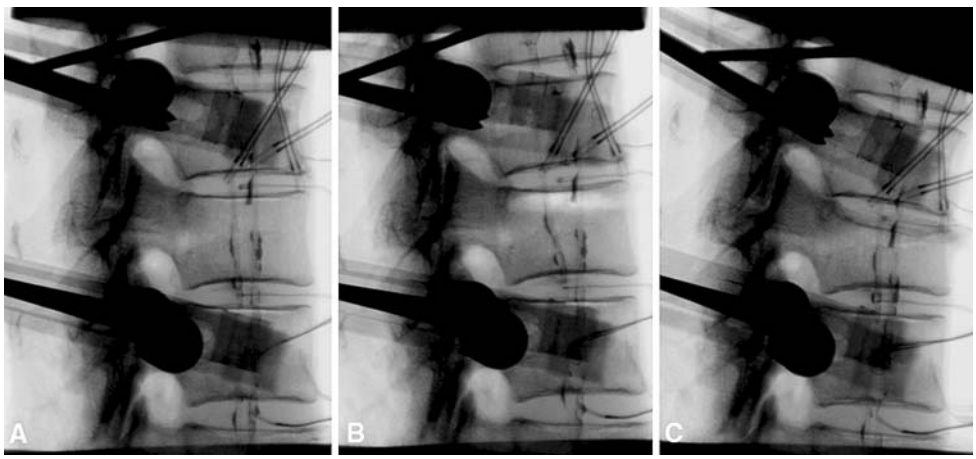

Fig. 2 Digital fluoroscopy images of a specimen. **a** Intact specimen. The bilateral loading cables, coated with radiopaque barium solution, are visible on the X-ray images. **b** Radiographic appearance of the void created under the upper endplate of the middle vertebra. **c** Image of the wedge fracture affecting only the upper part of the index vertebra

restore the pre-fracture anterior wall height and therefore correct the vertebral kyphosis angle (Fig. 3a). The extension moment was applied using upward force on the anterior loading arm fixed to the uppermost vertebra. After stabilization of the reduced fracture by cement injection into the void through the anterior opening, (Fig. 3b), the rest of the trabecular content in the middle VB was evacuated through a separate small anterior opening. The undamaged endplate was carefully scraped free of trabecular connections, and the rest of the VB was completely filled with cement under fluoroscopy to ensure proper cement distribution (Fig. 3c). Careful abrasion of both endplates ensured similar cement distribution near them. The specimen was then retested in flexion-extension (±6 Nm) under 400 N preload, and measurements of pressures at the discs adjacent to the middle vertebra and anterior wall compressive strains at the adjacent vertebrae were recorded.

Experimental creation of subsequent fractures

As a final step, the specimen was placed in flexion to 5 Nm and loaded in compression using the bilateral loading cables connected to actuators. The compressive load was gradually increased from 0 to 3,000 N or until a subsequent fracture was observed on fluoroscopy with a simultaneous sudden drop in the force versus time curve of the actuators.

Data analysis

The heights at the anterior wall and mid vertebral portion, as well as the vertebral kyphosis angle of the index vertebra were measured in the intact status, after the index fracture and after the reduction and augmentation. Mid vertebral height was measured using the depressed central endplate. Vertebral kyphosis angle was measured between the two end plates of the index vertebra. Measurements were performed on digital fluoroscopy images using computer software (Image Pro Plus, Media Cybernetics Inc). Flexion range of motion of the specimen was calculated as the angular change of the apical vertebra relative to the caudal one from the neutral posture to 6 Nm flexion. The force to failure for the index and the subsequent fractures was defined as the peak point of the force versus time curve.

The strain gauges used to measure anterior cortical strain were single element gauges and were connected in a quarter bridge (referring to Wheatstone bridge) configuration. In addition, the pressure sensors used to measure intervertebral disc pressure (model 060S) were quarter bridge diaphragm transducers. Strain gauges and transducers connected in a quarter bridge configuration are not capable of temperature compensation. These devices cannot be trusted to give absolute measurements since the output of the quarter bridge is a combination of thermal drift and measured value. Therefore, the disc pressure and adjacent vertebral wall compressive strain were normalized so that values in neutral position under 400 N preload were taken to zero, to compensate for thermal-drifting of sensors. As a result, the change in pressure and strain from neutral to full flexion before and after the creation and augmentation of the index fracture were used for analysis. Two specimens were excluded from pressure and strain analyses because of anterior slippage of pressure sensors during the experiment that resulted in inaccurate pressure recordings. The data were analyzed using repeated measures analysis of variance (ANOVA) with a significance level of $\alpha = 0.05$ using the commercial statistics package SPSS (SPSS Inc., Chicago, IL).

Results

In the intact specimens, vertebral kyphosis angle at the middle vertebra was 8.5 ± 2.2°, anterior wall height was 21.2 ± 2.7 mm, and mid vertebral height was

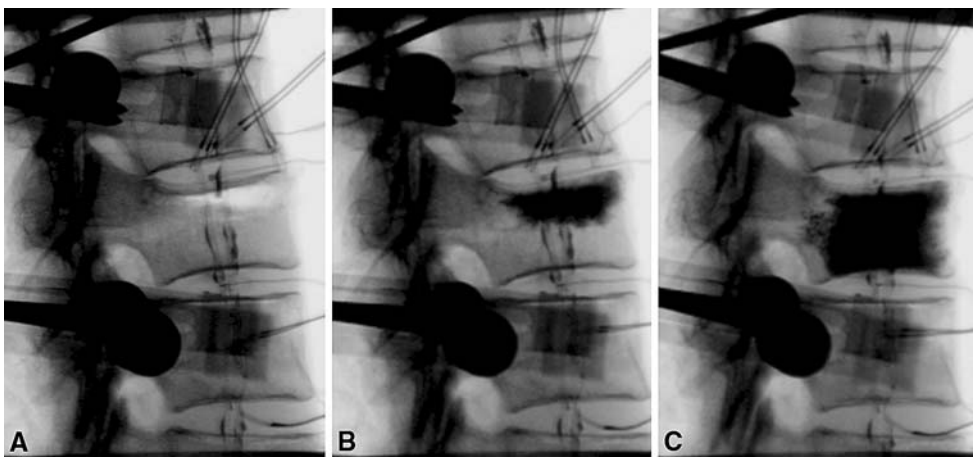

Fig. 3 Digital fluoroscopy images of a specimen **a** Reduction of anterior wall height and vertebral kyphosis angle with extension of the specimen while under 150 N preload. **b** Cement augmentation of the fracture. **c** Image showing the uniform distribution of cement under both endplates after careful abrasion of the un-fractured endplate

20.1 ± 2.9 mm. An average of 540 ± 150 N compressive load was required to fracture the target endplate of the index vertebra. No radiographic evidence of fractures at the non-target endplate or adjacent vertebral bodies was observed in any of the specimens. After the index fracture, vertebral kyphosis was 12.6 ± 2.4°, anterior wall height was 17.2 ± 3.1 mm and mid vertebral height was 14.3 ± 3.3 mm. A mean 4.6 ± 0.8 Nm extension moment, under 150 N preload, was sufficient to restore the kyphosis angle of the index vertebra to its intact value (8.8 ± 1.6°, $p = 0.38$). The anterior wall height was restored to 20.8 ± 2.6 mm, and the difference from the intact value, although statistically significant ($p = 0.04$), was small. Mid vertebral height remained significantly lower compared to intact (16.4 ± 3.0 mm, $p < 0.01$). Total flexion ROM of the specimens increased from 4.7 ± 1.4° in the intact status to 6.1 ± 2.4° after augmentation of the middle VB fracture. This increase was statistically significant ($p < 0.05$).

In the intact specimen, the pressure in the disc adjacent to the endplate assigned to remain un-fractured was 1.21 ± 1.82 MPa in the neutral posture under 400 N preload. Application of 6 Nm flexion moment increased disc pressure by 0.14 ± 0.11 MPa, representing an increase of 27.19 ± 17.4% from the pressure value in the neutral posture. After augmentation of the index fracture, the disc pressure in the neutral posture under 400 N preload was 1.34 ± 1.55 MPa. Application of 6 Nm flexion moment increased disc pressure by 0.13 ± 0.10 MPa, representing an increase of 15.8 ± 10.1% from the value in the neutral posture. The pressure change due to a flexion moment in the disc with undamaged endplates was not affected by the augmentation of the index fracture ($p = 0.55$). The disc pressure in the intact specimen adjacent to the endplate to be fractured was 0.51 ± 0.25 MPa in the neutral posture under preload. Application of 6 Nm flexion moment increased the pressure by 0.14 ± 0.10 MPa, representing an increase of 26.3 ± 9.5% from the pressure value in the neutral posture. After augmentation of the index fracture, the disc pressure at that level was 0.43 ± 0.13 MPa in the neutral posture under 400 N preload. Application of 6 Nm flexion decreased disc pressure by 0.07 ± 0.14 MPa, representing a decrease of 19.0 ± 26.8% from the value in the neutral posture (Fig. 4). The pressure change due to the application of the flexion moment in the disc with fractured endplate was significantly different from the intact ($p = 0.02$).

In the intact specimen, the compressive strain at the anterior wall of the VB adjacent to the endplate assigned to remain unfractured increased by 447.8 ± 100.4 microstrain due to the application of 6 Nm flexion moment as compared to the strain value in the neutral posture. After augmentation of the index fracture, the strain increased by 522.6 ± 131.5 microstrain from the neutral posture to 6 Nm flexion. (Fig. 4). This difference represents a non-significant change of 18.2 ± 7.1% in the anterior wall compressive strain of the adjacent vertebra next to the unfractured endplate, before and after the index fracture ($p > 0.05$). The strain at the anterior wall of the VB of the intact specimen adjacent to the endplate assigned for the index fracture increased by 413.2 ± 232.4 microstrain from the neutral posture to 6 Nm flexion. After augmentation of the index fracture, the strain increased by 836.2 ± 499.2 microstrain from the neutral posture to

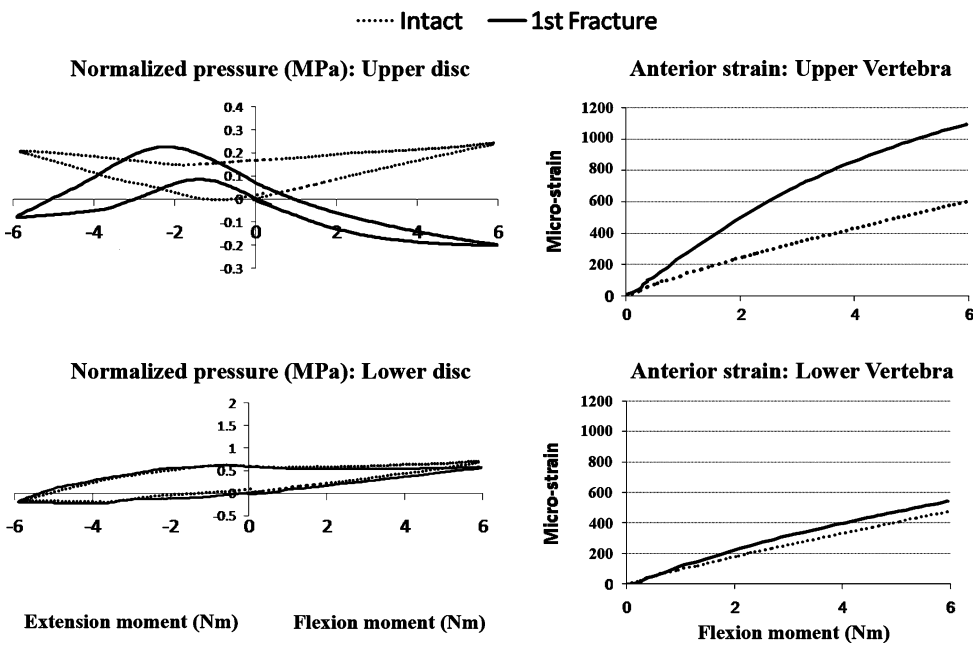

Fig. 4 Graphs showing the changes in the disc pressure (MPa) and anterior wall strain of the adjacent VBs (microstrain) after the selective damage to the upper endplate of the specimen shown in Figs. 2, 3. Data were collected during flexion-extension runs, under 400 N preload. Pressure and strain values were normalized so that values in neutral position under 400 N preload were taken to zero

6 Nm flexion. This difference represents a 94.2 ± 22.8% increase in the compressive strain of the anterior wall of the adjacent vertebra next to the damaged endplate, before and after the index fracture ($p < 0.05$). The maximum strain values seen in this study at 6 Nm of flexion were below 0.08% in all cases.

Subsequent compressive loading of the specimens in 5 Nm flexion resulted in a fracture of the adjacent VB close to the fractured endplate in six specimens and in a distal fracture at the uppermost VB in one specimen. Maximum load applied with the actuators failed to create a fracture in one of the specimens. The fractures of the adjacent vertebrae began as a depression in the anterior portion of the endplate (Fig. 5) that became gradually deeper as loading continued until the anterior wall finally failed. The failure load for the adjacent fractures was 1450 ± 402 N.

Discussion

This biomechanical study focused on the role of the endplate fracture as a risk factor for subsequent adjacent vertebral fractures. Cement was used only to stabilize the fracture and allow subsequent testing. The cementation technique used in this experiment is not relevant to any technique used in clinical practice. Because of the concerns existing in the literature about the presence of cement in the augmented vertebrae and how it may change their load bearing properties [5, 8, 34], both the endplates were carefully scraped free of any trabecular connections to ensure similar cement distribution underneath them. Therefore, any possible effect of cement presence under the endplates was a common denominator. Furthermore, restoration of the vertebral kyphosis angle by restoring the pre-fracture anterior wall height eliminated residual kyphosis as a risk factor for adjacent fractures leaving the endplate disruption as the only causal variable for the observed effects.

Experimental creation of a vertebral compression fracture is associated with uncertainty in both fracture pattern and location. Centrum defects have been previously used to assist in reproducing osteoporotic fractures in a target vertebra [12, 18]. The fracture model used in the current study allowed creating a predictable fracture not only at a target vertebra, but more specifically under the target endplate. The morphology of the fracture could also be controlled. The fracture began as depression of the weakened endplate and as the compressive load was increased, the anterior wall failed, progressing the fracture to a wedge shape while sparing the non-weakened endplate. In the current study, compressive loading was continued until the anterior wall height was reduced by approximately 25%.

Both in vivo [31, 39] and in vitro [4] studies have shown that in the intervertebral disc, the greatest pressures are exhibited in the forward flexed position under compression in activities such as lifting. The present study agrees with these findings. Furthermore, previous in vitro studies have documented that nuclear pressure is substantially reduced after an osteoporotic vertebral fracture [1, 2, 4, 10, 29] as more space becomes available for the nucleus. Our findings indicate a more specific impairment in the mechanical properties of the disc after endplate depression. The nucleus pressure is further decreased during flexion as compared to the already decreased value in the neutral posture reported in the literature. This abnormal mechanical behavior was accompanied with a simultaneous increase of the anterior wall compressive strain of the juxtaposed adjacent vertebra, which nearly doubled in

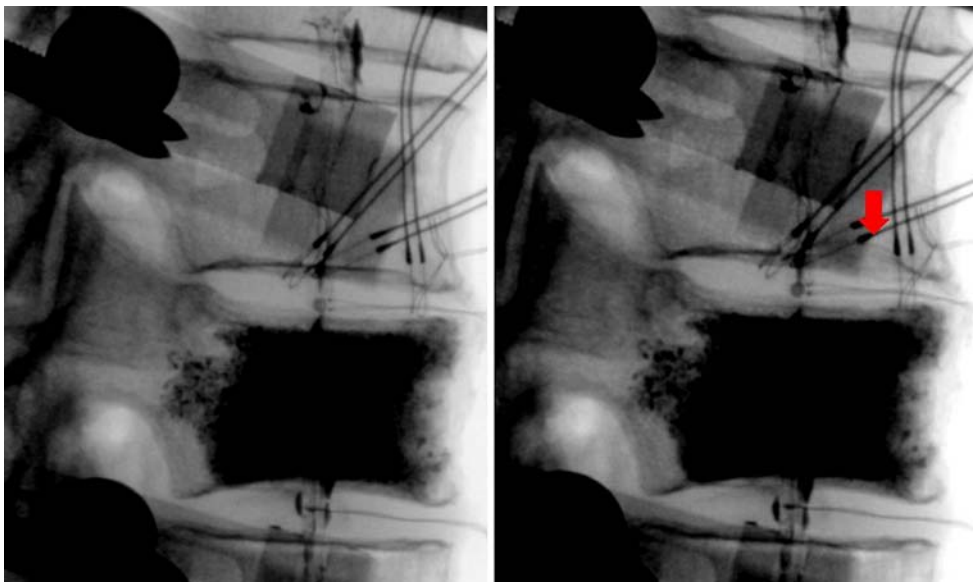

Fig. 5 Digital fluoroscopy images of the specimen shown in Figs. 2, 3 showing the initiation of a subsequent fracture at the anterior portion of the lower endplate of the upper adjacent vertebra (*arrow*), next to the damaged endplate of the index vertebra

flexion compared to the compressive stain in the intact status. On the contrary, the mechanical behavior of the undamaged disc of the fractured vertebra was not significantly affected and the compressive strain of the juxtaposed vertebral body was also not significantly altered. Previous investigators showed that anterior wall strain of adjacent vertebrae is increased with compressive load, but is more dramatically affected by flexion than by axial compression [15, 17, 18, 25, 36, 40]. Therefore, we can speculate that the small strain increase in the VB adjacent to the intact endplate found in this study could be explained by the increased flexion ROM that was observed after the fracture.

Cement augmentation using different surgical techniques, has been reported to only partially restore nucleus pressure, and the resultant pressure does not reach the pre-fracture condition [4, 10]. Our findings that after endplate fracture disc pressure is decreased during flexion as compared to the neutral posture are in contrast to previous experimental findings. Ananthakrishnan et al. [4] reported slightly higher disc pressure in flexion compared to the neutral position under axial compression after vertebroplasty for a VCF. In that study, pressure after vertebroplasty for an experimentally created vertebral fracture increased from 674 ± 111 kPa in the neutral posture under preload to 769 ± 165 kPa in the flexed position. This may suggest that the extension maneuver used in the present study to correct the vertebral kyphosis angle may have a detrimental effect on load transfer. Spinal extension exerts a ligamentotaxis effect through the anterior longitudinal ligament and annulus on the periphery of the fractured VB. Lacking tensile properties, the nucleus cannot exert a ligamentotaxis effect on the central part of the endplate, therefore central depression remains even after complete anterior wall reduction. In this context, elevation of the periphery of the endplate by spinal extension may enhance the relative central depression, leading to further compromise of nucleus mechanics. Clinical reports indicated that a greater degree of height restoration after vertebroplasty was associated with higher risk for new fractures [19, 26]. Similarly, another study reported that the rate of developing new symptomatic OVCFs after vertebroplasty was inversely correlated with the degree of wedge deformity of cemented vertebrae [23]. Although one might argue that higher cement volume in the less deformed vertebra may account for the increased rate of developing new fracture, those studies report that the risk of new fractures was not related to the volume of cement injected [23, 26]. Further clinical and biomechanical investigations are needed before reaching a definite conclusion.

It has been proposed that adjacent level load transfer through the vertebral centrum can be measured through adjacent disc pressure, while transfer through the vertebral shell can be measured through vertebral wall strain [4, 18]. Strain gauges bonded to the bone have been widely used to detect cortical bone deformation from load application. Surface strain distribution in the lumbar vertebrae measured by strain gauges has been shown to be directly proportional to compressive load [40]. Strain distribution, measured by surface strain gauges, has also been used as an indicator of the region where vertebral burst fracture initiates [15]. Similarly, stress concentration on the anterior cortex has been used to predict adjacent fracture risk after an osteoporotic compression fracture [17, 18]. Therefore, the findings from the current study support the hypothesis that endplate depression after fracture leads to significant reduction of load transfer through the centrum and increases adjacent level cortical strain, compensating for a lack of centrum support. The anterior shift of the load transfer path in flexion results in excessive load concentration in the anterior portion of the vertebra. After loading the cemented specimens to failure, nearly all subsequent fractures were located at the vertebra next to the damaged endplate. The fractures started as a depression of the anterior portion of the endplate close to the anterior wall, which subsequently led to anterior wall collapse as loading continued.

In vivo studies have reported that patients with degenerative discs have reduced nuclear pressure in all positions [39]. According to the hypothesis of the current study, those patients should also be at risk for osteoporotic vertebral fractures. This has been supported by a report that disc space narrowing is associated with an increased risk of vertebral fractures despite the higher BMD associated with spine osteoarthritis [43].

In conclusion, this study suggests that endplate depression after an osteoporotic vertebral fracture impairs the ability of the disc to distribute load evenly to the adjacent segments. Load concentration on the anterior portion of the adjacent vertebrae may contribute to increased subsequent fracture risk after an osteoporotic vertebral fracture. Current vertebral augmentation procedures for the treatment of osteoprotic VCFs have focused on the reduction of kyphosis angle and restoration of anterior vertebral body height with postural reduction or with the use of inflatable bone tamps [14, 16, 41]. The current study suggests that in addition to restoring spinal sagittal alignment, the ability to reduce the entire fractured endplate is important to restore load transmission across the fractured level.

Acknowledgments Institutional research support provided by the Department of Veterans Affairs, Washington, DC, and Kyphon Inc., Sunnyvale, CA.

References

1. Adams MA, McNally DS, Wagstaff J, Goodship AE (1993) Abnormal stress concentrations in lumbar intervertebral discs

following damage to the vertebral body: a cause of disc failure. Eur Spine J 1:214–221. doi:10.1007/BF00298362
2. Adams MA, McNally DS, Dolan P (1996) 'Stress' distributions inside intervertebral discs. The effects of age and degeneration. J Bone Joint Surg Br 78(6):965–972. doi:10.1302/0301-620X78B6.1287
3. Adams MA, Freeman BJ, Morrison HP, Nelson IW, Dolan P (2000) Mechanical initiation of intervertebral disc degeneration. Spine 25(13):1625–1636. doi:10.1097/00007632-200007010-00005
4. Ananthakrishnan D, Berven S, Deviren V et al (2005) The effect on anterior column loading due to different vertebral augmentation techniques. Clin Biomech (Bristol, Avon) 20:25–31. doi:10.1016/j.clinbiomech.2004.09.004
5. Baroud G, Nemes J, Heini P, Steffen T (2003) Load shift of the intervertebral disc after a vertebroplasty: a finite-element study. Eur Spine J 12(4):421–426. doi:10.1007/s00586-002-0512-9
6. Belkoff SM, Mathis JM, Deramond H et al (2001) An ex vivo biomechanical evaluation of hydroxyapatite cement for use with kyphoplasty. AJNR Am J Neuroradiol 22:1212–1216
7. Belkoff SM, Mathis JM, Fenton DC et al (2001) An ex vivo biomechanical evaluation of an inflatable bone tamp used in the treatment of compression fracture. Spine 26:151–156. doi:10.1097/00007632-200101150-00008
8. Berlemann U, Ferguson SJ, Nolte LP, Heini PF (2002) Adjacent vertebral failure after vertebroplasty: a biomechanical investigation. J Bone Joint Surg Br 84:748–752. doi:10.1302/0301-620X.84B5.11841
9. Black DM, Arden NK, Palermo L, Pearson J, Cummings SR (1999) Prevalent vertebral deformities predict hip fractures and new vertebral deformities but not wrist fractures. Study of Osteoporotic Fractures Research Group. J Bone Miner Res 14:821–828. doi:10.1359/jbmr.1999.14.5.821
10. Farooq N, Park JC, Pollintine P, Annesley-Williams DJ, Dolan P (2005) Can vertebroplasty restore normal load-bearing to fractured vertebrae? Spine 30(15):1723–1730. doi:10.1097/01.brs.0000171906.01906.07
11. Fribourg D, Tang C, Sra P, Delamarter R, Bae H (2004) Incidence of subsequent vertebral fracture after kyphoplasty. Spine 29(20):2270–2277. doi:10.1097/01.brs.0000142469.41565.2a
12. Gaitanis IN, Carandang G, Phillips FM, Magovern B, Ghanayem AJ, Voronov LI et al (2005) Restoring geometric and loading alignment of the thoracic spine with a vertebral compression fracture: effects of balloon (bone tamp) inflation and spinal extension. Spine J 5(1):45–54. doi:10.1016/j.spinee.2004.05.248
13. Grados F, Depriester C, Cayrolle G, Hardy N, Deramond H, Fardellone P (2000) Long-term observations of vertebral osteoporotic fractures treated by percutaneous vertebroplasty. Rheumatology 39:1410–1414. doi:10.1093/rheumatology/39.12.1410
14. Hadjipavlou AG, Tzermiadianos MN, Katonis PG, Szpalski M (2005) Percutaneous vertebroplasty and balloon kyphoplasty for the treatment of osteoporotic vertebral compression fractures and osteolytic tumours. J Bone Joint Surg Br 87(12):1595–1604. doi:10.1302/0301-620X.87B12.16074
15. Hongo M, Abe E, Shimada Y, Murai H, Ishikawa N, Sato K (1999) Surface strain distribution on thoracic and lumbar vertebrae under axial compression. Spine 24:1197–1202. doi:10.1097/00007632-199906150-00005
16. Hulme PA, Krebs J, Ferguson SJ, Berlemann U (2006) Vertebroplasty and kyphoplasty: a systematic review of 69 clinical studies. Spine 31(17):1983–2001. doi:10.1097/01.brs.0000229254.89952.6b
17. Kayanja MM, Ferrara LA, Lieberman IH (2004) Distribution of anterior cortical shear strain after a thoracic wedge compression fracture. Spine J 4(1):76–87. doi:10.1016/j.spinee.2003.07.003
18. Kayanja MM, Togawa D, Lieberman IH (2005) Biomechanical changes after the augmentation of experimental osteoporotic vertebral compression fractures in the cadaveric thoracic spine. Spine J 5(1):55–63. doi:10.1016/j.spinee.2004.08.005
19. Kim SH, Kang HS, Choi JA, Ahn JM (2004) Risk factors of new compression fractures in adjacent vertebrae after percutaneous vertebroplasty. Acta Radiol 45(4):440–445. doi:10.1080/02841850410005615
20. Kurowski P, Kubo A (1986) The relationship of degeneration of the intervertebral disc to mechanical loading conditions on lumbar vertebrae. Spine 11:726–731. doi:10.1097/00007632-198609000-00012
21. Lavelle WF, Cheney R (2006) Recurrent fracture after vertebral kyphoplasty. Spine J 6(5):488–493. doi:10.1016/j.spinee.2005.10.013
22. Ledlie JT, Renfro MB (2006) Kyphoplasty treatment of vertebral fractures: 2-year outcomes show sustained benefits. Spine 31(1):57–64. doi:10.1097/01.brs.0000192687.07392.f1
23. Lee WS, Sung KH, Jeong HT et al (2006) Risk factors of developing new symptomatic vertebral compression fractures after percutaneous vertebroplasty in osteoporotic patients. Eur Spine J 15(12):1777–1783. doi:10.1007/s00586-006-0151-7
24. Legroux-Gerot I, Lormeau C, Boutry N, Cotten A, Duquesnoy B, Cortet B (2004) Long-term follow-up of vertebral osteoporotic fractures treated by percutaneous vertebroplasty. Clin Rheumatol 23(4):310–317. doi:10.1007/s10067-004-0914-7
25. Lin HS, Liu YK, Adams KH (1978) Mechanical response of the lumbar intervertebral joint under physiological (complex) loading. J Bone Joint Surg 60(1):41–55
26. Lin CC, Chen IH, Yu TC, Chen A, Yen PS (2007) New symptomatic compression fracture after percutaneous vertebroplasty at the thoracolumbar junction. AJNR Am J Neuroradiol 28(6):1042–1045. doi:10.3174/ajnr.A0520
27. Lindsay R, Silverman SL, Cooper C et al (2001) Risk of new vertebral fracture in the year following a fracture. JAMA 285(3):320–323. doi:10.1001/jama.285.3.320
28. Liu L, Pei F, Song Y et al (2002) The influence of the intervertebral disc on stress distribution of the thoracolumbar vertebrae under destructive load. Chin J Traumatol 5:279–283
29. Luo J, Skrzypiec DM, Pollintine P, Adams MA, Annesley-Williams DJ, Dolan P (2007) Mechanical efficacy of vertebroplasty: influence of cement type, BMD, fracture severity, and disc degeneration. Bone 40(4):1110–1119. doi:10.1016/j.bone.2006.11.021
30. Melton LJ III, Atkinson EJ, Cooper C, O'Fallon WM, Riggs BL (1999) Vertebral fractures predict subsequent fractures. Osteoporos Int 10:214–221. doi:10.1007/s001980050218
31. Nachemson AL (1981) Disc pressure measurements. Spine 6(1):93–97. doi:10.1097/00007632-198101000-00020
32. Patwardhan AG, Havey RM, Meade KP, Lee B, Dunlap B (1999) A follower load increases the load-carrying capacity of the lumbar spine in compression. Spine 24:1003–1009. doi:10.1097/00007632-199905150-00014
33. Patwardhan AG, Havey RM, Carandang G, Simonds J, Voronov LI, Ghanayem AJ et al (2003) Effect of compressive follower preload on the flexion-extension response of the human lumbar spine. J Orthop Res 21:540–546. doi:10.1016/S0736-0266(02)00202-4
34. Polikeit A, Nolte LP, Ferguson SJ (2003) The effect of cement augmentation on the load transfer in an osteoporotic functional spinal unit, finite element analysis. Spine 28:991–996. doi:10.1097/00007632-200305150-00006
35. Pongchaiyakul C, Nguyen ND, Jones G et al (2005) Asymptomatic vertebral deformity as a major risk factor for subsequent fractures and mortality: a long-term prospective study. J Bone Miner Res 20(8):1349–1355. doi:10.1359/JBMR.050317

36. Ranu HS (1990) Measurement of pressures in the nucleus and within the annulus of the human spinal disc due to extreme loading. Proc Inst Mech Eng [H] 204:141–145. doi:10.1243/PIME_PROC_1990_204_248_02
37. Rohlmann A, Zander T, Bergmann G (2006) Spinal loads after osteoporotic vertebral fractures treated by vertebroplasty or kyphoplasty. Eur Spine J 15(8):1255–1264. doi:10.1007/s00586-005-0018-3
38. Ross PD, Genant HK, Davis JW, Miller PD, Wasnich RD (1993) Predicting vertebral fracture incidence from prevalent fractures and bone density among non-black, osteoporotic women. Osteoporos Int 3(3):120–126. doi:10.1007/BF01623272
39. Sato K, Kikuchi S, Yonezawa T (1999) In vivo intradiscal pressure measurement in healthy individuals and in patients with ongoing back problems. Spine 24(23):2468–2474. doi:10.1097/00007632-199912010-00008
40. Shah JS, Hampson WG, Jayson MI (1978) The distribution of surface strain in the cadaveric lumbar spine. J Bone Joint Surg 60-B(2):246–251
41. Shindle MK, Gardner MJ, Koob J, Bukata S, Cabin JA, Lane JM (2006) Vertebral height restoration in osteoporotic compression fractures: kyphoplasty balloon tamp is superior to postural correction alone. Osteoporos Int 17(12):1815–1819. doi:10.1007/s00198-006-0195-x
42. Silverman SL (1992) The clinical consequences of vertebral compression fractures. Bone 13(supp 1):261–267. doi:10.1016/8756-3282(92)90193-Z
43. Sornay-Rendu E, Munoz F, Duboeuf F, Delmas PD (2004) Disc space narrowing is associated with an increased vertebral fracture risk in postmenopausal women: the OFELY Study. J Bone Miner Res 19(12):1994–1999
44. Stanley SK, Ghanayem AJ, Voronov LI, Havey RM, Paxinos O, Carandang G et al (2004) Flexion-extension response of the thoracolumbar spine under compressive follower preload. Spine 29(22):E510–E514. doi:10.1097/01.brs.0000145417.94357.39
45. Tanigawa N, Komemushi A, Kariya S, Kojima H, Shomura Y, Sawada S (2006) Radiological follow-up of new compression fractures following percutaneous vertebroplasty. Cardiovasc Intervent Radiol 29(1):92–96. doi:10.1007/s00270-005-0097-x
46. The European Prospective Osteoporosis Study (EPOS) Group (2003) Determinants of the size of incident vertebral deformities in European men and women in the sixth to ninth decades of age: the European Prospective Osteoporosis Study (EPOS). J Bone Miner Res 18:1664–1673. doi:10.1359/jbmr.2003.18.9.1664
47. Tomita S, Kin A, Yazu M, Abe M (2003) Biomechanical evaluation of kyphoplasty and vertebroplasty with calcium phosphate cement in a simulated osteoporotic compression fracture. J Orthop Sci 8:192–197. doi:10.1007/s007760300032
48. Trout AT, Kallmes DF, Kaufmann TJ (2006) New fractures after vertebroplasty: adjacent fractures occur significantly sooner. AJNR Am J Neuroradiol 27(1):217–223
49. Trout AT, Kallmes DF, Layton KF, Thielen KR, Hentz JG (2006) Vertebral endplate fractures: an indicator of the abnormal forces generated in the spine after vertebroplasty. J Bone Miner Res 21(11):1797–1802. doi:10.1359/jbmr.060723
50. Uppin A, Hirsch J, Centenera L, Pfiefer B, Pazianos A, Choi I (2003) Occurrence of new vertebral fracture after percutaneous vertebroplasty in patients with osteoporosis. Radiology 226:119–124. doi:10.1148/radiol.2261011911
51. Voormolen MH, Lohle PN, Juttmann JR et al (2006) The risk of new osteoporotic vertebral compression fractures in the year after percutaneous vertebroplasty. J Vasc Interv Radiol 17(1):71–76
52. Yuan H, Brown C, Phillips FM (2004) Osteoporotic spinal deformity: a biomechanical rationale for the clinical consequences and treatment of vertebral body compression fractures. J Spinal Disord 17:236–242. doi:10.1097/00024720-200406000-00012